Examining neural circuitry models of affective psychopathology: novel insights from human lesion studies combined with functional imaging

by
Julian Chase Motzkin

A dissertation submitted in partial fulfillment of
the requirements for the degree of

Doctor of Philosophy
(Neuroscience)

at the
UNIVERSITY OF WISCONSIN-MADISON
2014

Date of final oral examination: 05/23/2014

The dissertation is approved by the following members of the Final Oral Committee:

Michael R. Koenigs, Assistant Professor, Psychiatry
Craig W. Berridge, Professor, Psychology
Richard J. Davidson, Professor, Psychology
Ned H. Kalin, Professor, Psychiatry
Vivek Prabhakaran, Assistant Professor, Radiology
Scott B. Reeder, Associate Professor, Radiology

Acknowledgements

To the neurological patients who participated in this research, I am so thankful for your patience, interest, and enthusiasm. Without you, these studies would not have been possible.

Thanks foremost to Mike, for giving me the freedom to pursue my interests and the guidance and structure to help me follow through. I have learned so much from you, and watching the lab grow over these last five years has been an incredible experience.

I owe a special debt of gratitude to Richie, who gave me an amazing opportunity as a first year medical student to travel to Madison and immerse myself in research. Thank you for welcoming me into your lab and your home with open arms. Meeting you changed the course of my life, and for that, I will be forever grateful.

Thanks to all of my committee members for your support over the years. Ned Kalin for your genuine excitement about my data. Discussions with you challenged me to dig deeper and discover not just answers, but new questions. Vivek Prabhakaran for your mentorship in research and medicine, and your enthusiasm. To Craig Berridge for your support and guidance.

Thanks to all the mentors I've had along the way, especially Gerald Pollack, my undergraduate research advisor, for giving me a truly interesting and difficult undergraduate project. A very special thanks to Thomas Anderson at Albany Medical College for giving me the tools to transform my interests in science in to a tangible reality. Your support gave me the courage to make this happen.

Thanks to Rasmus Birn for showing me the ropes of imaging analysis. Thanks also to the MRI technicians (especially Marti and Ginny) and the rest of the HERI community (DJ, Kristina, Maria) for making work feel less like work.

Thanks to all of my friends who've helped keep me sane, balanced, active, and a little bit musical on this journey: Bornali, Olga, Kim, Jeremy, Cliff, Joel, Mike, Felipe, Tim, Anthony, Jeff, Aaron, Drew, Jamie, Jonathan, and my labmates and great friends, Maia, Carissa, and Rick.

My family is amazing and so incredibly supportive. Thanks Mom, Dad, and Chel for being a perennial source of love and support. Big shout out to Mom for your unwavering enthusiasm for everything I've ever done. Your insight and curiosity are an inspiration.

Lastly, I would like to dedicate this document to my grandfathers, Gramps (Phil Chase) and Poppi (Alvin Motzkin). Gramps, you have always inspired me to put my mind to good use, and I am so proud to have followed in your footsteps as I pile it higher and deeper. Poppi, thanks for being my biggest fan. I miss you, but I know you'll be watching when I finally graduate from medical school.

Table of Contents

Abstract

Mood and anxiety disorders are psychiatric diagnoses characterized primarily by poorly controlled expression of negative emotion. Clinical neuroimaging studies have identified abnormalities in the structure and function of the ventromedial sector of the prefrontal cortex (vmPFC) in virtually all mood and anxiety disorders, suggesting that this brain area underlies some critical domain of affective function that cuts across diagnostic categories. However, the neural mechanisms by which vmPFC contributes to affective psychopathology are not fully understood. The predominant neural circuitry theory proposes that vmPFC regulates negative affect via top-down inhibition of areas involved in processing negative emotion—particularly the amygdala—and that pathologically elevated levels of negative affect characteristic of mood and anxiety disorders result from deficient vmPFC-mediated inhibition of amygdala activity. The goal of this dissertation is to test and refine this model through a novel combination of functional magnetic resonance imaging (fMRI) and human lesion methodologies. Subjects included neurosurgical patients with focal, bilateral vmPFC lesions and psychopathic prison inmates with similar deficits in affective processing. Using an fMRI task involving the cued presentation of aversive and neutral visual stimuli in the vmPFC lesion patients, we found evidence for a causal role of vmPFC in regulating amygdala activity. Building on the results of this first experiment, we examined the effects of vmPFC damage on brain regions outside of the amygdala. Patients with vmPFC damage exhibited altered anticipatory processing of uncertain outcomes in bilateral insula and reduced resting perfusion in the bed nucleus of stria terminalis, highlighting the

distributed effects of vmPFC damage on brain regions and psychological processes relevant to affective psychopathology. In a final study of prison inmates with psychopathy, we discovered reduced structural and functional connectivity between the amygdala and vmPFC, underscoring the relevance of circuit-level connections with vmPFC across a range of affective dysfunction. Taken together, the findings summarized in this dissertation provide direct evidence of a causal role of vmPFC in the modulation of neural, physiological, and behavioral expressions of negative affect. These studies highlight a need to refine and elaborate prevailing neurocircuitry models of affective psychopathology.

List of Figures

List of Tables

Chapter 1. Introduction and Significance

Recent epidemiological survey data indicate that nearly one third of the United States population currently meets diagnostic criteria for one or more psychiatric disorders in the Diagnostic and Statistical Manual (DSM) of Mental Disorders (Kessler et al., 2005a). Mood and anxiety disorders, characterized primarily by deficits in the expression and regulation of negative emotion, are two of the most common diagnoses, with prevalence rates of 18 and 10 percent, respectively (Kessler et al., 2005b; Kessler et al., 2005a). Despite the considerable burden these disorders pose to individuals and to society (Bereza et al., 2009), depression and anxiety remain poorly understood and, in many cases, resistant to treatment (Bruce et al., 2005; Gibbons et al., 2012; Cuijpers et al., 2014). Substantial individual variability in their presentation, course, and response to treatment introduce significant barriers to effective clinical management. Unlike many other disorders treated within the contemporary medical establishment, for which clinicians use reliable biomarkers to effectively guide diagnosis, prognosis, and treatment, the identification of consistent and meaningful biological substrates of psychiatric disorders has remained elusive (Kapur et al., 2012).

Although current diagnostic categories based on clinical consensus have provided an invaluable foundation for clinical diagnosis and research, many clinicians and researchers see poor treatment outcomes as an indictment of overly rigid diagnostic categories that fail to capture the underlying mechanisms of dysfunction (Insel et al., 2010; Kapur et al., 2012). Therefore, a major goal of modern psychiatric medicine is to develop a system of diagnosis and treatment that is based on the pathophysiological mechanisms underlying

mental illness, irrespective of diagnostic category (Insel et al., 2010; Kapur et al., 2012; Cuthbert and Insel, 2013). This framework places a particular emphasis on the objective assessment of neural circuits responsible for particular domains of psychological or behavioral dysfunction that may be shared across traditional diagnoses (Insel et al., 2010; Kapur et al., 2012; Cuthbert and Insel, 2013).

Brain structure and function, readily measured *in vivo* using modern neuroimaging techniques, are beginning to emerge as potential diagnostic and prognostic markers for a host of psychiatric disorders (Mayberg et al., 2000; Whalen et al., 2008; Nitschke et al., 2009; Pizzagalli, 2011; Heller et al., 2013; McGrath et al., 2013). However, to date, neuroscientific study of the biological substrates of psychopathology in humans has been dominated by research comparing individuals with a clinical diagnosis to typically developing, or psychiatrically "healthy", adults. Although these studies have yielded undeniable insights to the patterns of brain structure and (dys)function associated with mood and anxiety disorders, they are inherently limited in their capacity to assess the causal contributions of observed neurobiological differences to dysfunctional behavior; in other words, while these studies succeed in "mapping" dysfunction to particular systems and circuits, they are unable to determine whether observed neurobiological differences are indicative of a diathesis, or pre-existing risk, or whether they instead reflect changes that emerge as a consequence of the disorder. This limitation has clear implications for the utility and predictive validity of neuroimaging in the diagnosis and treatment of mental illness. The development of more reliable and predictive biomarkers for mood and anxiety disorders would therefore benefit from a complementary approach to more fully

illuminate the neural circuitry responsible for affective functions commonly disrupted in these disorders.

The ventromedial sector of prefrontal cortex (vmPFC) is a brain area of critical importance in this regard. Clinical neuroimaging studies have identified abnormalities in vmPFC function and structure in virtually all mood and anxiety disorders, including major depression (Drevets et al., 1992; Mayberg et al., 1999; Mayberg et al., 2000; Mayberg et al., 2005; Greicius et al., 2007; Etkin and Schatzberg, 2011), post-traumatic stress disorder (Rauch et al., 2006; Shin et al., 2006; Etkin and Wager, 2007; Koenigs and Grafman, 2009b; Kuhn and Gallinat, 2012), obsessive-compulsive disorder (Harrison et al., 2012; Stern et al., 2012), generalized anxiety disorder (Etkin and Schatzberg, 2011; Greenberg et al., 2013), panic disorder (Uchida et al., 2008), bipolar disorder (Almeida et al., 2009; Versace et al., 2010), social anxiety disorder (Blair et al., 2010), and specific phobias (Hermann et al., 2007, 2009). The pervasive involvement of vmPFC dysfunction in mood and anxiety disorders suggests that vmPFC underlies some critical domain (or domains) of affective function that cut across traditional diagnostic categories.

Research Strategy

The lesion method has traditionally been the gold standard for interrogating whether a brain region is a critical neural substrate for a particular functional domain. The strength of the lesion method lies in its unique capacity to ascertain whether damage to a particular brain region is *causally* related to the impaired function. Examining patterns of brain activity, peripheral physiology, and behavior following focal damage to key brain regions implicated in anxious and depressive psychopathology could be a key step toward

elucidating the critical neural substrates of affective dysfunction in these disorders. The ubiquity of studies reporting alterations in structure and function of vmPFC, across diagnostic categories, highlights the necessity of research investigating the mechanisms by which this brain region contributes to observed behavioral phenotypes.

Using the lesion method, in concert with human neuroimaging techniques, the aim of this dissertation is to better understand the varied roles of vmPFC in affective function and dysfunction. In the following sections, I briefly introduce the reader to the concepts of emotion and emotion regulation, summarize data linking these processes to specific brain regions and networks (particularly vmPFC), and conclude the introduction by outlining a widely accepted neural circuitry model of affective dysfunction in mood and anxiety disorders. In the ensuing empirical chapters, I describe a series of experiments that test and refine central predictions of this model in pursuit of a more complete understanding of the role of vmPFC in affective processes relevant to psychopathology. Using existing models as a guiding framework, I conclude by presenting alternative explanations to better reconcile the full complement of available data.

Chapter 2. Emotion Regulation and Psychopathology

Emotion is an evolving concept. Throughout recorded human history, emotions have alternately been viewed as supernatural intrusions, signs of virtue, disruptive influences on cold reason, and adaptive biological phenomena (Solomon, 2010; Stearns, 2010). The emergence of Darwinian perspectives on psychology in the 19th century heralded a palpable shift toward a more functionalist approach to emotion (Darwin, 1872; James, 1884). This approach highlights the potential adaptive functions of emotions, suggesting that emotional states can serve as visceral guidance cues to bias action tendencies, guide decision-making, enhance memory, and facilitate social interaction (Campos et al., 1994). Emotional states, like fear, sadness, anger, and disgust, are each associated with loosely coupled but coordinated changes in autonomic and endocrine physiology, behavior, and subjective experience that anticipate and guide behavioral responses based on the context of the situation and the goals of the individual.

Inherent in the functionalist perspective is the capacity for emotions to influence and potentially disrupt higher-order cognitive and intellectual processes (Campos et al., 1994). In other words, the mechanisms by which one evaluates and controls one's emotions and with which one's emotions affect control processes are mutually influential. At times, the disruptive influences of emotion can seem overwhelming: fear of an impending public speech directing attention to negative feedback, sadness leading to withdrawal from important and personally meaningful goals, unchecked or misplaced anger disrupting valuable interpersonal relationships. Each of these situations provides an example of the power of our emotions to guide our thoughts and behavior in ways that

are maladaptive and potentially harmful to wellbeing. Thus, in most situations, we must regulate our emotions to conform to our current goals, or to the environmental and social context within which the emotion occurs.

An emerging field of research on emotion regulation has largely focused on conscious, cognitive strategies that can be used to deliberately regulate emotional experience (Gross, 2002; Ochsner and Gross, 2005; Ochsner and Gross, 2008). However, the expression of any given emotional response may be highly variable depending on any number of mutually influential factors, such as: the environmental or social context of the experience, previously learned associations, expectations about the experience, awareness or attention, effortful attempts to regulate or reappraise the experience, and even the current emotional state, to name a few. Evidently, any given emotional experience can be influenced by a variety of intrinsic and extrinsic psychological processes involved in monitoring, evaluating, and modifying emotional reactions (Thompson, 1994). For the purposes of this dissertation, I will define emotion regulation as a set of conscious and unconscious processes by which individuals modulate their emotions to appropriately respond to contextual demands (Aldao et al., 2010).

The burden of dysregulation

In certain cases, unchecked emotional expression or an impaired capacity for regulation can have profound effects on physical and psychological health (McEwen and Sapolsky, 1995; Sapolsky, 1996; Aldao et al., 2010). Indeed, problems with emotion or emotion regulation feature prominently in the diagnostic criteria for the majority of DSM diagnoses (American Psychiatric Association, 2013). Mood and anxiety disorders in

particular are largely defined by deficits in emotional expression and regulation. For example, across anxiety disorders, the principle diagnostic criterion is “marked fear or anxiety” about particular objects, situations, or events (American Psychiatric Association, 2013). In major depressive disorder, diagnostic criteria include persistent depressed mood and feelings of sadness (American Psychiatric Association, 2013). In both disorders, affective pathology is typically characterized by context-inappropriate emotional expression—the experience and display of a potentially normative emotional response that does not match the guidelines of current goals or situations (Davidson et al., 2000). Thus, although fear and sadness may be perfectly normal emotional responses in the appropriate context, when they are expressed at inappropriate times, or in situations in which most individuals would not express such emotions, they become pathological. In modern society, such contextually inappropriate response patterns can encourage social isolation and further reinforce maladaptive patterns of emotional expression and modulation.

Clearly, a better understanding of the neurobiological underpinnings of effective and dysfunctional emotional expression and regulation could have a profound impact on the way clinicians diagnose and treat mood and anxiety disorders. In the next section, I review evidence supporting a key role for the vmPFC in affective processing.

Chapter 3. Neurobiological underpinnings of adaptive and maladaptive emotion regulation

Phineas Gage and modern insights from the lesion method

In 1848, the physician John Harlow published what is now considered the first reported link between brain injury and emotional dysfunction (Harlow, 1848). In September of that year, Harlow was called upon to treat Phineas Gage, a 25-year-old railroad foreman on the Rutland & Burlington line in Vermont. Gage had been preparing blasting powder with a tamping rod when, suddenly, the iron rod sparked against the rock, triggering an explosion that sent the tapered end of the roughly 4-foot long, 1.25 inch diameter rod through the side of Gage's face and up through the midline of his brain before exiting through the top of his head and landing some distance away. Despite the mortal nature of his injury, Gage regained consciousness within a few minutes and was able to walk under his own power shortly after arriving to a nearby town for treatment.

In a retrospective report published two decades after the accident, Harlow described the unique changes that befell Gage in the wake of his brain injury:

> "His contractors, who regarded him as the most efficient and capable foreman in their employ previous to his injury, considered the change in his mind so marked that they could not give him his place again. The equilibrium or balance, so to speak, between his intellectual faculties and animal propensities, seems to have been destroyed. He is fitful, irreverent, indulging at times in the grossest profanity (which was not previously his custom), manifesting but little deference for his fellows, impatient of restraint or advice when it conflicts with his desires, at times pertinaciously obstinate, yet capricious and vacillating, devising many plans of future operation, which are no sooner arranged than they are cloned in turn for others appearing more feasible. […] Previous to his [injury] though

> untrained in the schools, he […] was looked upon by those who knew him shrewd smart business man, very energetic and [persistent] executing all his plans of operation. In this regard [he] was radically changed, so decidedly that his [friends] and acquaintances said he was 'no longer Gage.'" (Harlow, 1868)

Harlow paints the picture of a man who, once a model of persistence, respect, and strength of character, was immediately and permanently transformed following his injury. After his recovery, Gage was profane, obstinate, and animalistic, absent any overt alterations in his cognitive faculties of language, memory, reason, and general intelligence. In sum, the injury left Gage with profound disruptions in affect, behavioral control, and decision-making.

From the anatomical description of Harlow (Harlow, 1868) and subsequent modern anatomical reconstructions (Damasio et al., 1994), we now know that Gage suffered damage restricted primarily to the ventral and medial sectors of his frontal lobes. This region, commonly referred to as ventromedial prefrontal cortex (vmPFC), covers a large swath of the frontal lobes, extending from the medial surface of the orbitofrontal cortex to the ventral third of the medial prefrontal cortex. Although the exact boundaries of vmPFC remain a subject of debate in the literature, this area is generally thought to subsume Brodmann's cytoarchitectonic areas 11, 12, 13, 24, 25, 32, and the medial portion of 10 below the level of the genu of the corpus callosum (**Figure 1**). Therefore, vmPFC encompasses a heterogeneous population of cytoarchitectonically and functionally distinct subregions sharing a common gross anatomical location and a largely conserved pattern of connectivity with other brain areas. The vmPFC is a higher

order association cortex with extensive inputs and outputs, especially to limbic[1] regions like the insula, cingulate gyrus, amygdala, hippocampus, and dorsomedial thalamus (**Figure 1**). This network of connections affords the vmPFC the ability to receive and monitor large amounts of sensory data and to influence a host of other brain regions, particularly the amygdala. Importantly, damage to vmPFC, in addition to affecting local processing within this region, disrupts the majority of bidirectional connections between the frontal lobes and subcortical and limbic regions (Eslinger and Damasio, 1985).

In more than a century since the first description of Gage's injury, similar reports of profound, yet specific, alterations in personality and emotion began to emerge in the literature. In most cases, these patients suffered damage similar to Gage, restricted largely to the orbital and medial surfaces of the frontal lobes, commonly resulting from large anterior cranial fossa meningiomas or anterior communicating artery aneurysms. The patterns of behavior in these patients stood in stark contrast to other descriptions of frontal lobe damage following more extensive cortical lesions to the dorsal and lateral cortex. Whereas global prefrontal lesions elicited variable behavioral deficits in executive functions (e.g., attention, memory, and planning) depending on the location and extent of damage, nearly all cases of vmPFC damage were accompanied by disruptions in emotion, social behavior, and decision-making (Fuster, 2008b). In 1975, Blumer and Benson coined the term "pseudopsychopathy" to describe the personality changes characteristic

[1] The "limbic system" refers to a network of brain areas linked by common cytoarchitectonic organization, similar functional properties, and overlapping anatomical connectivity to brainstem and hypothalamic regions involved in the control of visceral and physiological processes. The word "limbic" comes from the Latin word "limbus", meaning, "border" or "edge." Indeed, the brain regions comprising the limbic system form a sort of border, or interface, between higher order cortical structures and brainstem and hypothalamic structures controlling the internal physiological milieu (Papez, 1937; Maclean, 1954).

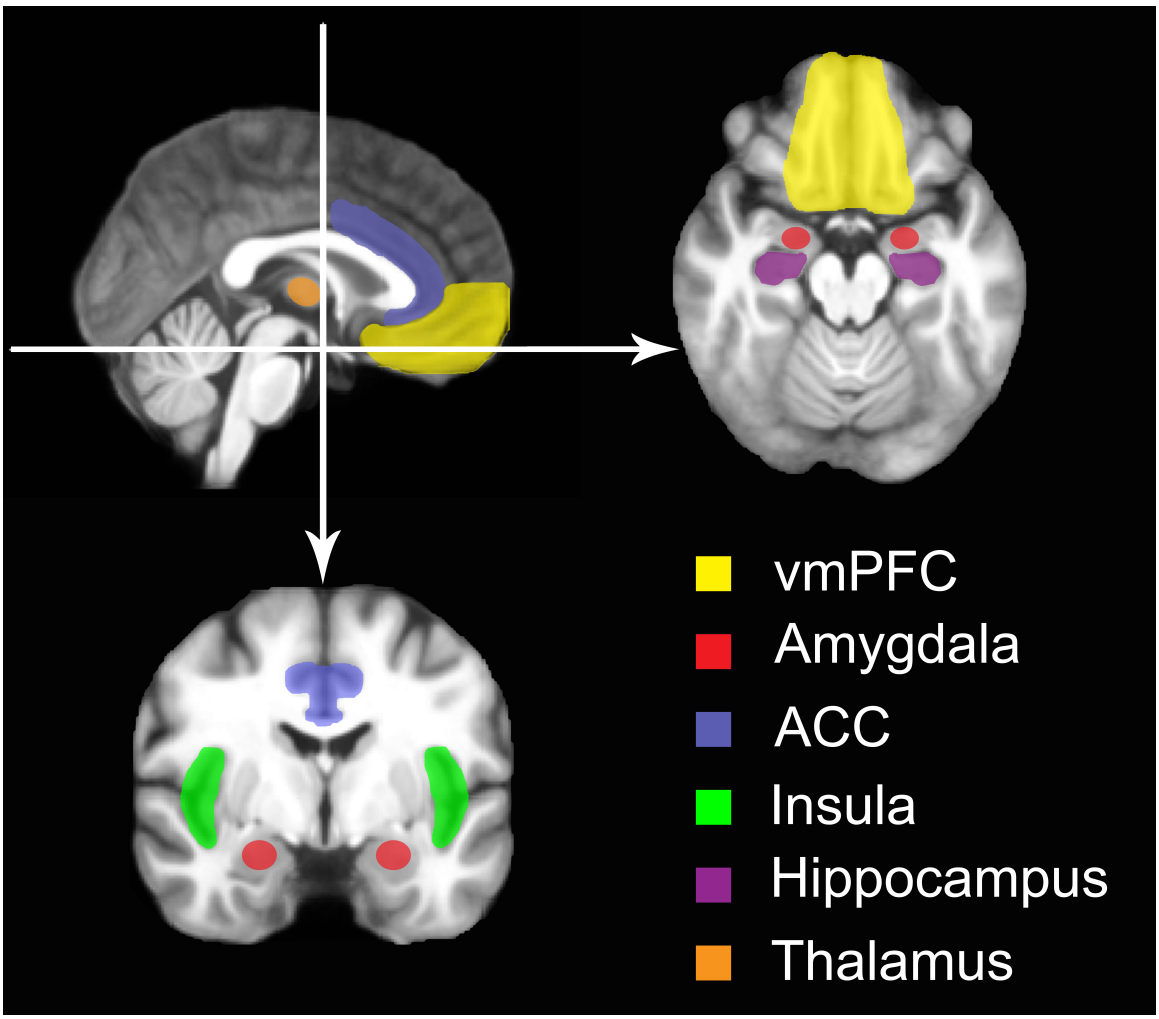

Figure 1. Illustration of ventromedial prefrontal cortex and interconnected structures. The area shaded in yellow on sagittal midline (top left) and axial (top right) sections of the brain denotes vmPFC. Ventral areas of the ACC, shown in blue on sagittal (top left) and coronal (bottom left) sections, are sometimes included in anatomical descriptions of vmPFC. ACC, Anterior Cingulate Cortex; vmPFC, ventromedial Prefrontal Cortex.

of these patients (e.g., blunted affect, lack of empathy, irresponsibility, and poor decision-making), in light of their striking resemblance to hallmark psychopathic personality traits (Blumer and Benson, 1975).

In recent decades, groups of patients with focal vmPFC lesions have been more carefully studied, permitting more thorough characterization of the specific affective processing deficits associated with damage to this brain region. For example, utilizing the

Iowa Rating Scale of Personality Change (IRSPC)[2], Barrash and colleagues found that, relative to patients with lesions outside vmPFC, patients with focal vmPFC damage exhibited dampening of emotional experience and poorly modulated emotional reactions, in addition to other deficits in decision-making and goal-directed behavior (Barrash et al., 2000). In other studies, adult-onset vmPFC damage has been associated with increased aggression and emotional lability, especially in response to frustrating situations (Grafman et al., 1996; Blair and Cipolotti, 2000). More recently, vmPFC damage has been linked to variable deficits in recognizing emotional expressions in others (Heberlein et al., 2008; Wolf et al., 2014).

One of the most consistently reported deficits in vmPFC lesion patients is attenuation of the autonomic and physiological components of an emotional response. Electrodermal skin conductance responses (SCRs) are commonly used peripheral indices of autonomic arousal, reliably elicited by stimuli with emotional or arousing content (Bradley et al., 2001; Dawson and Schell, 2007). Damasio and colleagues observed that patients with vmPFC damage exhibited blunted SCRs to emotionally evocative stimuli, despite exhibiting normative SCRs to orienting stimuli like loud noises (Damasio et al., 1990). In a similar study investigating the recall and re-experience of a previous emotional event, Tranel and colleagues observed decreased SCRs and decreased self-reported emotional intensity in patients with vmPFC damage (Tranel et al., 1998). Several studies have linked vmPFC damage to reduced anticipatory arousal under conditions of risk and

[2] The Iowa Rating Scale of Personality Change is a structured clinical assessment of 30 specific personality changes obtained from a close associate (usually spouse or family member) that is familiar with the change in the patient's real-world behavior before and after brain damage. Using information from collateral sources is necessary because patients with vmPFC lesions are notable for their lack of insight to their own behavior (Barrash et al., 2000).

uncertainty (Bechara et al., 1997; Bechara et al., 1999), which correspond directly to decision-making deficits in tasks involving uncertain or risky outcomes (Bechara et al., 1994; Fellows and Farah, 2003; Tsuchida et al., 2010).

In spite of the profound alterations in affect observed in these patients, neuropsychological testing indicates that intellectual and cognitive abilities of speech, language, vocabulary, general intelligence, and memory remain intact, and in some cases, above average. This profile is largely consistent with a putative role of vmPFC in the generation and modulation of affect, sparing higher order cognitive and intellectual capacities.

Modern insights from human brain imaging and post-mortem analysis

With the emergence and popularization of *in vivo* magnetic resonance imaging (MRI) in the 1990s, the vmPFC has become the focus of significant attention as researchers attempt to better understand psychiatric disorders characterized by disruptions in affective processing, like depression and anxiety. As group lesion studies revealed large-scale disruptions in social and affective processing following vmPFC damage, clinical neuroimaging studies began to identify consistent differences in vmPFC structure, function, and connectivity in mood and anxiety disorders (Mayberg et al., 2000; Etkin and Wager, 2007; Greicius et al., 2007; Drevets et al., 2008; Etkin and Schatzberg, 2011; Stern et al., 2012). For example, neuroanatomical studies of cortical volume in major depressive disorder have found reduced volume in the subgenual cingulate region of vmPFC (Drevets et al., 1997), with some studies indicating that volume increases following successful pharmacological treatment (Manji et al., 2000). Post-mortem

analyses of the brains of patients with major depressive disorder largely support the structural imaging results, finding reduced numbers of glial cells and reduced neuronal cell density within the vmPFC (Ongur et al., 1998; Cotter et al., 2001). In contrast, functional imaging with positron emission tomography (PET) has revealed *increases* in glucose metabolism in vmPFC in major depression (after correcting for reductions in gray matter volume)(Drevets et al., 1997; Mayberg et al., 1999), with reductions in resting metabolism observed after successful pharmacological treatment (Mayberg et al., 2000; Drevets et al., 2002).

Although alterations in structure and function have been observed in a number of additional brain regions linked to affective processing—including, but not limited to the amygdala, insula, posterior cingulate/precuneus, lateral prefrontal cortex, and ventral striatum—the vmPFC and amygdala are perhaps the most commonly cited neural correlates of affective psychopathology in the extant literature, and have thus been the focus of considerable investigation (Quirk and Gehlert, 2003; Quirk and Beer, 2006; Rauch et al., 2006; Shin et al., 2006). Taken together, the brain lesion and imaging data support the hypothesis that vmPFC is a critical neural substrate of emotion and social behavior. In the following section, I outline the prevailing neurobiological model of emotion regulation, which draws heavily upon previous human and animal research implicating the vmPFC in affective psychopathology.

Chapter 4. A model of vmPFC function in emotion regulation

The predominant neural circuitry model of emotion regulation, based largely on animal studies of fear conditioning and extinction, proposes that vmPFC serves to regulate negative affect via top-down inhibition of brain regions involved in processing negative emotion—particularly the amygdala—and that pathologically elevated levels of negative affect in mood and anxiety disorders result from deficient vmPFC-mediated inhibition of amygdala activity (Quirk and Gehlert, 2003; Milad et al., 2006; Rauch et al., 2006). Multiple lines of convergent evidence support this inhibitory model of vmPFC function, described in turn below.

The role of amygdala in negative emotion

Abundant convergent data from human and animal studies implicate the amygdala as a principal neural substrate of negative emotions, including fear and sadness (Davis and Whalen, 2001; Dolan and Vuilleumier, 2003; Phelps and LeDoux, 2005). The amygdala projects to brainstem and hypothalamic structures that coordinate the physiological, autonomic, and musculoskeletal components of an emotional response (LeDoux et al., 1988), and the central role of the amygdala in the acquisition and expression of conditioned fear is well documented (Phelps and LeDoux, 2005). Stimulation of human amygdala is sufficient to induce subjective experience of fear, anxiety, and sadness, which are accompanied by concomitant increases in peripheral indices of autonomic arousal (Lanteaume et al., 2007). Furthermore, human amygdala lesions are associated with an increased tendency to approach potentially dangerous stimuli and reduced

recognition and display of negative emotional expressions (Adolphs et al., 2005; Tranel et al., 2006; Feinstein et al., 2011), although these patients have recently been shown to exhibit anxious behavior under certain extreme conditions (Feinstein et al., 2013). Together, these data implicate the amygdala as a critical neural substrate for the expression of negative emotional states**.**

vmPFC-amygdala interactions and emotion regulation

Using fear conditioning and extinction paradigms, an elegant set of rodent studies have demonstrated a causal chain between activity in infralimbic cortex (the purported homolog of human vmPFC), inhibition of amygdala, and extinction of conditioned behavioral and physiological fear responses (Milad and Quirk, 2002; Quirk et al., 2003; Milad et al., 2006; Quirk et al., 2006). Projection fibers from rodent infralimbic cortex synapse on inhibitory intercalated cells that strongly inhibit the output of the amygdala (Royer et al., 2000), electrophysiological studies in rodents have demonstrated that medial PFC stimulation directly decreases the responsiveness of amygdala neurons (Quirk et al., 2003; Rosenkranz et al., 2003), with corresponding reductions in the behavioral and physiological expression of conditioned fear (Milad and Quirk, 2002).

In humans, functional imaging studies have demonstrated that activity in vmPFC and amygdala is inversely related during the extinction of conditioned fear (Phelps et al., 2004) and during the volitional suppression of negative emotion (Urry et al., 2006; Johnstone et al., 2007; Delgado et al., 2008), with the inverse coupling between vmPFC and amygdala commonly disrupted in mood and anxiety disorders (Milad et al., 2006; Rauch et al., 2006; Johnstone et al., 2007). More recently, both anxiety and depression

have been associated with decreases in structural and functional connectivity between the amygdala and medial PFC (Kim and Whalen, 2009; Kim et al., 2010; Kim et al., 2011).

Anatomical tracing studies in rodents and non-human primates indicate that the amygdala and prefrontal cortex (PFC) are extensively and reciprocally connected (Amaral and Price, 1984; McDonald et al., 1996; Ghashghaei et al., 2007), with orbital and medial regions of the PFC exhibiting the highest concentration of projected (McDonald et al., 1996) and received fibers (Ongur and Price, 2000), providing a viable anatomical substrate for the observed functional relationship.

Taken together, these studies strongly support the assertion that the PFC, with a particular emphasis on ventral and medial sub-regions, is an important regulator of the amygdala (Davidson, 2002; Ochsner et al., 2002), and further, that the exaggerated negative affect typical of mood and anxiety disorders may be due to deficient regulation of amygdala by vmPFC (Drevets, 2003; Quirk and Gehlert, 2003; Rauch et al., 2006).

Limitations of the top-down inhibition model

Given the putative role of vmPFC in emotion regulation, one might predict that individuals with damage to this region would exhibit patterns of behavior consistent with pathological anxiety or depression. Although the data presented above are consistent with the proposal that vmPFC plays a critical and causal role in regulating amygdala activity, the characteristic presentation of human vmPFC lesion patients (summarized in the previous section) reveals a discrepancy between predicted and observed behaviors. Human vmPFC lesions are commonly associated with changes in personality and behavior that are notably distinct from those typical of anxious and depressive

psychopathology (Eslinger and Damasio, 1985; Barrash et al., 2000). Rather, personality changes accompanying vmPFC damage (e.g., lack of empathy, social disinhibition, blunted affect, irresponsibility, and poor decision-making) bear striking resemblance to hallmark psychopathic personality traits, and have been dubbed "pseudopsychopathy" (Blumer and Benson, 1975) and "acquired sociopathy" (Eslinger and Damasio, 1985). Similarly, patients with vmPFC damage typically exhibit blunted (not enhanced) physiological responses to emotionally evocative stimuli, more akin to individuals with psychopathy than patients with depression and anxiety (Hare, 1965; Hare et al., 1978; Damasio et al., 1990; Bechara et al., 1997; Bechara et al., 1999). Focal vmPFC damage has actually been shown to *reduce* the likelihood of developing post-traumatic stress disorder (PTSD) and depression (Koenigs et al., 2008a; Koenigs et al., 2008b). These observations are largely consistent with previous studies of resting glucose metabolism in major depression, indicating that metabolism in the subgenual cingulate region of vmPFC is increased (not decreased) in depression (Mayberg et al., 2000), and that successful treatment is associated with reductions in resting metabolism. Thus, increased vmPFC activity in depression may reflect the generation and expression (rather than the regulation) of negative affective states. Finally, a recent study of non-human primates found that orbitofrontal cortex lesions impinging on the major outflow tracts between vmPFC and amygdala were associated with *reduced* activity in the extended amygdala and *reduced* anxiety behaviors (Fox et al., 2010).

Thus, it remains unknown whether the disruption of vmPFC function would in fact significantly disinhibit amygdala activity in humans. These seemingly contradictory findings suggest that a more thorough understanding of the interaction between the

vmPFC and amygdala (or other brain regions involved in negative affect) will be necessary to elucidate the contribution of vmPFC to emotional psychopathology.

Chapter 5. Objectives and Hypotheses

Despite substantial convergent evidence supporting a putative role of vmPFC in the modulation of emotion through direct regulation of amygdala activity, there are several apparent limitations to this model of vmPFC function in its current form. Most notably, human vmPFC lesions elicit changes in behavior and physiology in direct opposition to what might be expected if vmPFC were indeed critical for top-down regulation of negative affect. These ostensibly contradictory findings suggest that a more nuanced understanding of the interaction between the vmPFC and other brain regions implicated in the expression of negative emotion, like the amygdala, will be necessary to clarify the role of vmPFC in the modulation of negative affective states.

To date, much of the insight linking particular brain regions to the psychological processes of emotion regulation has been gleaned from electrophysiological studies in animals and functional imaging studies in humans with psychiatric illness. Although these sources of data have significantly advanced our understanding of the neural bases of mood and anxiety disorders, there are significant limitations associated with each approach. Animal models are inherently restricted in their capacity to address the uniquely human features of psychiatric illness, and the correlative nature of human neuroimaging data precludes causal inferences between observed brain activity and behavior. Therefore, a more complete understanding of the neurobiological mechanisms underlying mood and anxiety disorders requires a complementary experimental approach.

As outlined in the introduction, the lesion method has traditionally been the gold standard for interrogating whether a brain region is a critical and causal neural substrate

for a particular functional domain. The inconsistency between current neurobiological models of emotion regulation and extant human lesion data highlights the necessity of research investigating the mechanisms by which brain regions implicated in affective processing contribute to observed behavioral phenotypes. Examining patterns of brain activity, physiology, and behavior following focal damage to vmPFC will be a fundamental step toward elucidating the critical role of this brain region in the modulation and expression of negative affect.

In the next three chapters of this dissertation, I deploy the method outlined above to a group of rare human patients with focal, stable vmPFC lesions. In Chapter 6, I use structural and functional imaging techniques, together with peripheral recordings of cardiac physiology, to examine how damage to the vmPFC affects amygdala activity and peripheral physiological responses to aversive stimuli. Building on the results of this first experiment, the subsequent two chapters examine the effects of vmPFC damage on brain regions outside of the amygdala, and how individual differences in brain activity in these regions contribute to behavioral and physiological processes relevant to the pathogenesis of anxiety and depression. Finally, in Chapter 9, I apply the insights from previous chapters to a separate clinical population with marked impairments in affective function—prison inmates with psychopathy. As mentioned above, psychopathic individuals are notable for their similarity to patients with vmPFC damage. This final experiment illustrates the generalizability of new perspectives of vmPFC function gleaned from the previous chapters. I conclude with a summary and integration of the research findings, with special consideration given to neurobiological models of affective psychopathology.

Chapter 6. Ventromedial prefrontal cortex is critical for the regulation of amygdala activity in humans

As described in the previous sections, despite considerable evidence from cellular and electrophysiological studies in animals and functional imaging studies in humans, the prevailing model of emotion regulation is unable to reconcile the predicted and observed patterns of behavior following human vmPFC lesions. Whereas the model predicts that vmPFC damage should promote amygdala hyperactivity and downstream enhancement of behavioral and physiological indices of negative affect, patients with focal vmPFC lesions characteristically present with blunted physiological and behavioral indices of emotion and are *less* likely to develop anxious and depressive psychopathology than patients with lesions outside vmPFC (Damasio et al., 1990; Koenigs et al., 2008a; Koenigs et al., 2008b).

Thus, it remains unknown whether the disruption of vmPFC function would in fact significantly disinhibit amygdala activity in humans. In this chapter, I address this empirical gap through a novel application of functional magnetic resonance imaging (fMRI) to four neurosurgical patients with focal, bilateral vmPFC lesions. The aim of this chapter is to determine whether patients with vmPFC damage exhibit increased amygdala activation to aversive stimuli, as would be predicted by the prevailing model of vmPFC function in emotion regulation.

Previous work in human populations indicates that pictures with aversive content (e.g., images of interpersonal violence, accidents, dismemberment, and otherwise aversive material) robustly activate the amygdala in neurologically and psychiatrically

healthy adults, as well as in mentally ill populations (Phan et al., 2002; Costafreda et al., 2008; Ewbank et al., 2009). To examine the effects of focal vmPFC damage on amygdala reactivity, the present study used fMRI and a peripheral measure of cardiac physiology during a task involving the cued presentation of aversive and neutral picture stimuli. A finding of increased amygdala activation to aversive stimuli in the vmPFC lesion group would provide support for the hypothesis that vmPFC exerts a causal influence on amygdala activity in humans.

Methods

Participants

The target lesion group consisted of four adult neurosurgical patients with extensive bilateral parenchymal damage, largely confined to the vmPFC—defined as the medial one-third of the orbital surface and the ventral one-third of the medial surface of prefrontal cortex, bilaterally (**Figure 2**). Each of the four patients underwent surgical resection of a large anterior cranial fossa meningioma via craniotomy. Initial clinical presentations included subtle or obvious personality changes over several months preceding surgery. On post-surgical MRI, although vasogenic edema largely resolved, there were persistent T_2-weighted signal changes, consistent with gliosis, in the vmPFC bilaterally. All experimental procedures were conducted more than three months after surgery, when the expected recovery was complete. At the time of testing, all patients had focal, stable MRI signal changes and resection cavities and were free of dementia and substance abuse.

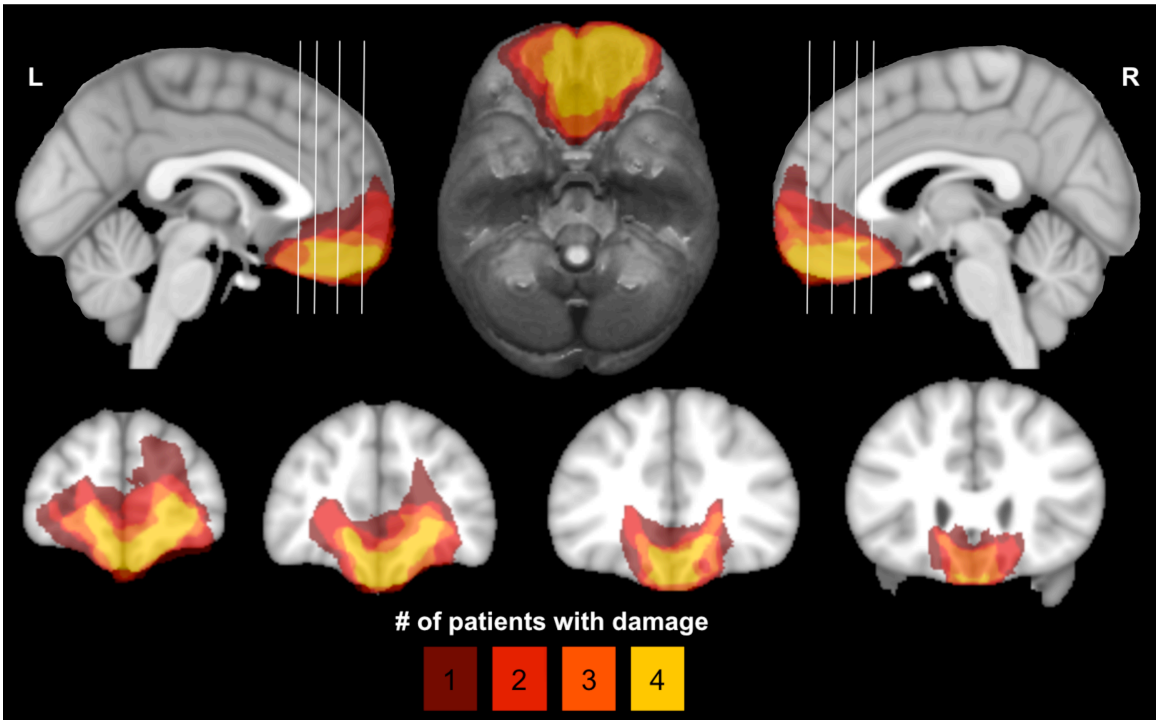

Figure 2. Lesion overlap of vmPFC patients. Color indicates the number of overlapping lesions at each voxel. All vmPFC patients had damage to the medial one-third of the orbitofrontal cortex and the ventral one-third of medial surface of prefrontal cortex, bilaterally. This area includes Brodmann areas 11, 12, 13, 24, 25, 32, and the medial portion of 10 below the level of the genu of the corpus callosum, as well as subjacent white matter.

Nineteen healthy adults with no history of brain injury, neurological or psychiatric illness, or current use of psychoactive medication were recruited as a normal comparison (NC) group. From the full NC group, we selected a subsample of n=10 subjects who were more closely matched to the vmPFC patients in age and gender, to corroborate results from the larger NC sample. Demographic and neuropsychological data for the vmPFC and NC groups are summarized in **Table 1**.

Event-related fMRI task

During the fMRI task, adapted from a previous paradigm shown to elicit strong amygdala activation in healthy subjects (Sarinopoulos et al., 2010), subjects viewed 64

Table 1. Subject Characteristics: Lesion Study

	Age	Sex	Edu	IQ	Pos Aff	Neg Aff	BDI-II	STAI-T
vmPFC (n=4)	58.5 (6.2)	3 M 1 F	15.5 (4.1)	103.8 (12.4)	36 (8.4)	17.0 (8.7)	7.0 (3.2)	34.3 (9.5)
NC (n=19)	51.7 (9.9)	11 M 8 F	17.7 (3.5)	110.9 (7.2)	37.8 (4.9)	13.0 (2.4)	4.0 (3.3)	31.6 (6.0)
NC age 50+ (n=10)	59.8 (4.7)	8 M 2 F	16.8 (2.3)	113.1 (7.2)	39.2 (5.4)	12.6 (2.7)	3.7 (2.9)	29.6 (5.0)
P (vmPFC vs NC)	0.16	0.63	0.51	0.25	0.56	0.73	0.11	0.44
P (vmPFC vs NC age 50+)	0.95	0.99	0.64	0.14	0.54	0.64	0.13	0.28

Means are presented with standard deviations in parentheses. Edu, years of education; IQ, intelligence quotient estimated by the Wide Range Achievement Test 4, Blue Reading subtest (Wilkinson and Robertson, 2006); Pos/Neg Aff, scores from the Positive and Negative Affect Schedule (PANAS) (Watson et al., 1988); BDI-II, Beck Depression Inventory-II (Beck et al., 1996) ; STAI-T, trait version of the Spielberger State Trait Anxiety Inventory (Spielberger et al., 1983).

unique images drawn from the International Affective Picture System (IAPS) (Lang et al., 2008), divided evenly among pictures with aversive and neutral content (see **Figure 3 and Supplementary Table 1** for details). Aversive stimuli consisted of 32 negative/unpleasant and arousing images, based on published norms (Ewbank et al., 2009; Lang et al., 2008) (Valence: 2.01±0.39; Arousal: 6.25±0.7). Neutral stimuli consisted of 32 images with neutral valence and low arousal ratings (Valence: 4.96±0.21; Arousal: 2.95±0.77). All images were preceded by one of three visual cues ("X", "O", or "?"). The "X" and "O" cues indicated that the subsequent image would be aversive or neutral, respectively, whereas the "?" cue provided no information regarding the emotional content of the image (equal likelihood of aversive or neutral content). Each experimental trial consisted of a cue presented for 2 s, followed—after a jittered inter-stimulus interval (ISI) (range: 2-8 s)—by a 1 s picture presentation. After a second jittered ISI (range: 5-9 s), subjects had 4 s to rate their emotional response to the image

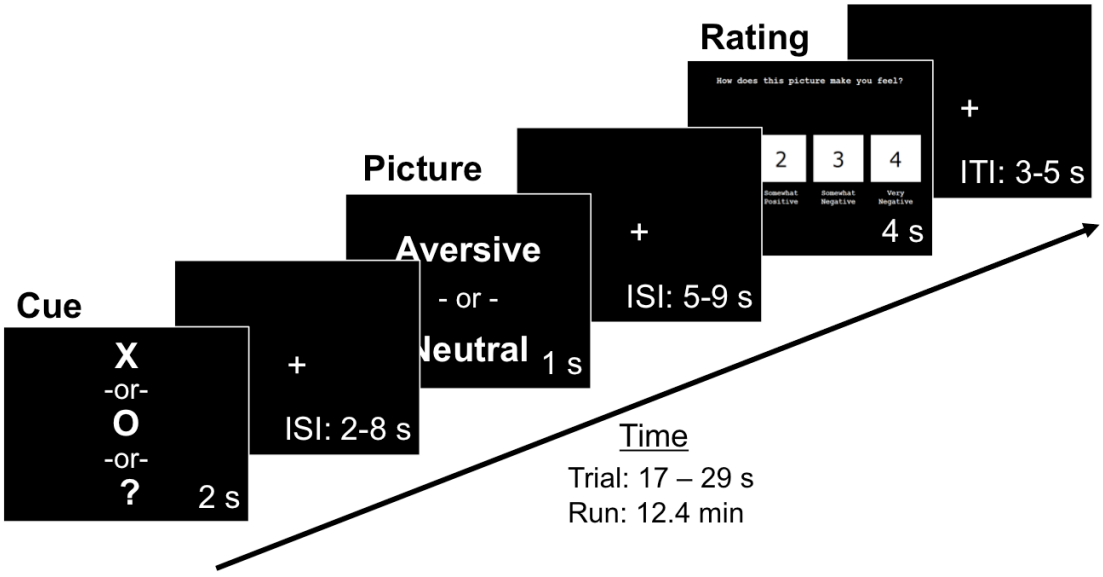

Figure 3. fMRI task used to assess amygdala responses to aversive and neutral pictures. Each experimental trial (pictured) consisted of a cue ("X", "O", or "?") presented for 2 s, followed—after a jittered inter-stimulus interval (ISI) (range: 2-8 s)—by a 1 s picture presentation (Aversive or Neutral). After a second jittered ISI (range: 5-9 s), subjects had 4 s to rate their emotional response to the image using a 4-item likert scale ranging from 1 ("very positive") to 4 ("very negative"). There were two experimental runs of 32 trials each, with each run lasting ~12.4 min.

using a 4-item scale ranging from 1 ("very positive") to 4 ("very negative") (see **Supplementary Table 2** for rating data). Prior to scanning, subjects were informed of all cue-picture contingencies and completed a practice task consisting of 16 unique trials (4 per cue-picture pair) to ensure task comprehension.

MRI data acquisition

All structural and functional MRI data were acquired using a 3.0 T GE Discovery MR750 scanner equipped with an 8-channel radio-frequency head coil array (General Electric Medical Systems; Waukesha, WI). High-resolution T_1-weighted anatomical images were acquired using an inversion-recovery spoiled GRASS [SPGR] sequence

(TR=8.2ms, TE=3.2ms, α=12°, FOV=256x256mm, matrix=256x256, in-plane resolution=1x1mm^2, slice thickness=1mm, 1024 axial slices). To facilitate lesion segmentation, we collected a separate T_2-weighted FLAIR scan (TR=8650ms, TE=136ms, α=0°, FOV=220x220mm^2, matrix=512x512, in-plane resolution=0.43x0.43mm^2, slice thickness=5 mm, gap 1mm, 25 axial slices).

Baseline resting cerebral blood flow (CBF) was estimated using a 3D fast spin echo spiral sequence with pseudocontinuous arterial spin labeling (pcASL) (Dai et al., 2008; Xu et al., 2010; Okonkwo et al., 2012) and background suppression for quantitative perfusion measurements (TR=4653ms, TE=10.5ms, post-labeling delay=1525ms, labeling duration=1450ms, eight interleaved spiral arms with 512 samples at 62.5 kHz bandwidth and 38 4-mm thick slices, number of excitations=3, scan duration=4.5min).

Whole-brain functional scans were acquired using a T_2*-weighted gradient-echo echoplanar imaging (EPI) sequence (TR=2000ms; TE=22ms; α=79°; FOV=224x224mm^2; matrix=64x64, in-plane resolution=3.5x3.5mm^2, slice thickness=3mm, gap=0.5mm, 38 interleaved axial oblique slices). Field maps were acquired using two separate acquisitions (TR=600ms, TE_1=7ms, TE_2=10ms, α=60°, FOV=240x240mm^2, matrix=256x128, slice thickness=4mm, 33 axial oblique slices). The two task runs lasted 12.4 minutes each. Scans were acquired in the following order: pcASL, field map, rest, task, T1, T2-FLAIR.

*Heart rate data acquisition***.**

Cardiac data were acquired at 100 Hz with GE's photoplethysmograph, affixed to the left index finger throughout the scan session. Heart rate data were available for n=12 NC subjects and all n=4 vmPFC lesion patients.

Lesion segmentation and image normalization.

Individual vmPFC lesions were visually identified and manually segmented on the T_1-weighted images. Lesion boundaries were drawn to include areas with gross tissue damage or abnormal signal characteristics on T_1 or T_2 FLAIR images. T_1-weighted images were skull-stripped, rigidly co-registered with a functional volume from each subject, then diffeomorphically aligned to the Montreal Neurological Institute (MNI) coordinate system using a Symmetric Normalization (SyN) algorithm (Avants and Gee, 2004) with constrained cost-function masking to prevent warping of tissue within the lesion mask (Brett et al., 2001). We created the lesion overlap map (**Figure 2**) by computing the sum of aligned binary lesion masks for all four vmPFC patients.

fMRI task preprocessing and analysis.

Data analysis was conducted using AFNI (Cox, 1996) and FSL (http://www.fmirb.ox.ac.uk/fsl) software. Individual task runs were slice time corrected, field map corrected (Jezzard and Clare, 1999), motion corrected, smoothed with a 6-mm full-width half-maximum (FWHM) Gaussian kernel, and scaled to percent signal change. Preprocessed task data were concatenated and analyzed using a general linear model (GLM) with separate regressors for each cue and picture type, the rating period, and

several regressors of no interest, including six motion covariates from rigid-body alignment (Johnstone et al., 2006) and a fourth-order polynomial to model baseline and slow signal drift. Blood oxygen level-dependent (BOLD) signal was modeled by convolving each event with AFNI's default canonical hemodynamic response function (HRF; gamma function). Because the identity of the cue did not significantly alter amygdala responses to the aversive pictures in either group (**Supplementary Table 3**), analyses were limited to aversive and neutral stimuli, irrespective of cue. Responses to the cues themselves are described at length in Chapter 7. To avoid potential confounds introduced by subject motion, volumes in which more than 10% of voxels were time series outliers were censored prior to conducting the GLM; there were no group differences in the average proportion of censored volumes (χ^2=2.09, P=0.15), or in mean framewise displacement (NC: 0.06±0.06mm, vmPFC: 0.04±0.02mm; W=28, P=0.44). Resulting whole-brain maps of voxelwise β-values for aversive and neutral pictures were aligned to MNI space and resampled to $3mm^3$ isotropic resolution for second-level analyses.

To identify brain regions responsive to aversive stimuli, we performed a whole-brain, two-tailed paired-sample t-test between responses to aversive and neutral pictures in the full NC group. Resulting statistical maps were family-wise error (FWE) corrected for multiple comparisons across the whole brain at the cluster level (P_{FWE}<0.05), using a height threshold of P<0.001 (Forman et al., 1995; Carp, 2012). A corrected P_{FWE}<0.05 was achieved using a cluster extent threshold of 38 voxels ($1026mm^3$), calculated using Monte Carlo simulations with 3dClustSim in AFNI. Significant clusters from the

aversive>neutral contrast (10 total) were used as functional regions of interest (ROIs) for subsequent between-groups analyses.

To visualize group-averaged BOLD responses to pictures within individual ROIs, we conducted a second GLM, replacing the canonical HRF with a series of nine TENT functions in order to deconvolve the raw BOLD signal. This model yielded β-values for each of 9 TRs from 0-16 seconds after picture onset. Because functional ROIs were derived using the canonical HRF, estimated response data from the deconvolution model were used for display only.

In light of the small sample size of vmPFC lesion patients, we used non-parametric Mann-Whitney-Wilcoxon tests to evaluate our main *a priori* hypothesis regarding amygdala activity. Specifically, we focused our between-groups analyses on percent signal change estimates extracted from functionally-derived right and left amygdala ROIs (amygdala clusters from the aversive>neutral contrast in the NC group). We used functional ROIs to ensure that group comparisons were conducted within functionally homogenous regions within the amygdala (i.e., regions that respond strongly to aversive relative to neutral stimuli) (Poldrack, 2007). However, to confirm that group comparisons within functionally-derived amygdala ROIs reflected differences in amygdala activity *per se*, we conducted additional between-groups tests using values extracted from atlas-defined anatomical ROIs in the right and left amygdala, created using the Talairach daemon in AFNI (Talairach and Tournoux, 1988). To examine subregions of the amygdala, we conducted follow-up analyses using hand-drawn, atlas-defined ROIs in the central nucleus of the amygdala (CeA) (Oler et al., 2012).

To test the specificity of observed effects to the amygdala, we conducted follow-up analyses on percent signal change values extracted from the eight remaining functionally-derived non-amygdala comparison ROIs (e.g., bilateral visual cortex, lateral temporal cortex, thalamus, etc.), in which we predicted normal responses to pictures for the vmPFC patients. All group comparisons were corroborated with the subsample of n=10 age- and gender-matched NC subjects in order to verify that group effects were not driven by potential differences in demographic variables. All tests were considered significant at $P<0.05$.

Cerebral perfusion analysis.

Quantitative CBF images from pcASL were rigidly co-registered with a T_2*-weighted EPI volume from the task scan and normalized to MNI space. Normalized CBF volumes were scaled to whole-brain CBF (after masking out the lesion in vmPFC patients) and smoothed with a 6mm FWHM Gaussian kernel. To rule out differences in baseline cerebral perfusion, we examined group differences in mean whole-brain CBF, as well as differences in scaled CBF for all ROIs using non-parametric Mann-Whitney-Wilcoxon tests.

Heart rate analysis

To assess cardiac responses to picture stimuli, we computed trial-wise estimates of heart rate change for each subject, as previously described (Bradley et al., 2001). Cardiac R-spikes were identified using interactive beat detection software. Trials with ectopic beats, missed beats, or periods of noisy signal (where beat detection failed), were

excluded from further analysis (NC group: n=2 with one excluded trial, n=1 with two excluded trials, n=2 with three excluded trials; vmPFC group: n=1 with two excluded trials). R-R intervals were transformed into heart rate in beats per minute, in 500 ms bins. Changes in heart rate were determined by subtracting the mean heart rate for 1 s preceding each picture from the heart rate at each 500 ms after picture onset. As in previous studies, the maximum cardiac deceleration (i.e., heart rate decrease) during the first 3 s of picture viewing was used as an index of the physiological response to each picture (Bradley et al., 2001). Group differences in cardiac deceleration were computed separately for aversive and neutral pictures using non-parametric Mann-Whitney-Wilcoxon tests.

Results

fMRI task

During the fMRI task, both groups rated aversive pictures as significantly more negative than the neutral pictures, with no differences between groups in ratings for either emotion category (**Supplementary Table 2**). Relative to neutral pictures, aversive pictures elicited robust bilateral amygdala activation in both the NC subjects (**Figure 4a** and **Table 2**) and vmPFC lesion patients (**Figure 4b**). To examine group differences in amygdala activity, we extracted percent signal change estimates from functionally-derived right and left amygdala ROIs—clusters of supra-threshold amygdala voxels from the aversive>neutral contrast in the NC group (**Figure 5a**). In support of our main hypothesis, vmPFC lesion patients exhibited significantly greater right amygdala activation to aversive pictures than did NC subjects (W=6, P=0.006;**Figure 5b, Table 3**).

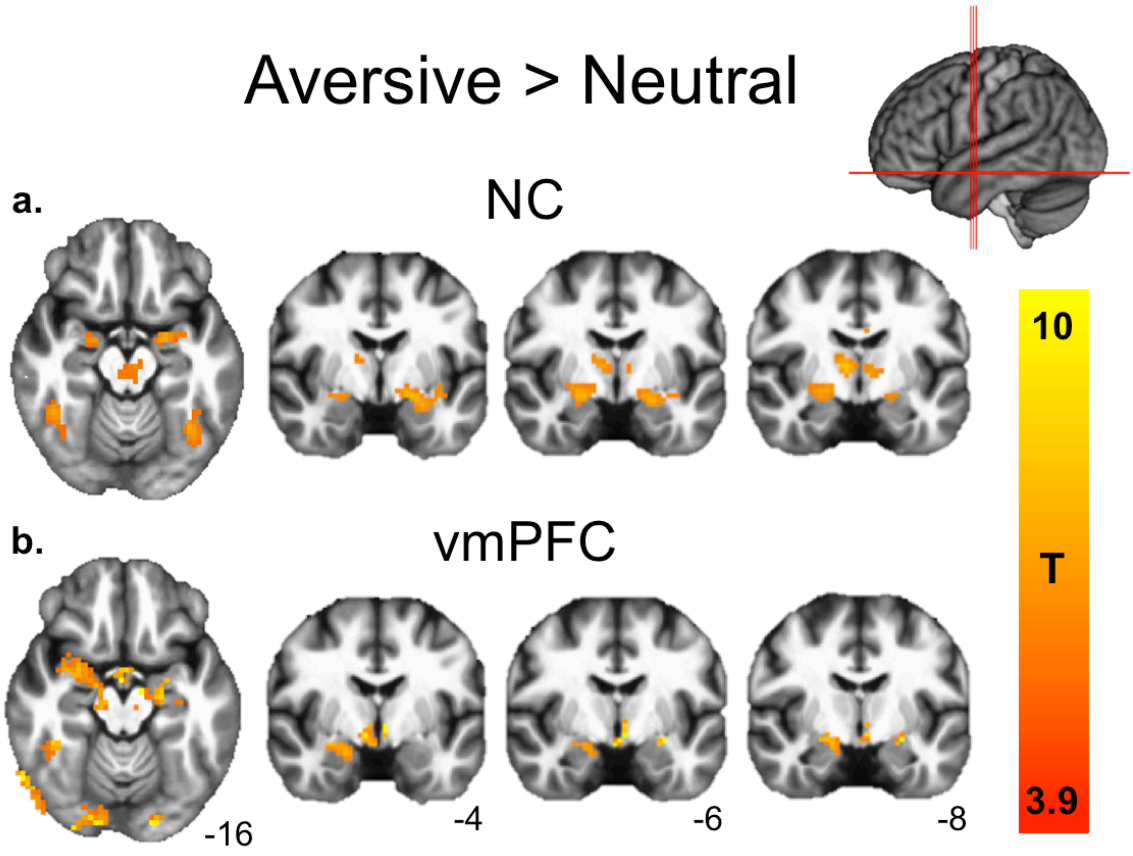

Figure 4. Neural responses to aversive>neutral pictures. (a) NC subjects (P_{FWE}<0.05; FWE, family wise error). **(b)** vmPFC lesion patients (displayed at corrected NC threshold of T=3.9 for comparison). Both groups exhibited robust bilateral amygdala responses, as well as responses in visual cortex, lateral temporal cortex, thalamus, and cingulate gyrus (see **Table 2** for full cluster list).

We observed similar group differences in activation to aversive pictures using an anatomically-defined right amygdala ROI (W=13, P=0.04) as well as an anatomically-defined right CeA ROI (W=13, P=0.04). This central finding was corroborated in a smaller sample of ten NC subjects closely matched in age and gender to the vmPFC group (W=2, P=0.008; **Supplementary Table 4**), suggesting that the findings were not driven by group differences in demographic factors. No significant group differences were observed in any left amygdala ROI (Functional ROI: W=28, P=0.46; Anatomical

Table 2. Cluster maxima for regions with statistically significant increased BOLD signal for aversive pictures relative to neutral pictures

NC group								vmPFC group	
				Peak voxel					
Brain region	**BA**	**Clust size**	***P* (FWE)**	**T**	**x**	**y**	**z**	**T**	***P***
R ITG	37	684	<0.0001	12.50	47	-68	-3	3.47	0.040
Thal		337	<0.0001	11.16	-1	-27	-4	1.99	0.141
L MTG	37	597	<0.0001	8.84	-52	-69	6	3.07	0.055
R Lingual	17	283	<0.0001	7.00	17	-90	-3	1.36	0.267
L Amyg	28	72	<0.005	6.49	-19	-3	-12	2.23	0.112
R Amyg	28	39	<0.05	6.03	20	-6	-12	3.38	0.043
R Precun	31	64	<0.005	6.00	5	-48	33	-0.85	0.458
L MFG	9	68	<0.005	5.23	-7	51	27	0.90	0.434
L ACC	24/32	72	<0.005	4.86	-1	6	39	0.87	0.448
L PCC	23	62	<0.005	4.58	-7	-24	27	-1.55	0.219

Clusters ordered by T score, for the aversive>neutral contrast in the NC group. Corrected p thresholds indicate minimum FWE-corrected p-value for each cluster. Uncorrected p values for the vmPFC group are derived from a voxelwise paired t-test in the vmPFC group, estimated at the peak coordinates for the NC group. R, right; L, left; ITG, inferior temporal gyrus; Thal, thalamus; MTG, middle temporal gyrus; Lingual, lingual gyrus; Amyg, amygdala; Precun, precuneus; MFG, medial frontal gyrus; ACC, anterior cingulate cortex; PCC, posterior cingulate cortex.

ROI: W=24, *P*=0.29; CeA ROI: W=24, *P*=0.29; **Figure 5c, Table 3, Supplementary Table 4)**.

To test the specificity of group differences to the amygdala, we conducted follow-up analyses in the eight remaining functionally-derived ROIs from the aversive>neutral picture contrast (e.g. visual cortex, lateral temporal cortex, thalamus, etc.) and found no consistent group differences in the response to aversive or neutral pictures in the non-amygdala comparison ROIs (**Table 3, Supplementary Table 4**). To ensure that group differences in the amygdala were not due to baseline differences in amygdala perfusion following vmPFC damage, we estimated CBF using pcASL prior to both functional scans in all subjects. There were no significant differences between the NC and vmPFC groups

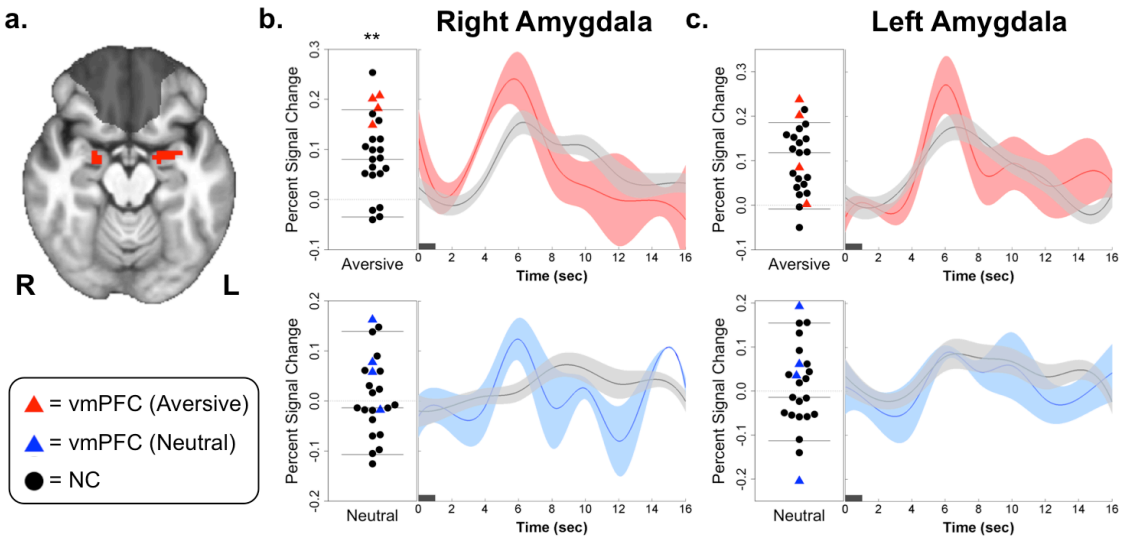

Figure 5. Greater right amygdala responses to aversive pictures in vmPFC lesion patients. (a) Task-derived right and left amygdala ROIs (red) used to extract mean percent signal change (PSC) estimates for group comparisons. vmPFC lesion overlap shaded in gray for reference. **(b)** Left, plots of right amygdala PSC for individual NC (black circles) and vmPFC (red and blue triangles) subjects in response to aversive pictures (top) and neutral pictures (bottom). Horizontal lines represent the mean and 95% confidence intervals of PSC values in the NC group. Right, mean timeseries of right amygdala PSC in response to aversive and neutral pictures for vmPFC (red, blue) and NC (black) subjects (width of shaded area corresponds to ±1 s.e.m.). **(c)** Plot and mean timeseries of PSC extracted from the left amygdala ROI. Dark horizontal bars on timeseries plots indicate picture duration (1 s). ***P*<0.01

in whole brain CBF, nor were there differences in relative CBF for any ROI used in group comparisons, including right amygdala (**Supplementary Table 5, Supplementary Table 6**). Finally, it is unlikely that the observed findings are due to systematic group differences in the shape of the hemodynamic response, since there were no apparent differences in the estimated hemodynamic response in motor cortex to button press (**Supplementary Figure 1**) or in visual and temporal comparison ROIs in response to aversive pictures (**Supplementary Figure 2**).

Table 3. Group differences in percent signal change to aversive and neutral pictures in functional and anatomical ROIs

	Aversive pictures				Neutral pictures			
Brain Region	**NC mean (SD)**	**vmPFC mean (SD)**	**W**	***P***	**NC mean (SD)**	**vmPFC mean (SD)**	**W**	***P***
R Amyg (Func ROI)	0.08 (0.07)	0.18 (0.03)	6	**0.006**	0.00 (0.08)	0.07 (0.07)	20	0.162
R Amyg (Anat ROI)	0.09 (0.08)	0.19 (0.07)	13	**0.044**	0.02 (0.08)	0.05 (0.12)	31	0.611
R Amyg (CeA ROI)	0.09 (0.08)	0.18 (0.06)	13	**0.044**	0.00 (0.09)	0.06 (0.09)	23	0.25
L Amyg (Func ROI)	0.10 (0.07)	0.13 (0.11)	28	0.456	0.01 (0.08)	0.02 (0.17)	31	0.611
L Amyg (Anat ROI)	0.10 (0.08)	0.16 (0.11)	24	0.286	0.02 (0.09)	0.03 (0.14)	32	0.667
L Amyg (CeA ROI)	0.12 (0.09)	0.19 (0.11)	24	0.286	0.01 (0.09)	0.01 (0.19)	31	0.612
R ITG	0.34 (0.13)	0.42 (0.11)	23	0.25	0.22 (0.11)	0.31 (0.07)	20	0.162
L MTG	0.30 (0.12)	0.35 (0.07)	26	0.366	0.20 (0.10)	0.25 (0.02)	22	0.218
Thal	0.14 (0.08)	0.18 (0.02)	24	0.286	0.06 (0.08)	0.11 (0.07)	23	0.25
R Lingual	0.48 (0.18)	0.50 (0.14)	31	0.611	0.38 (0.14)	0.44 (0.08)	24	0.286
L ACC	0.10 (0.06)	0.10 (0.06)	40	0.907	0.02 (0.09)	0.07 (0.06)	23	0.25
L MFG	0.03 (0.09)	0.01 (0.12)	41	0.845	-0.08 (0.07)	-0.04 (0.06)	26	0.366
R Precun	-0.01 (0.06)	-0.02 (0.04)	45	0.611	-0.06 (0.07)	0.01 (0.03)	17	0.097
L PCC	0.05 (0.05)	-0.03 (0.12)	56	0.162	-0.02 (0.06)	0.02 (0.08)	27	0.409

p-values for significant group differences are in bold. MNI coordinates for each ROI can be found in Table 2. Func ROI, functionally-defined ROI; Anat ROI, anatomically-defined ROI.

Heart rate response to pictures

To determine whether group differences in amygdala activity were accompanied by comparable differences in peripheral physiological responses, we investigated stimulus-evoked reductions in heart rate in response to the picture stimuli. Consistent with previous studies using the same stimuli, both groups exhibited cardiac deceleration in response to aversive and neutral pictures (Bradley et al., 2001; Codispoti et al., 2001). However, contrary to the amygdala fMRI results, the magnitude of stimulus-evoked cardiac deceleration was significantly *lower* in vmPFC lesion patients than in the NC subjects for aversive pictures (NC: -1.3±0.67; vmPFC: -0.52±0.31; W=6, *P*=0.03; **Supplementary Figure 3**). We observed similar, though non-significant, reductions in cardiac deceleration in response to neutral pictures (NC: -1.4±0.89; vmPFC: -0.60±0.30; W=11, *P*=0.13). There was no significant difference between groups in overall mean heart rate across the scan session (NC: 62.7±9; vmPFC: 75.9±12; W=11, *P*=0.13).

Discussion

Through a novel application of fMRI in human lesion patients with bilateral vmPFC damage, we have demonstrated a critical role for vmPFC in regulating amygdala activity. Specifically, we found that vmPFC lesions were associated with increased right amygdala reactivity to aversive stimuli. These findings are directly relevant to neural circuitry models of emotion regulation and affective psychopathology.

The model of vmPFC function in affective psychopathology posits two key features: (i) vmPFC dysfunction results in disinhibition of the amygdala and (ii) the resultant amygdala hyperactivity engenders pathologically high levels of anxiety and negative

affect (Quirk and Gehlert, 2003; Milad et al., 2006; Rauch et al., 2006). Although our results unequivocally support feature (i) of this model, they seem to complicate feature (ii), at least as it pertains to human affective processing. Using fear conditioning and extinction paradigms, an elegant set of rodent studies have demonstrated a causal chain between activity in infralimbic cortex (the purported homolog of human vmPFC), inhibition of amygdala, and extinction of conditioned behavioral and physiological fear responses (Milad and Quirk, 2002; Quirk et al., 2003; Milad et al., 2006; Quirk et al., 2006). Human functional imaging studies have provided correlative data consistent with this model (Phelps et al., 2004; Milad et al., 2006; Rauch et al., 2006; Urry et al., 2006; Johnstone et al., 2007; Delgado et al., 2008). However, the causal relationships among vmPFC activity, amygdala activity, and negative affect appear to be more complicated in humans. At least two lines of research argue for a more comprehensive model. One line of research involves patients with major depressive disorder (MDD). A number of neuroimaging studies indicate that patients with MDD exhibit abnormally high levels of activity within vmPFC (particularly in the subgenual cortex) (Mayberg et al., 2000; Mayberg et al., 2005; Greicius et al., 2007; Matthews et al., 2008; Keedwell et al., 2009). In addition, MDD patients who are responsive to antidepressant medication or deep brain stimulation tend to exhibit decreased activity in both the subgenual vmPFC and amygdala after treatment (Mayberg et al., 2000; Sheline et al., 2001; Drevets et al., 2002; Mayberg et al., 2005). Furthermore, activity within the subgenual vmPFC has been shown to correlate positively with negative affect in healthy subjects (Mayberg et al., 1999; Zald et al., 2002; Kross et al., 2009). These data suggest that increased vmPFC activity in depression may reflect the generation and expression (rather than the regulation) of

negative affective states. The second line of research involves vmPFC lesion patients. It is well established that vmPFC damage results in personality changes more reminiscent of psychopathy (e.g., blunted emotional experience, low emotional expressivity, impulsivity, lack of empathy, reckless decision-making) than anxiety or depression (Blumer and Benson, 1975; Eslinger and Damasio, 1985; Barrash et al., 2000). Critically, vmPFC damage has been shown to *reduce* (not increase) the likelihood of developing depression (Koenigs et al., 2008a) and post-traumatic stress disorder (Koenigs et al., 2008b). Moreover, vmPFC damage is associated with diminished physiological reactions (e.g., skin conductance responses) to aversive stimuli (Damasio et al., 1990; Bechara et al., 1997; Camille et al., 2004). Our heart rate data are consistent with these prior physiological findings. Rather than observing increased cardiac deceleration in response to aversive pictures in the vmPFC lesion patients (as the model might predict based on the amygdala hyperactivity in these patients), we observed *reduced* deceleration in the vmPFC lesion patients relative to the NC subjects. It should be noted, however, that the finding of similar group differences in cardiac deceleration in response to neutral pictures suggests a more general orienting deficit in the vmPFC group. Together, these findings indicate that the role of vmPFC in affective processing is not simply the regulation of negative emotion through inhibition of the amygdala. Rather, vmPFC appears to play a more multifaceted role that could include processes related to self-awareness and self-reflection (Koenigs and Grafman, 2009a; Qin and Northoff, 2011), and/or more direct modulation of emotion-related physiological responses and negative affect (Price and Amaral, 1981; Neafsey, 1990; Ongur and Price, 2000; Barbas et al., 2003; Ghashghaei et al., 2007).

Although we did not have any *a priori* hypothesis regarding lateralization, significant group differences in amygdala reactivity to aversive pictures were observed only in the right amygdala (**Figure 5**, **Table 3**). Previous meta-analyses offer some support for a functional dissociation of right and left amygdala in rapid, automatic stimulus processing and sustained stimulus evaluation, respectively (Wager et al., 2003; Baas et al., 2004; Costafreda et al., 2008). However, the laterality effects observed here may be due to the lesion characteristics of our vmPFC patient sample. Although all lesions involved significant bilateral damage to vmPFC, each patient had slightly greater damage on the right side (**Supplementary Table 7**). Future work in larger samples with more heterogeneous vmPFC lesions will be necessary to more conclusively determine the link between lateralization of vmPFC damage and amygdala hyperactivity.

Future studies could also expand the scope of the present findings by using more diverse stimuli and/or task paradigms. One possibility would be to use a fear extinction paradigm, to allow more direct comparisons with rodent data (Milad et al., 2006; Quirk and Beer, 2006). Moreover, previous studies indicate that the amygdala responds to positive valence and may be more sensitive to stimulus arousal than to valence, per se (Wager et al., 2003; Costafreda et al., 2008; Sabatinelli et al., 2009). To maximize our power to detect group differences in amygdala activation, we limited stimuli to aversive and neutral pictures and used a simple four-item valence rating scale. Future studies could include images with positive valence and more detailed ratings of valence and arousal in order to determine whether changes in amygdala activity following vmPFC damage are specific to negative affect or more broadly related to subjective arousal.

In conclusion, here we demonstrate a critical role for the vmPFC in regulating amygdala activity. Our findings provide unique evidence regarding the causal interactions among brain regions subserving emotion regulation in humans, and offer novel support for the inhibitory influence of vmPFC on amygdala, as proposed in neurocircuitry models of affective dysfunction in mental illness. The current results also raise a host of further questions. Namely, if vmPFC is in fact necessary for amygdala regulation in humans, as our results suggest, yet amygdala hyperactivity in individuals with vmPFC lesions is not accompanied by the cardinal signs of hyperactivity—increased peripheral autonomic activity and fearful/anxious behavior—then it follows that there should be other brain regions with which the vmPFC interacts that could explain the divergence of neural, physiological, and behavioral data in the present study. There are a number of viable candidate brain regions and psychological processes by which vmPFC damage could exert such effects. In the following two chapters, I describe two research studies that build on the present results, investigating the effects of vmPFC damage on anticipatory brain activity (**Chapter 7**) and resting brain perfusion (**Chapter 8**).

Chapter 7. Ventromedial prefrontal cortex lesions alter neural and physiological correlates of anticipation under uncertainty

The anticipatory processing of uncertain and potentially aversive future outcomes is one viable psychological process by which vmPFC activity could influence affective function. How one copes with the uncertainty that pervades daily life can have a substantial impact on one's psychological wellbeing. Indeed, excessive worry about potential future aversive events is a core feature of anxiety disorders (APA, 1994). As recent clinical studies have highlighted the central role that intolerance of uncertainty plays in anxiety disorders (Garfinkle and Behar, 2012; McEvoy and Mahoney, 2012; Grupe and Nitschke, 2013), studies in cognitive and affective neuroscience have begun to delineate the neural circuitry involved in the anticipation of uncertain future events. Research in healthy adult populations has revealed a network of brain regions that become active during the anticipation of unpredictable or uncertain outcomes, including insula, amygdala, ventromedial/orbital prefrontal cortex, and anterior cingulate cortex (Critchley et al., 2001; Dunsmoor et al., 2007; Sarinopoulos et al., 2010; Somerville et al., 2013). These same brain areas have been widely implicated in the pathogenesis of anxiety disorders (Lorberbaum et al., 2004; Rauch et al., 2006; Simmons et al., 2006; Etkin and Wager, 2007; Nitschke et al., 2009; Grupe and Nitschke, 2013). However, the mechanisms of interaction among these brain regions during anticipatory uncertainty remain unclear.

With respect to anticipatory affective processing, the ventromedial prefrontal cortex (vmPFC) is a key node in this network. Several previous neuroimaging studies in healthy

adult populations have observed vmPFC activation during the anticipation of aversive stimuli, including pain, affect-laden negative pictures, and risky choices (Ploghaus et al., 1999; Critchley et al., 2001; Nitschke et al., 2006), with the magnitude of vmPFC activity associated with self-reported anticipatory anxiety and negative affect (Kwan et al., 2000; Sawamoto et al., 2000). Patients with vmPFC damage reliably exhibit decision-making deficits in tasks involving uncertain or risky outcomes (Bechara et al., 1994; Fellows and Farah, 2003; Tsuchida et al., 2010), as well as diminished anticipatory arousal preceding risky, uncertain choices (Bechara et al., 1997; Bechara et al., 1999). Anatomical connectivity data provide additional support for this view; vmPFC shares reciprocal connections with subcortical, hypothalamic, and brainstem regions responsible for somatic components of emotion, as well as with cortical regions, such as lateral prefrontal and anterior cingulate cortex, that mediate cognitive and behavioral control (Neafsey, 1990; Ongur and Price, 2000; Barbas et al., 2003; Ghashghaei et al., 2007). Together, these previous findings suggest that vmPFC may play a pivotal role in coordinating neural and peripheral physiological responses to uncertainty during the anticipation of aversive stimuli.

To test this hypothesis, we employed fMRI and a measure of heart rate variability (HRV) in the same sample of four human neurosurgical patients with focal bilateral vmPFC damage, while they completed a task involving the cued anticipation of aversive and neutral picture stimuli. We predicted that vmPFC damage would significantly alter fMRI and HRV correlates of uncertainty.

Methods

Details about research participants, lesion tracing, and fMRI acquisition are presented in Chapter 6.

Event-related fMRI task

During the fMRI task, described in detail in the previous chapter (**Chapter 6**), subjects viewed 64 unique images drawn from the International Affective Picture System (IAPS) (Lang et al., 2008), divided evenly among pictures with aversive and neutral content (**Figure 3**). All images were preceded by one of three visual cues ("X", "O", or "?"). The "X" and "O" cues indicated that the subsequent image would be aversive or neutral, respectively, whereas the "?" cue provided no information regarding the emotional content of the image (equal likelihood of aversive or neutral content). Thus, aversive ("X") and neutral ("O") cues predicted certain outcomes, whereas ambiguous ("?") cues indicated uncertainty about the impending stimulus.

Heart rate data acquisition

Heart rate data were acquired at 100 Hz with GE's photoplethysmograph, affixed to the left index finger throughout the scan session. Heart rate data were available for n=10 NC subjects and all n=4 vmPFC lesion patients during the task and n=11 NC subjects and all n=4 vmPFC lesion patients during the resting scan.

fMRI task preprocessing and analysis.

Preprocessing of fMRI data was conducted as described in the previous chapter. Because the aim of the present study was to examine effects of vmPFC damage on anticipatory neural activity, preprocessed task data were concatenated and analyzed as previously described to separately model phasic and sustained components of anticipation (Grupe et al., 2013). Phasic activity was modeled using stick regressors at the onset of each cue and sustained activity was modeled using a duration-modulated boxcar regressor, beginning at cue offset and spanning the 2- to 8-second anticipatory ISI. All six cue regressors were included in a general linear model (GLM) with additional regressors for each picture type, a single regressor for the rating period, and several regressors of no interest, including six motion covariates from rigid-body alignment (Johnstone et al., 2006) and a fourth-order polynomial to model baseline and slow signal drift. Blood oxygen level-dependent (BOLD) signal was modeled by convolving each regressor with AFNI's default canonical hemodynamic response function (HRF; gamma function). To avoid potential confounds introduced by subject motion, volumes in which more than 10% of voxels were time series outliers were censored prior to conducting the GLM; there were no group differences in the average proportion of censored volumes (χ^2=2.09, *P*=0.15), or in mean framewise displacement (NC: 0.06±0.06mm, vmPFC: 0.04±0.02mm; W=28, *P*=0.44). Resulting whole-brain maps of voxelwise β-values for phasic responses to each cue were aligned to MNI space and resampled to $3mm^3$ isotropic resolution for second-level analyses.

To identify brain regions responsive to the manipulation of certainty during the cue period, we performed a voxel-wise linear mixed effects (LME) analysis on phasic cue β-

values from the first-level GLMs, using only the n=19 NC subjects (Chen et al., 2013). Cue identity ("?", "X", "O") was modeled as a within-subjects factor, with age (mean centered) and gender included as between-subjects covariates. General linear tests for the contrast of ambiguous ("?") versus certain ("X" + "O") cues were used to identify brain regions sensitive to uncertainty in the NC group.

To identify brain regions in which cue-related activity differed between groups, we conducted a second LME analysis including data from the four vmPFC lesion patients. This full LME model included cue ("?", "X", "O"), group (NC vs. vmPFC), and the group-by-cue interaction, as well as between-subjects covariates for age (mean centered) and gender. The group-by-cue interaction map was used to identify brain regions in which the magnitude of the phasic cue response differed between NC and vmPFC groups. All statistical maps were family-wise error (FWE) corrected for multiple comparisons across the whole brain at the cluster level ($P_{FWE}<0.05$), using a height threshold of $P<0.001$ (Forman et al., 1995; Carp, 2012). A corrected $P_{FWE}<0.05$ was achieved using a cluster extent threshold of 38 voxels (1026 mm^3), calculated using Monte Carlo simulations with 3dClustSim in AFNI.

To visualize the timecourse of BOLD responses to cues within significant clusters, we conducted a second GLM, replacing the canonical HRF with a series of nine TENT functions in order to deconvolve the raw BOLD signal. This model yielded β-values for each of 9 TRs from 0-16 seconds after cue onset. Because significant clusters were derived using the canonical HRF, estimated response data from the deconvolution model were used for display only.

Cerebral perfusion analysis

Quantitative CBF images from pcASL were preprocessed and aligned as described in the previous chapter. To rule out differences in baseline cerebral perfusion, we examined group differences in mean whole-brain CBF, as well as differences in scaled CBF for significant clusters from the group-by-cue interaction using non-parametric Mann-Whitney-Wilcoxon tests.

Heart rate variability analysis

To assess HRV, we analyzed cardiac plethysmography data to compute separate estimates of heart rate and variability for the resting and task scans. Individual cardiac R-spikes were identified using interactive beat detection software. Resulting interbeat interval (IBI) series were visually inspected for outliers, which were hand-corrected prior to analysis with CMETx software (Allen et al., 2007). CMETx-derived estimates of mean heart rate and heart rate variability (logHRV: the natural-log transformed variance of the unfiltered IBI series) were estimated for each scan. Task HRV estimates for each subject were calculated by averaging estimates across both task scans.

To ascertain whether individual differences in HRV were related to neural responses to the cue stimuli, we regressed task HRV estimates on percent signal change values extracted from clusters identified in the group-by-cue interaction LME analysis. The dependent variables were parameter estimates from the linear contrast of ambiguous vs. certain cues, which we conceptualized as an index of the modulation of neural activity by cue certainty. This analysis was intended to assess whether individual differences in the modulation of neural activity by cue certainty was related to overall HRV during the task.

Two separate linear regression models were conducted, one examining the strength of the relationship in the NC group alone, and a second examining the relationship across both the NC and vmPFC groups together. Group differences in both task and resting HRV were assessed using non-parametric Mann-Whitney-Wilcoxon tests, considered significant at $p < 0.05$.

Results

First, we determined whether the expectancy manipulation in our task (ambiguous versus certain cues) elicited the predicted pattern of neural activity in the NC subject group. Consistent with previous studies, our whole-brain analysis revealed greater bilateral insula activity for ambiguous relative to certain cues (**Figure 6, Table 4**). We also observed two clusters in bilateral lingual gyrus in which responses were greater for certain relative to ambiguous cues.

Next, we identified regions of the brain in which phasic cue responses differed between the NC and vmPFC groups (a significant group-by-cue interaction). This analysis revealed three significant clusters: bilateral insula and left dorsolateral prefrontal cortex (dlPFC) (**Figure 7, Table 5**). Importantly, the bilateral insula regions from the interaction analysis overlapped substantially with the uncertainty-sensitive bilateral insula clusters identified in the NC group (**Figure 8**), indicating that vmPFC damage significantly altered cue-related insula activity. Follow-up analyses revealed that group-by-cue interactions were driven largely by significant group differences in response to the certain aversive cues in the left insula (W=0, $P<0.001$), and by significant group differences in the right insula in response to both the certain aversive cues (W=7,

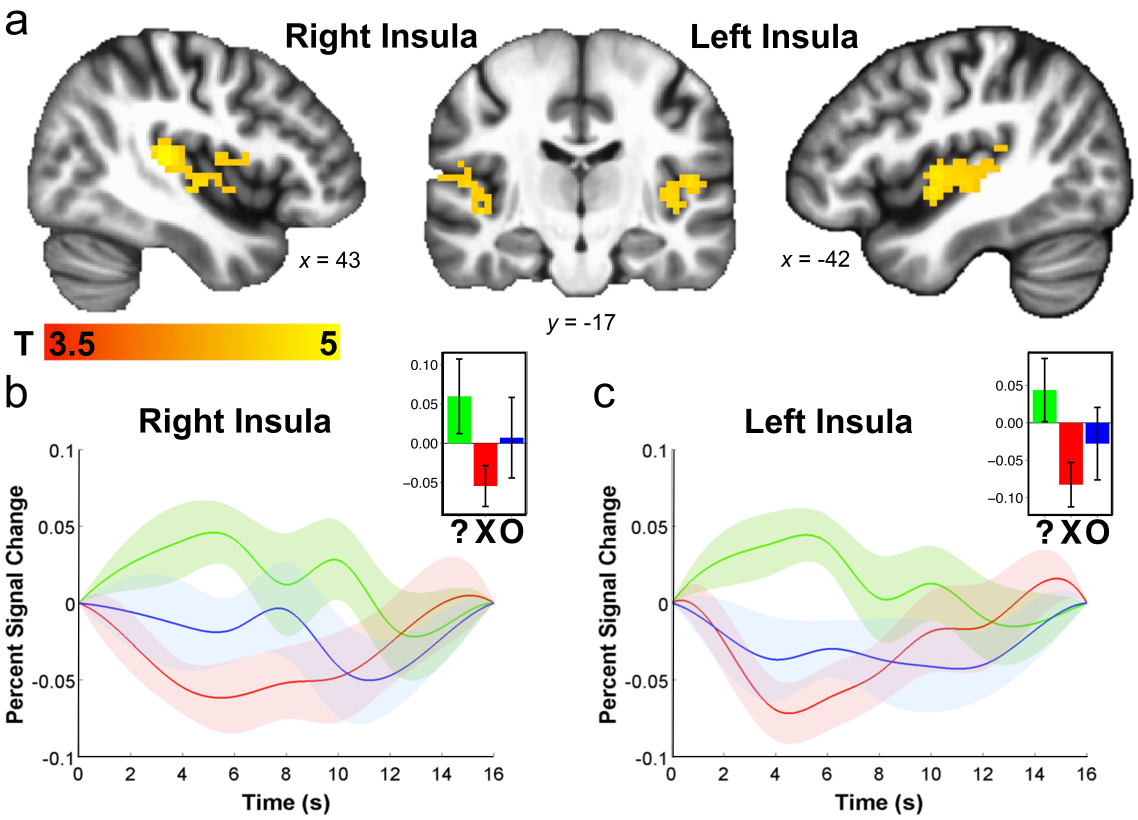

Figure 6. Brain regions with greater activation to ambiguous, relative to certain, cues in n=19 NC subjects. (a) Significant insula clusters from the ambiguous > certain contrast ($P_{FWE} < 0.05$). Slice coordinates (in mm) are presented in Montreal Neurological Institute (MNI) template space. **(b)** Mean timeseries of percent signal change (PSC) in response in response to ambiguous (?, green), certain aversive (X, red), and certain neutral (O, blue) cues within the right insula cluster (width of shaded area corresponds to ±1 SEM). **(c)** Mean timeseries of PSC in response to cues within the left insula cluster. Inset figures display the mean PSC response by cue (error bars indicate ±1 SEM). Dark horizontal bars on plots indicate cue duration (2 sec).

P=0.008) and ambiguous cues (W=64, *P*=0.035) (**Figure 7**). On average, the NC group showed greater activation to ambiguous cues, relative to certain-aversive and certain-neutral cues, in bilateral insula clusters, whereas vmPFC lesion patients exhibited the greatest difference between certain-aversive and certain-neutral cues. Activity in the dlPFC cluster followed a different pattern, with consistent deactivation in response to all three cues in the NC group but cue-dependent differences in activity in the vmPFC lesion group.

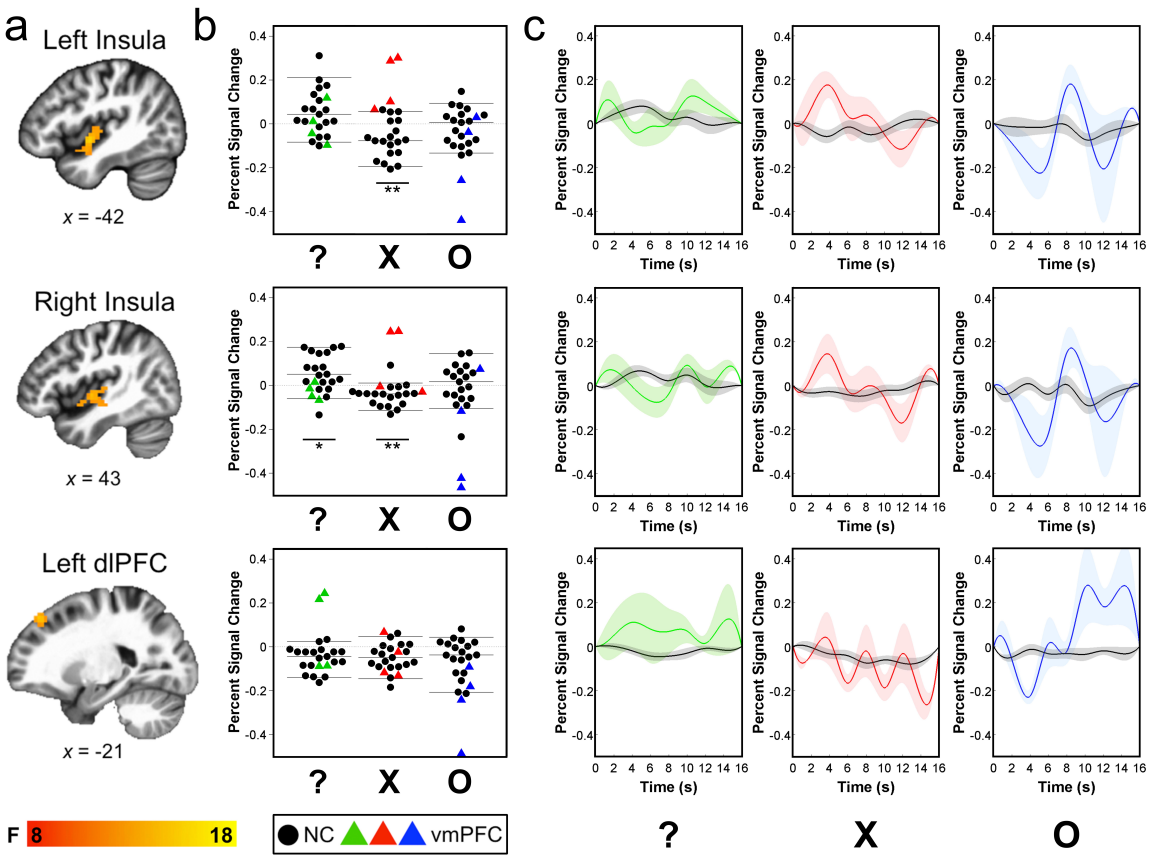

Figure 7. Brain regions showing significant group-by-cue interactions ($P_{FWE} < 0.05$). (a) Group differences in cue reactivity were observed in left insula (top row), right insula (middle row), and left dlPFC (bottom row). Slice coordinates (in mm) are presented in Montreal Neurological Institute (MNI) template space. **(b)** Scatterplots depict the distribution of individual PSC values for vmPFC lesion patients (green, red, and blue triangles) and NC subjects (black circles) in response to ambiguous (?), certain aversive (X), and certain neutral (O) cues within each cluster. Black horizontal lines on scatter plots represent the mean and 95% confidence intervals of PSC values in the NC group. **(c)** The mean timeseries in response to each cue type are displayed for vmPFC lesion patients (green, red, and blue ribbons) and NC subjects (gray ribbons). The width of the shaded ribbons in timeseries plots corresponds to ±1 SEM. $*P < 0.05$, $**P < 0.01$.

Table 4. Brain regions sensitive to uncertainty in NC group

		Cluster			Peak Voxel			
Contrast	**Structure**	**BA**	**Size**	P_{FWE}	**T**	**x**	**y**	**z**
Ambiguous > Certain	L Insula	13/41	290	< 0.001	5.56	-51	-20	6
	R Insula	13/41	205	< 0.001	5.56	48	-19	10
Certain > Ambiguous	R Cuneus	18	135	< 0.001	-5.74	20	-94	7
	L Cuneus	18	48	< 0.05	-4.68	-15	-99	8

Cluster size in number of voxels (3 x 3 x 3 mm^3). Corrected *P* thresholds indicate minimum FWE-corrected *P* value for each cluster. Peak voxel coordinates (mm) are presented in MNI space. BA, Brodmann area; FWE, familywise error; L, left; R, right.

Table 5. Significant clusters identified in the group-by-cue interaction analysis

	Cluster			Peak Voxel			
Structure	**BA**	**Size**	P_{FWE}	**F**	**x**	**y**	**z**
L Insula	13	86	< 0.001	13.73	-44	-5	-5
R Insula	13/41	79	< 0.001	13.26	46	-8	-2
L dlPFC	8/9	42	< 0.05	12.56	-21	38	46

Cluster size in number of voxels (3 x 3 x 3 mm^3). Corrected *P* thresholds indicate minimum FWE-corrected *P* value for each cluster. Peak voxel coordinates (mm) are presented in MNI space. BA, Brodmann area; dlPFC, dorsolateral prefrontal cortex; FWE, familywise error; L, left; R, right.

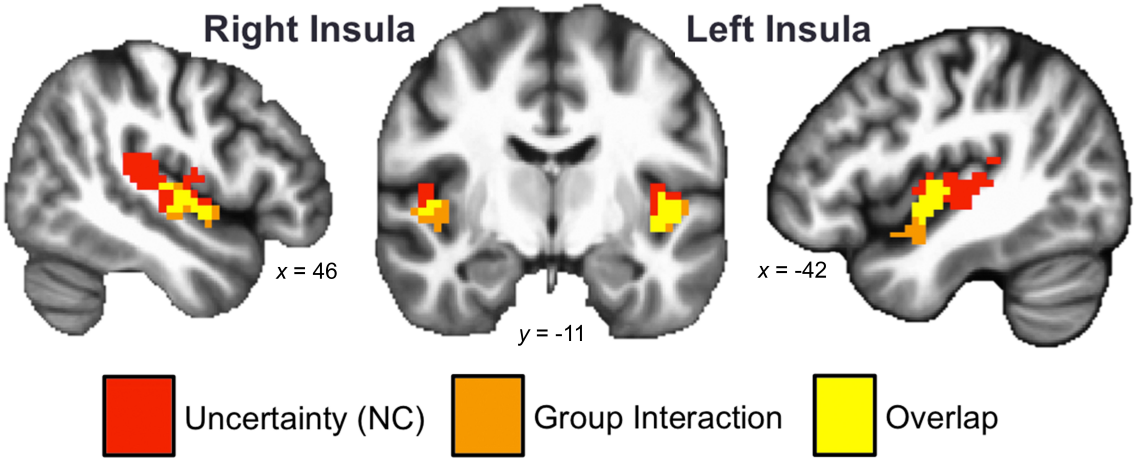

Figure 8. Conjunction analysis. Regions showing significant activity in the ambiguous > certain contrast in the NC group (red) and a significant group-by-cue interaction (orange). There is significant overlap in bilateral mid insula (yellow). All whole-brain maps are corrected for multiple comparisons at $P_{FWE} < 0.05$. Slice coordinates (in mm) are presented in Montreal Neurological Institute (MNI) template space.

To ensure that group differences in insula or dlPFC activity were not due to baseline differences in insula perfusion following vmPFC damage, we estimated cerebral blood flow (CBF) using pseudocontinuous arterial spin labeling (pcASL) prior to functional scans in all subjects. There were no significant differences between the NC and vmPFC groups in whole brain CBF (NC = 36.30 ± 8.73, vmPFC = 40.09 ± 13.65, W=31, *P*=0.611), nor were there differences in relative CBF for the left insula (NC = 1.42 ± 0.19, vmPFC = 1.35 ± 0.15, W=45, *P*=0.611) and left dlPFC clusters (NC = 0.99 ± 0.21, vmPFC = 0.98 ± 0.10, W=43, *P*=0.725), although the vmPFC group had significantly lower CBF in the right insula cluster (NC = 1.50 ± 0.21, vmPFC = 1.29 ± 0.12, W=63, *P*=0.044).

Finally, we investigated whether group differences in neural responses to cue stimuli were accompanied by differences in peripheral physiology. Consistent with a proposed role for vmPFC in the context-dependent modulation of peripheral physiological activity, the vmPFC lesion group had significantly lower HRV during the experimental task than the NC group (NC = 7.23 ± 0.66, vmPFC = 6.08 ± 0.71, W=36, *P*=0.024). However, a similar group difference in HRV was also present during the resting scan (NC = 7.42 ± 0.74, vmPFC = 6.14 ± 0.55, W=41, *P*=0.010), indicating a more general reduction in HRV in the vmPFC lesion group. There were no significant differences in mean heart rate between groups during either the resting or task scans (Resting: NC = 62.43 ± 10.37, vmPFC = 74.70 ± 14.49, W=10, *P*=0.138; Task: NC = 64.52 ± 9.16, vmPFC = 75.94 ± 12.03, W=11, *P*=0.240). To directly examine the relationship between neural responses to cues and HRV, we regressed HRV during the task on contrast estimates for ambiguous versus certain cues drawn from significant clusters identified in the group-by-cue

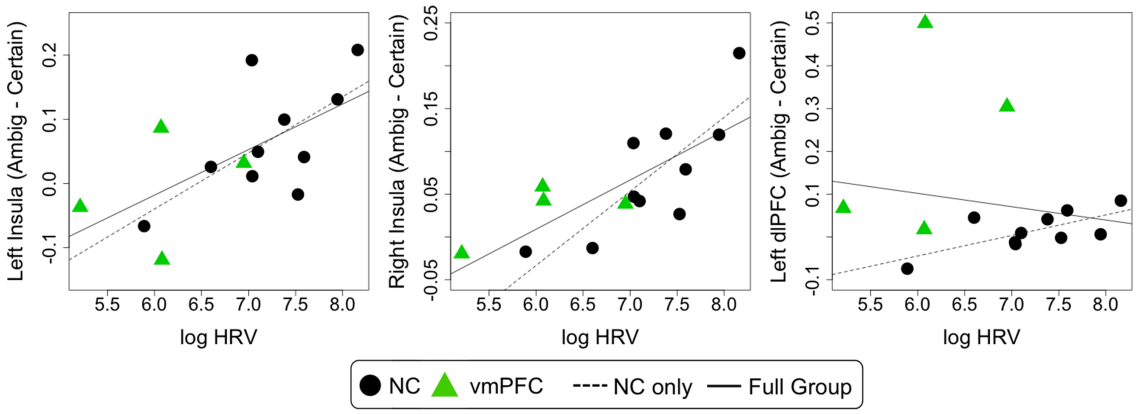

Figure 9. Relationship between uncertainty-related activity and HRV. Scatter plots depicting the relationship between task HRV and uncertainty-related activation (ambiguous – certain) in left insula (left), right insula (middle), and left dlPFC (right) clusters identified in the group-by-cue interaction. Green triangles represent vmPFC lesion patients and black circles represent NC subjects. Solid lines indicate the regression line across all subjects with HRV data (n=4 vmPFC lesion patients, n=10 NC subjects), whereas dotted lines indicate the regression line for the n=10 NC subjects. Ambig=ambiguous, dlPFC=dorsolateral prefrontal cortex.

interaction analysis. For both insula clusters, larger differences between ambiguous and certain cues were associated with greater HRV during the task (both within the NC group and across the entire sample), indicating that greater sensitivity to cue certainty in bilateral insula is accompanied by greater variability in physiological reactivity during the task (**Figure 9**) (left insula: $r_{NC\text{-}only}$=0.65, P=0.043, r_{FULL} =0.64, P=0.013; right insula: $r_{NC\text{-}only}$=0.80, P=0.005, r_{FULL} =0.75, P=0.002). On average, vmPFC lesion patients exhibited patterns of neural and physiological activity consistent with the prediction line derived in the NC group, with reduced modulation of insula activity by cue certainty and lower HRV. No such relationship was present for the left dlPFC cluster, although uncertainty-related activity in this region was significantly correlated with task HRV within the NC group (left dlPFC: $r_{NC\text{-}only}$=0.69, P=0.027, r_{FULL} =0.18, P=0.549).

Discussion

In this chapter, we report four main findings: (1) among NC subjects, ambiguous cues elicited stronger bilateral insula activity than certain cues, (2) vmPFC lesion patients exhibited an abnormal pattern of neural activity—particularly in bilateral insula—in response to the cues, (3) vmPFC damage was associated with attenuated HRV, and (4) across subjects, uncertainty related insula activity was related to individual differences in HRV. Here we discuss each of these main findings in turn.

First, with respect to the finding of greater bilateral insula activity for the ambiguous versus certain cue contrast in the NC subjects, we note that this result is broadly consistent with several previous fMRI studies of healthy adult subjects (Dunsmoor et al., 2007; Sarinopoulos et al., 2010; Somerville et al., 2013). Using virtually the same task, Sarinopoulos and colleagues found that bilateral insula responses to aversive pictures were larger following the ambiguous cue than the certain cue (Sarinopoulos et al., 2010). Our data show a similar bilateral insula finding in response to the cues themselves. Another study using neutral and aversive pictures, which were presented in conditions of either certain/predictable temporal sequence or uncertain/unpredictable temporal sequence, found greater anterior insula activity for the uncertain condition (Somerville et al., 2013). An analogous study of Pavlovian conditioning manipulated the certainty of the pairing of the conditioned (CS) with the unconditioned stimuli (UCS) (Dunsmoor et al., 2007). Greater bilateral insula activity was observed when the CS-UCS pairing was uncertain/unpredictable, as compared to when the pairing was certain/predictable. Hence, our findings bolster an emerging literature that implicates the insula in responding to the uncertain anticipation of aversive stimuli.

Next we consider the major novel finding from our study—the effect of vmPFC damage on cue-related neural activity. We observed a significant interaction between group and cue type within the same regions of mid-insular cortex that we found to be sensitive to uncertainty in the NC group, indicating that vmPFC lesions affect the processing of uncertainty in the insula. This finding supports theoretical accounts that highlight the role of vmPFC and insula in the anticipation of ambiguous, potentially aversive outcomes (Schoenbaum et al., 2009; Singer et al., 2009; Thayer et al., 2012; Grupe and Nitschke, 2013). Insula and vmPFC are themselves reciprocally interconnected and share overlapping projections to subcortical brain regions implicated in physiological and somatic components of an emotional response (Neafsey, 1990; Allen et al., 1991; Shi and Cassell, 1998; Barbas et al., 2003). With respect to the processing of risk and uncertainty, vmPFC is thought to be a critical neural substrate of context-dependent regulation of affect and behavior. This assertion is based on several sources of data: (1) vmPFC plays a key role in learned safety during fear extinction (Milad and Quirk, 2002; Phelps et al., 2004), (2) vmPFC is active during cognitive reappraisal of affective stimuli (Urry et al., 2006), (3) vmPFC encodes representations of expected future outcomes (Summerfield et al., 2006), and (4) vmPFC tracks relative value of competing choices (Hare et al., 2009; Schoenbaum et al., 2009; Fellows, 2011). The insular cortex has been associated with a wide range of functions, but is perhaps most commonly implicated in the encoding and representation of bodily sensations and subjective emotional "feeling" states (Craig, 2002; Singer et al., 2009). In relation to vmPFC, it has been proposed that insula stores representations (i.e., "somatic markers") of previous affective states for retrieval and interpretation by vmPFC (Damasio, 1994).

Lesions to both areas have been associated with abnormal patterns of decision-making under conditions of risk and uncertainty (Bechara et al., 1994; Fellows and Farah, 2003; Clark et al., 2008; Tsuchida et al., 2010). The present results offer novel support for a critical role of vmPFC in modulating the processing of uncertainty in the insular cortex.

Our heart rate data provide complementary evidence of the effect of vmPFC lesions on anticipatory processing. Variability in resting heart rate is crucial for maintaining homeostasis across variable environmental conditions, and primarily reflects central modulation of sympathetic and parasympathetic innervation to the heart (Jose and Collison, 1970). Thus, high levels of HRV are thought to reflect a greater capacity to adapt to evolving environmental demands (Thayer et al., 2012). Indeed, higher resting HRV is associated with the production of more context-appropriate behavioral and physiological responses and with greater emotion regulation ability (Appelhans and Luecken, 2006; Melzig et al., 2009; Thayer et al., 2012). Conversely, low HRV is associated with delayed recovery from psychological stressors, as well as an increased risk of depression, anxiety, and all-cause mortality (Gorman and Sloan, 2000; Weber et al., 2010). Importantly, vmPFC activity is consistently associated with heart rate changes during emotional and cognitive tasks (Lane et al., 2009; Thayer et al., 2012). Our HRV data provide unique lesion evidence for a causal role of vmPFC in controlling HRV; patients with vmPFC damage exhibited significantly lower HRV during both the resting scan and the experimental task. To our knowledge, this is the first study showing reduced HRV in patients with vmPFC lesions, although this finding is consistent with several previous reports demonstrating blunted physiological responses to aversive stimuli and their anticipation following vmPFC damage (Damasio et al., 1990; Bechara et al., 1997;

Bechara et al., 1999). Furthermore, the magnitude of uncertainty-related insula activation was associated with task HRV both within the NC group and across all subjects, indicating that increased sensitivity to cue certainty in the insula was related to overall HRV during the task.

Although our results conclusively demonstrate a critical role for vmPFC in modulating insula responses to uncertainty, it remains unclear exactly *how* vmPFC and insula interact during the anticipation of potentially aversive outcomes. Similarly, it remains unclear whether vmPFC lesions alter peripheral physiological responses through the loss of direct projections to brainstem and hypothalamic nuclei, or whether they do so by altering activity in other cortical regions, like the insula. One possibility is that vmPFC damage directly impairs the regulation of physiological responses, and consequently, alters somatic representations in the insular cortex. Our data appear to be consistent with this proposal. Patients with vmPFC damage exhibited lower HRV both at rest and during the experimental task. The generalizability of physiological dysfunction outside of the task suggests that vmPFC damage directly attenuates adaptive control of peripheral physiology, which is then differentially represented by the insula. However, it is also possible that vmPFC damage deprives insula of input regarding relevant contextual cues, which in turn leads to altered stimulus processing and downstream effects on physiology and behavior. It has been shown that insular cortex stimulation in human neurosurgical patients can elicit robust changes in heart rate and blood pressure (Oppenheimer et al., 1992), and that insular lesions can have profound effects on cardiac physiology (Cereda et al., 2002). Thus, it is feasible that the observed effects of vmPFC lesions on peripheral physiology could be mediated by deficient interactions between insula and vmPFC, even

at rest. Future work including patients with insular cortex lesions will be necessary to disentangle the unique contributions of each brain region to the observed neural, physiological, and behavioral responses to uncertainty. Additionally, studies employing more aversive stimuli, such as acute pain or shock, could help to determine the causality of neural activity on physiology and behavior at the single trial level. Further studies could also investigate the role of the dlPFC in processing uncertainty and anticipation; our unexpected finding of a group-by-cue interaction in left dlPFC suggests that this cortical area may interact with vmPFC and insula in this context. Lateral prefrontal cortex has previously been shown to be active during the anticipation of aversive stimuli (Nitschke et al., 2006; Aupperle et al., 2012), and given the dense reciprocal connections among dlPFC, vmPFC, and insula (Yeterian et al., 2012), and the putative involvement of dlPFC in goal maintenance, response selection, and attentional allocation (Miller and Cohen, 2001), dlPFC may be an important node of this circuit.

In sum, the findings of this study demonstrate a crucial role for vmPFC in coordinating neural and physiological responses to uncertainty during anticipation. Our results offer new insight into the functional interactions between vmPFC and insula, two key components of the brain circuitry underlying human affective function, and provide an alternative mechanism by which vmPFC damage could alter context-dependent emotion regulatory processes implicated in the pathogenesis of mood and anxiety disorders.

Chapter 8. Ventromedial prefrontal cortex damage alters resting blood flow to the bed nucleus of stria terminalis

In the previous two chapters, we have seen evidence that human vmPFC lesions are associated with increased amygdala activation to aversive stimuli, altered insula responses during uncertain anticipation, and blunted peripheral physiological indices of emotion. These findings elaborate on the leading neural circuitry model of vmPFC function in mood and anxiety disorders by showing that (1) although patients with vmPFC lesions exhibit increased amygdala activity in response to aversive stimuli (consistent with the top-down amygdala regulation model of vmPFC function), such changes are not accompanied by the predicted enhancement of physiological and behavioral responses to aversive stimuli, and (2) that altered uncertainty-related anticipatory activity in the insula following vmPFC lesions is more closely related to observed physiological indices of emotion regulation. These findings suggest that vmPFC may coordinate multiple neural processes (beyond amygdala inhibition) that are critical for the expression of negative affect in humans. In this chapter, we examine this hypothesis further by investigating the effect of human vmPFC lesions on resting cerebral blood flow in subcortical structures closely linked to the expression of peripheral indices of negative emotion, in particular, the bed nucleus of the stria terminalis (BNST).

The BNST and vmPFC are strongly interconnected (Avery et al., 2014), and previous human and animal work has linked BNST activity to anxiety-related behavior (Davis and Whalen, 2001; Walker et al., 2003; Kalin et al., 2005; Somerville et al., 2010; Somerville et al., 2013). Moreover, a previous neuroimaging study in non-human primates found that

bilateral orbitofrontal lesions (which included regions of vmPFC) were associated with reduced BNST metabolism and reduced anxious behavior in an intruder paradigm (Fox et al., 2010). Across the lesioned and non-lesioned monkeys, the level of BNST metabolism positively correlated with the degree of anxious behavior. These findings suggest that vmPFC/OFC may play a crucial role in generating or maintaining negative affect by promoting BNST activity.

To test this hypothesis in humans, we employ an MRI measure of resting cerebral blood flow in the sample of four neurosurgical patients with circumscribed bilateral vmPFC lesions. We predict that, consistent with the results of the non-human primate study (Fox et al., 2010), humans with bilateral vmPFC damage will exhibit reduced BNST perfusion, which will in turn correlate with self-report measures of negative affect and anxiety.

Methods

Details about research participants, lesion tracing, and MRI acquisition are presented in Chapter 6.

Cerebral perfusion analysis

Quantitative CBF images from pcASL were rigidly co-registered with a T_2*-weighted EPI volume from the task scan and normalized to MNI space. Normalized CBF volumes were scaled to whole-brain CBF (after masking out the lesion in vmPFC patients) and smoothed with a 6mm full-width at half-maximum (FWHM) Gaussian kernel. To test the main study hypothesis, we used regions-of-interest (ROIs) corresponding to the right and

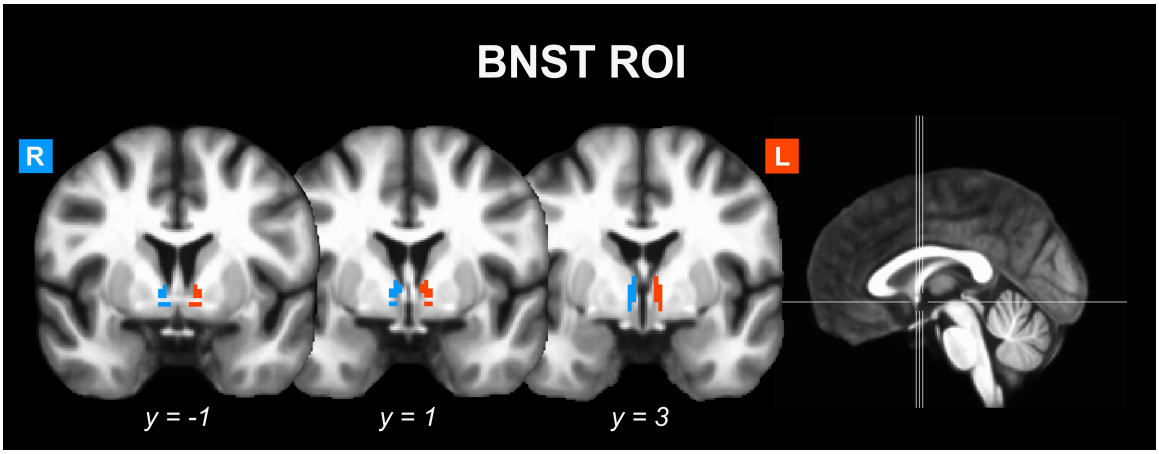

Figure 10. BNST Regions of Interest (ROIs). Right (blue) and left (orange) BNST ROIs used to examine group differences in perfusion.

left BNST (**Figure 10**). BNST ROIs were hand-drawn on the MNI template brain using neuroanatomical boundaries from the human brain atlas of Mai (Mai et al., 2003). To determine the specificity of between-group differences, we also examined group differences in mean unscaled whole-brain CBF, as well as differences in scaled CBF for additional subcortical ROIs that are known to be directly connected with vmPFC (amygdala, mediodorsal nucleus of the thalamus, hypothalamus, periaqueductal gray, and ventral striatum) as well as for several subcortical areas not densely or directly connected with vmPFC (lateral geniculate nucleus, caudate nucleus, putamen). Mediodorsal thalamus, hypothalamus, and lateral geniculate nucleus ROIs were generated using Talairach atlas labels from AFNI's built-in Talairach Daemon (Talairach and Tournoux, 1988). Striatal ROIs (ventral striatum, caudate nucleus, and putamen) were generated using spheres with a radius of 3.5 mm centered on coordinates corresponding to the inferior ventral striatum, dorsal caudate, and dorsal rostral putamen ROIs reported in a previous functional connectivity study (Di Martino et al., 2008), which was based on a

large-scale meta-analysis of striatal connectivity (Postuma and Dagher, 2006). The periaqueductal gray ROI was hand-drawn using MRIcron software (Rorden et al., 2007) on the group average anatomical volume in MNI template space, based on neuroanatomical boundaries from the human brain atlas of Mai (Mai et al., 2003). All between-group comparisons were assessed using non-parametric Mann-Whitney-Wilcoxon tests.

Rest state fMRI preprocessing and analysis

Rest-state fMRI data analysis was performed using AFNI (Cox, 1996) and FSL (http://www.fmirb.ox.ac.uk/fsl/). EPI volumes were slice time corrected using the first slice as a reference (sequential acquisition, Fourier interpolation), field map corrected (Jezzard and Clare, 1999), and motion corrected by rigid body alignment to the first EPI acquisition. Next, images were deobliqued and the first three volumes were omitted from the EPI time series. Data were then motion corrected (3dvolreg) and despiked to remove extreme time series outliers. Finally, the time series data were band-pass filtered ($0.01<f<0.1$) and spatially smoothed with a 4mm FWHM Gaussian kernel. Two NC subjects were excluded from the rest-state analysis (n=1 with excessive head motion (>2mm) (Power et al., 2012), n=1 due to errors in field map correction) for a total sample size of n=17 NC subjects. Functional connectivity was assessed using the hand-drawn anatomical ROIs in right and left BNST as seeds. Functional connectivity was computed using a GLM with the mean resting-state BOLD time series extracted from each subject-specific ROI and eight regressors of no interest, including six motion covariates, and average time series from white matter and ventricles. To further control for subject

motion, volumes in which more than 10% of voxels were time series outliers were censored in the GLM. Correlation coefficients were converted to z-scores via Fisher's r-to-z transform and corrected for degrees of freedom. Resulting z-score maps were aligned to MNI space and resampled to $3mm^3$ isotropic resolution for subsequent second-level analyses.

To specifically examine whether the BNST ROIs used in this study exhibited significant functional connectivity with vmPFC in the NC group, we conducted a whole brain voxel-wise one-sample t-test against zero using z-transformed BNST connectivity maps from each subject. Resulting statistical maps were FWE-corrected for multiple comparisons across the whole brain at the cluster level ($P_{FWE}<0.05$), using a height threshold of $P<0.001$ (Forman et al., 1995; Carp, 2012). A corrected $P_{FWE}<0.05$ was achieved using a cluster extent threshold of 37 voxels (999 mm^3), calculated using Monte Carlo simulations.

Relationship to anxiety measures

To investigate whether individual differences in anxiety were related to CBF in BNST, we regressed self-report measures of negative affect and anxiety on CBF values in BNST ROIs. Self-report scales were validated measures of trait anxiety (STAI-T) (Spielberger et al., 1983), depression (BDI) (Beck et al., 1996), and negative affect (PANAS-negative) (Watson et al., 1988). Two separate linear regression models were conducted for each measure, one examining the strength of the relationship in the NC group alone, and a second examining the relationship across both the NC and vmPFC groups together. Regression analyses were considered significant at $P<0.05$.

Results

In support of the main study hypothesis, the vmPFC lesion patients exhibited significantly lower perfusion in the right BNST, as compared to NC subjects (W=65, p=0.027). There was no significant difference between groups for the left BNST (W=50, p=0.37). Among the comparison ROIs, the groups differed in only one region—the right mediodorsal nucleus of the thalamus (W=72, p=0.003). This unpredicted result survives Bonferroni correction for the total number of comparison ROIs (α=0.05/13=0.004). Complete ASL results are presented in **Table 6**.

As a follow-up to the main study result (reduced right BNST metabolism in the vmPFC lesion group), we used rest-state fMRI to determine whether the BNST ROI used in this study is functionally connected with the vmPFC among the neurologically healthy subjects. As expected, the NC subjects exhibited significant rest-state functional connectivity between the right BNST and a 116-voxel cluster within the vmPFC (**Figure 11**). Importantly, the region of significant BNST functional connectivity was located in an area in which all four vmPFC patients had significant damage. The left BNST seed exhibited a similar pattern of resting state connectivity in the NC group, with two significant clusters of 45 and 91 voxels located within the vmPFC.

Contrary to the previous study of non-human primates with OFC lesions, there were no significant relationships between any of the three self-reported measures of negative affect (BDI, STAI, and PANAS) and right or left BNST CBF, both within the NC group and across the full sample (all *P*'s>0.10).

Table 6. ASL cerebral perfusion data

ROI	NC mean	NC s.d.	vmPFC mean	vmPFC s.d.	W	*P*
Whole Brain	36.30	8.73	40.09	13.65	31	0.611
BNST						
L BNST	1.07	0.14	1.00	0.16	50	0.366
R BNST	*1.03*	*0.16*	*0.83*	*0.07*	*65*	*0.027*
vmPFC network						
L amygdala	1.11	0.15	1.23	0.11	20	0.162
R amygdala	1.1	0.15	1.01	0.19	46	0.557
L ventral striatum	1.43	0.21	1.31	0.13	51	0.324
R ventral striatum	1.36	0.23	1.14	0.07	58	0.116
L MD thalamus	1.28	0.09	1.23	0.05	51	0.324
R MD thalamus	*1.32*	*0.10*	*1.11*	*0.10*	*72*	*0.003*
L hypothalamus	1.08	0.16	1.01	0.09	46	0.557
R hypothalamus	1.07	0.18	0.91	0.04	61	0.067
Periaqueductal gray	0.94	0.12	0.96	0.11	33	0.725
Non-vmPFC network						
L caudate	1.24	0.21	1.17	0.23	45	0.611
R caudate	1.29	0.22	1.18	0.14	52	0.286
L putamen	1.26	0.23	1.26	0.17	36	0.907
R putamen	1.32	0.23	1.27	0.18	42	0.785
L LGN thalamus	1.04	0.17	1.08	0.08	28	0.456
R LGN thalamus	1.14	0.22	1.03	0.09	50	0.366

Significant group differences are in italics. L, left; R, right; BNST, bed nucleus of stria terminalis; LGN, lateral geniculate nucleus; MD, mediodorsal.

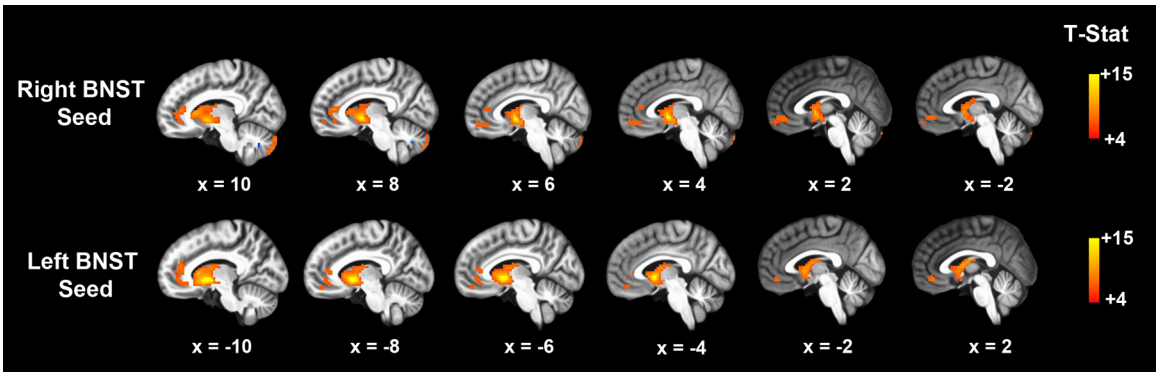

Figure 11. Rest-state functional connectivity for the right and left BNST ROI in n=17 NC subjects. Significant functional connectivity was observed between the right BNST and a region of vmPFC in which all four vmPFC patients had damage (top row). A similar pattern of functional connectivity with the vmPFC was found for the left BNST ROI (bottom row). Coordinates presented (in mm) in MNI template space, thresholded at $P_{FWE}<0.05$.

Discussion

In this chapter, we demonstrate a significant and rather selective reduction in right BNST perfusion in patients with bilateral vmPFC lesions. This finding squarely supports our main hypothesis, which was based on a previous PET study showing reduced BNST metabolism in primates with bilateral OFC lesions (Fox et al., 2010). This study is the first to use functional imaging in human lesion patients to show an effect of vmPFC damage on resting cerebral perfusion, thereby providing unique and novel data on the causal relationship between vmPFC and BNST. More specifically, these data suggest that vmPFC normally serves to promote BNST activity, which in turn could enhance behavioral and physiological components of negative emotion (Davis and Shi, 1999; Walker et al., 2003). This vmPFC-BNST interaction could explain in part why vmPFC damage in humans has been associated with blunted affect (Barrash et al., 2000), diminished physiological arousal to emotionally evocative stimuli (Damasio et al., 1990), and a reduced likelihood of developing PTSD and depression (Koenigs et al., 2008a; Koenigs et al., 2008b). A putative interaction between vmPFC and BNST is supported by our functional connectivity analysis (**Figure 11**) as well as by previous human neuroimaging data documenting robust functional and structural connections between the two regions (Avery et al., 2014). This vmPFC-BNST interaction could thus constitute an important addition to neural circuitry models of mood and anxiety disorders, which have predominantly focused on the role of vmPFC in inhibiting amygdala activity (Quirk and Gehlert, 2003; Milad et al., 2006; Rauch et al., 2006).

The model of vmPFC-BNST interaction proposed above is based largely on previous research linking BNST activity to the expression of trait-like anxiety (Davis and Whalen,

2001; Walker et al., 2003; Kalin et al., 2005). Unlike the amygdala, which has been implicated in rapid, time-limited fear responses consistent with orienting towards potentially threatening stimuli, BNST is thought to be involved in generating and maintaining responses consistent with sustained anxiety (Walker et al., 2003). Although direct axonal connections between vmPFC and BNST have not been well characterized in primates, high-resolution tracing studies in rodents have identified robust direct projections from rodent infralimbic cortex—the putative homologue of human vmPFC—to BNST (McDonald et al., 1999), in addition to well-documented indirect connections through other limbic regions like the amygdala, insula, and mediodorsal thalamic nucleus (McDonald et al., 1999; Dong et al., 2001a; Dong et al., 2001b). Each of these areas in turn project to brainstem and hypothalamic nuclei involved in coordinating peripheral aspects of an emotional response (Heimer et al., 1997; Tye et al., 2011; Jennings et al., 2013; Kim et al., 2013). Together, these regions form a network well-suited for the modulation and expression of behavioral and physiological components of emotion.

Unlike the previous lesion study in non-human primates (Fox et al., 2010), we did not observe a significant relationship between BNST perfusion and measures of anxiety. There are several plausible explanations for this null finding. One is that the ASL perfusion measure employed here may be too coarse of an index of BNST activity to correlate with specific aspects of emotional experience. Recent evidence indicates that BNST consists of distinct subregions with divergent roles in emotional expression. A study using optogenetics to activate and deactivate discrete subpopulations of BNST neurons found that focal stimulation of adjacent BNST subregions elicited opposing anxiolytic and anxiogenic effects (Jennings et al., 2013; Kim et al., 2013). Thus, the lack

of an association between BNST perfusion and anxiety in the present may study reflect the conflicting effects of changes in blood flow on anatomically distinct and functionally antagonistic regions of BNST. Secondly, given that previous associations between BNST metabolism and anxiety phenotypes were observed using PET scanning under conditions designed to elicit anxious responses (Kalin et al., 2005; Fox et al., 2010), our approach of simply examining resting blood flow inside the MRI environment (with no anxiety-inducing stimulus) may be insufficient to observe the expected relationships between BNST function and anxious behavior. Finally, there was a narrow range of self-reported negative affect in our healthy adult comparison sample. All subjects were well within the subclinical range (Spielberger et al., 1983; Watson et al., 1988; Beck et al., 1996), which may have limited our ability to detect a correlation between BNST perfusion and self-reported anxiety. Future work in larger samples using more robust emotion induction paradigms and a broader range of anxiety levels will be necessary to more fully elucidate the relationship between BNST activity and psychopathology.

Several additional findings from this study warrant further consideration. One is the unpredicted effect of vmPFC damage on mediodorsal thalamus perfusion. Among all comparison ROIs, only the right mediodorsal thalamus exhibited a significant group difference. This finding can likely be explained by the fact that the mediodorsal nucleus is the region of thalamus that is the most densely interconnected with vmPFC (Ongur and Price, 2000). However, it is important to note that not all regions that are densely interconnected with vmPFC exhibited reductions in perfusion; no significant group differences were observed in either hemisphere for amygdala, ventral striatum, hypothalamus, or periaqueductal gray. This pattern of results suggests that vmPFC may

play an especially critical role in modulating the activity of BNST and mediodorsal thalamus. Alternatively, the null effects in other brain regions could be due the small sample of vmPFC lesion patients, though the primate PET study also found no significant effect of OFC damage on amygdala metabolism (Fox et al., 2010). Another noteworthy finding is that the significant reductions in BNST and mediodorsal thalamus perfusion were observed only in the right hemisphere. These lateralized effects may be due to the lesion characteristics of our vmPFC patient sample. Although all patients' lesions involved significant bilateral damage to vmPFC, each patient had slightly greater damage on the right side (**Supplementary Table 7**). Future work in larger patient samples with more heterogeneous vmPFC lesions could more conclusively determine the link between lateralization of vmPFC damage and BNST perfusion.

One limitation of the present study is the single functional imaging measure (ASL) used to index BNST activity. Because resting cerebral blood flow is tightly coupled to cerebral metabolism (Fox and Raichle, 1986), ASL can be interpreted as a proxy measure of cerebral metabolism—and hence underlying neural activity—similar to PET (Xu et al., 2010; Okonkwo et al., 2012). However, the ASL data in this study only reflect resting state activity. Future fMRI studies could build upon the present results by determining whether vmPFC damage also diminishes stimulus-evoked BNST activity in anxiogenic tasks (Alvarez et al., 2011; Grupe et al., 2013; Somerville et al., 2013).

In sum, through a unique application of ASL cerebral perfusion imaging in patients with bilateral vmPFC lesions, we have demonstrated a critical role of vmPFC in promoting BNST activity. This finding corroborates non-human primate data and yields novel insight on the brain circuitry underlying human affective function. Together with

the results from the previous two chapters, this result highlights the critical importance of reciprocal interactions between vmPFC and subcortical brain regions like the amygdala and BNST, as well as cortical regions, like the insula, in driving behavioral and physiological components of an emotional response. These insights have direct implications for a range of neuropsychiatric disorders characterized by affective dysfunction, as we will see in the next chapter.

Chapter 9. Reduced prefrontal connectivity in psychopathic prison inmates

The results described in the previous three chapters offer compelling support for a view of vmPFC function in affective psychopathology that depends critically on complex reciprocal interactions among brain regions implicated in emotional processing. This assertion has important implications for disorders across a broad spectrum of affective dysfunction. Most notably, given previous findings of reduced structural and functional connectivity between amygdala and vmPFC in depression and anxiety (interpreted as neurobiological evidence for a failure of top-down regulation of amygdala by vmPFC), the more inclusive model suggests that disorders at the opposite end of the spectrum of affective dysfunction (e.g., blunted affect, social disinhibition) could exhibit the same gross patterns of neuroanatomical dysfunction, yet present with a divergent pattern of behavior. Psychopathy is an ideal neuropsychiatric disorder in which to test this hypothesis.

Typified by callous and impulsive antisocial behavior, psychopathy is present in roughly a quarter of adult prison inmates, and is associated with a disproportionately high incidence of violent crime and recidivism (Hare, 2003). Perhaps the most compelling support for a central role of vmPFC dysfunction in psychopathy has emerged from the study of neurological patients with focal vmPFC lesions. For decades, neurologists have noted that the personality changes accompanying vmPFC damage (e.g., blunted affect, social disinhibition, lack of empathy, irresponsibility, and poor decision-making) bear striking resemblance to hallmark psychopathic personality traits. Indeed, the personality changes associated with vmPFC damage have been dubbed “pseudopsychopathy”

(Blumer and Benson, 1975) and "acquired sociopathy" (Eslinger and Damasio, 1985). Early research in psychopathic prison inmates revealed blunted SCRs during the anticipation of punishment (suggesting an anticipatory arousal deficit), consistent with what would later be observed in human vmPFC lesion patients (Hare, 1965; Hare et al., 1978; Tharp, 1980). More recently, it has been shown that psychopaths perform remarkably similar to vmPFC lesion patients on measures of social economic choice (Koenigs et al., 2010) and moral judgment (Koenigs et al., 2012). Taken together, these data suggest that vmPFC dysfunction may be a critical neurobiological substrate underlying psychopathy.

In this chapter, we employ two complementary neuroimaging methods to quantify the structural and functional connectivity of vmPFC in psychopathic and non-psychopathic prison inmates. Using diffusion tensor imaging (DTI), we test the hypothesis that psychopathy is associated with reduced structural integrity of the uncinate fasciculus (UF), the primary white matter pathway connecting vmPFC with anterior temporal lobe structures, including the amygdala. Using functional magnetic resonance imaging (fMRI), we test the hypothesis that psychopathy is associated with lower levels of correlated activity between vmPFC and amygdala at rest.

Methods

Participants

Participants were adult male inmates recruited from a medium-security Wisconsin correctional institution. Inmates were eligible if they met the following criteria: under 45 years of age, IQ greater than 70, no history of psychosis or bipolar disorder, and not

currently taking psychotropic medications. Informed consent was obtained both orally and in writing.

The Psychopathy Checklist-Revised (PCL-R) (Hare, 2003) was used to assess psychopathy. The PCL-R assessment involves a 60-90 minute interview and file review to obtain information used to rate 20 psychopathy-related items as 0, 1, or 2, depending on the degree to which each trait characterizes the individual. A substantial literature supports the reliability and validity of PCL-R assessments with incarcerated offenders (Hare, 2003). To evaluate interrater reliability, a second rater who was present during interviews provided independent PCL-R ratings for 8 inmates. The intraclass correlation coefficient was 0.85. PCL-R Factor 1 and 2 scores were computed following procedures outlined in the PCL-R manual (Hare, 2003).

Participant Groups

Participants were classified as psychopathic if their PCL-R scores were 30 or greater and non-psychopathic if their PCL-R scores were 20 or less (Hare, 2003). (The use of these cut scores affords clear distinction between high and low levels of psychopathy, but precludes the correlation of imaging data with PCL-R factor or facet scores, which would require a more continuous range of PCL-R scores.)

MRI Data Collection

All MR imaging data were acquired using the Mind Research Network's mobile Siemens 1.5 T Avanto Mobile MRI System with advanced SQ gradients (max slew rate 200T/m/s, 346 T/m/s vector summation, rise time 200 μs) equipped with a 12-element

head coil. Head motion was limited using padding and restraint. All prisoners were scanned on correctional facility grounds.

DTI preprocessing and analysis

A total of 27 inmates (n=14 psychopaths and n=13 non-psychopaths) meeting the inclusion criteria participated in the DTI study (**Table 7**).

Diffusion weighted echo-planar magnetic resonance images were acquired by applying diffusion sensitizing gradients along 30 non-collinear directions (b-value = 800 s/mm^2). Five interleaved non-diffusion-weighted (b-value = 0 s/mm^2) volumes were collected during each run to enable corrections for motion and eddy current distortions. Images were collected with the following parameters: repetition time (TR) = 9,200 ms, echo time (TE) = 84 ms, Field of View (FOV) = 256 mm x 256 mm, matrix size = 128 x 128, slice thickness = 2 mm, no gap, voxel size = 2 mm x 2 mm x 2 mm, 70 slices. The sequence was repeated twice and the data combined to improve SNR.

Data processing was conducted using the FSL (http://www.fmrib.ox.ac.uk/fsl/) and CAMINO (Cook et al., 2006) software packages. Eddy current distortions and head movements were corrected by affine registration of all images to the first non-diffusion-weighted volume (FSL). Non-brain tissue was removed using the brain extraction toolbox (BET) in FSL (Smith, 2002) and the resulting brain masks were carefully inspected before performing non-linear diffusion tensor estimation using CAMINO (Jones and Basser, 2004; Alexander and Barker, 2005). Diffusion tensor images for each subject were screened for extreme outlier voxels and resampled to 1.75 mm x 1.75 mm x 2.5 mm resolution. Fractional anisotropy (FA), a scalar measure of

Table 7. Participant group characteristics: Psychopathy Study

	DTI Study			Rest-fMRI Study		
Variable	Non-psychopaths (n=13)	Psychopaths (n=14)	p	Non-psychopaths (n=20)	Psychopaths (n=20)	p
Demographic						
Age	31.7 (7.9)	32.9 (6.9)	0.69	31.1 (7.5)	32.6 (6.8)	0.53
Race (Cauc/Afr Am)	12/1	10/4	0.33	18/2	15/5	0.41
Neuropsychological						
IQ[a]	102.3 (12.5)	97.9 (11.1)	0.36	101.4 (12.6)	99.6 (10.2)	0.63
Digit Span Back	7.1 (2.6)	6.4 (3.3)	0.57	6.9 (2.2)	6.7 (3.4)	0.84
Anxiety/Neg Affect[b]	13.5 (10.7)	13.2 (7.2)	0.93	11.2 (9.5)	13.4 (8.3)	0.44
Psychopathy						
PCL-R total	14.6 (2.7)	32.2 (1.8)	<0.001	14.2 (3.4)	31.9 (1.7)	<0.001
Factor 1	5.3 (1.9)	12.1 (1.7)	<0.001	4.7 (2.1)	11.8 (1.8)	<0.001
Factor 2	7.5 (3.0)	17.4 (1.4)	<0.001	7.9 (3.1)	17.2 (1.5)	<0.001
Substance Abuse[c]						
Alcohol						
Prevalence	5/10	7/11	0.67	9/16	11/16	0.72
Age of onset	21.0 (5.2)	17.7 (2.2)		22.4 (6.5)	19.0 (3.4)	
Cannabis						
Prevalence	4/10	7/11	0.39	7/16	11/16	0.29
Age of onset	19.8 (4.7)	19.7 (8.6)		17.9 (4.7)	19.3 (6.8)	
Cocaine						
Prevalence	2/10	3/11	0.99	3/16	6/16	0.43
Age of onset	17,18	16,16,26		19.7 (2.9)	20.2 (5.4)	
Stimulants						
Prevalence	1/10	2/11	0.99	2/16	4/16	0.65
Age of onset	30	20,23		16,18	15,20,23,30	
Opioids						
Prevalence	2/10	2/11	0.99	3/16	6/16	0.43
Age of onset	15,35	16,20		20.7 (5.1)	21.7 (7.3)	
Sedatives						
Prevalence	0/10	1/11	0.99	1/16	2/16	0.99
Age of onset	n/a	20		27	20/22	
Hallucinogens						
Prevalence	0/10	3/11	0.21	1/16	4/16	0.33
Age of onset	n/a	15,20,21		20	15,17,20,21	

[a]based on Shipley Institute of Living Scale (Zachary, 1986), [b]based on Welsh Anxiety Scale, [c]based on diagnosis of abuse or dependence in the Structured Clinical Interview for DSM-IV Disorders (SCID) (First, 2002), which was administered to 10/13 non-psychopaths and 11/14 psychopaths in the DTI study and 16/20 non-psychopaths and 16/20 psychopaths in the rest-fMRI study. P-values for race distribution and substance abuse prevalence were computed with Fisher's Exact Test. All other p-values are based on t-tests (means presented followed by standard deviations in parentheses). P-values were not calculated for substance abuse age of onset due to relatively small sample sizes of abusers for most substances.

fiber coherence and microstructural white matter integrity, was calculated from the diffusion tensors at each brain voxel.

FA maps for each subject were non-linearly registered to the standard MNI152 white matter template and resampled to 1 mm^3 resolution (Andersson et al., 2007). Aligned images were averaged into a group mean FA image, which was thinned to create a study-specific white matter skeleton mask. This mask was projected onto each subject's native space FA image and whole brain estimates were acquired by extracting the mean FA value across the white matter skeleton. Group differences were examined in the Uncinate Fasciculus (UF), the primary structural connection between the amygdala and ventromedial prefrontal cortex (vmPFC), and in comparison tracts with documented frontal and temporal connectivity, in which no group differences were expected (Inferior Longitudinal Fasciculus/Inferior Fronto-Occipital Fasciculus, ILF/IFOF; Superior Longitudinal Fasciculus, SLF; Superior Fronto-Occipital Fasciculus, SFOF). Individual FA estimates for each ROI were acquired by projecting the John's Hopkins University (JHU) white matter atlas onto each subject's native space FA image and computing the mean value across the tract labels of interest (Mori et al., 2005). FA values for each ROI were scaled to whole-brain FA and entered into two-sample t-tests to assess group differences between psychopaths and non-psychopaths. All DTI analyses were considered significant at $p<0.05$.

To confirm the anatomical validity of UF regions of interest (ROIs) used in the between-groups analysis, UF tracts were verified in every subject using tractography. Briefly, fiber tracking was performed from every voxel in the brain ("brute force" method) using the tensor deflection (TEND) algorithm in CAMINO (Lazar et al., 2003).

Individual UF tracts were isolated by filtering tractography results to include only those tracts that passed through the UF ROI defined by the JHU atlas (**Figure 12a**). Tracts acquired in this way were compared to tracts derived using the manual two-ROI approach, a technique shown to reliably identify tracts with the characteristic "C" shape of UF fibers (Wakana et al., 2007; Hua et al., 2008). Fiber trajectories for each subject were confirmed using known neuroanatomical landmarks and white matter atlases to verify that the ROIs sampled from white matter regions containing predominantly UF fibers. All tractography data were processed and analyzed using TrackVis software (Wang et al., 2007).

Rest state fMRI preprocessing and analysis

A total of 40 inmates (n=20 psychopaths and n=20 non-psychopaths) meeting the inclusion criteria participated in the rest-fMRI study (**Table 7**). Twenty-six inmates had both DTI and rest-fMRI data.

Resting state functional images were collected while subjects lay still and awake, passively viewing a fixation cross. T2*-weighted gradient-echo echoplanar functional images (EPIs) were acquired with the following parameters: TR= 2000 ms, TE = 39 ms, flip angle = 75 °, FOV = 24 x 24 cm, matrix = 64 x 64, slice thickness = 4 mm, gap = 1 mm, voxel size = 3.75 mm x 3.75 mm x 5 mm, 27 sequential axial oblique slices. Resting-state scans lasted 5.5 minutes (158 volumes). A high-resolution T1-weighted structural image was acquired using a four-echo MPRAGE sequence (TR = 2530; TE = 1.64, 3.5, 5.36, 7.22 ms; flip angle = 7°, FOV = 256 x 256 mm, matrix = 128 x 128, slice thickness = 1.33 mm, no gap, voxel size = 1 mm x 1 mm x 1.33 mm, 128 interleaved

sagittal slices). All four echos were averaged into a single high-resolution image, which was used to aid in the spatial normalization of EPI volumes and visualization of group statistics.

All fMRI data analysis was performed using AFNI (Cox, 1996) and FSL (http://www.fmrib.ox.ac.uk/fsl/). EPI volumes were slice time corrected using the first slice as a reference (sequential acquisition, fourier interpolation) and motion corrected by rigid body alignment to the first EPI acquisition. Any subject with motion greater than 4 mm in any direction was excluded from further analysis. The first 3 volumes were omitted from the EPI time series and the data were despiked to remove extreme time series outliers. Time series data were bandpass filtered ($0.009 < f < 0.08$) before spatially smoothing with a 4-mm full width at half maximum (FWHM) Gaussian kernel. EPI time series data and high-resolution T1 images were normalized to the Talairach coordinate system (Talairach and Tournoux, 1988) using a 12-parameter linear warp and the EPI data were resampled to 3 mm cubic voxels for subsequent functional connectivity analyses. Normalized T1 anatomical images were segmented into gray matter, white matter, and cerebrospinal fluid (CSF) segments using FAST in FSL (Zhang et al., 2001). White matter and CSF segments were used as masks to extract a representative time series from each tissue type.

To investigate differences in vmPFC connectivity between psychopaths and non-psychopaths, we examined two functional networks with documented vmPFC involvement. To test the hypothesis that psychopathy is associated with reduced vmPFC-amygdala connectivity, we seeded the right and left amygdala in each subject. Amygdala ROIs were manually traced on the Talairaich-aligned group average T1 anatomical image

(Nacewicz et al., 2006) and subsequently edited by cycling through each subject's T1 image, excluding voxels in which the group mask overlapped with adjacent, non-amygdalar, tissue (**Figure 13a**). The final exclusionary mask contained only voxels overlying the amygdala in all subjects.

Functional connectivity was assessed by computing whole brain correlations with the mean time series derived from each of the seed ROIs. The mean time series was included in a GLM with eight regressors of no interest, including six motion parameters (3 translations, 3 rotations) obtained from the rigid body alignment of EPI volumes, the ventricular time series acquired by averaging across the CSF mask, the white matter time series acquired by averaging across the white matter mask, and a second order polynomial to model baseline signal and slow drift. Voxelwise correlation coefficients for each ROI were converted to z scores via Fisher's r to z transform and the resulting z-score maps were entered into second level statistical analyses.

To investigate differences in functional connectivity between psychopathic and non-psychopathic prisoners, we performed unpaired two-sample t-tests on the z-score maps derived from each seed region of interest. Based on our *a priori* interest in connectivity with the vmPFC, we restricted group comparisons to a region encompassing the medial surface of the PFC bilaterally, ventral to the genu of the corpus callosum (z=-6.5; **Figure 13a**). The vmPFC ROI was created using the WFU pickatlas (Maldjian et al., 2003) and subsequently edited in AFNI to exclude regions dorsal to the genu. Group difference maps were corrected for multiple comparisons using cluster-extent thresholding at an uncorrected $p<0.005$, $\alpha=0.05$ (cluster size=14 voxels, 378 mm^3). Cluster extents were computed using Monte Carlo simulations implemented in the 3dClustSim program

(AFNI). Group correlation maps were overlaid on the normalized mean anatomical image. All coordinates are reported in Talairach space.

To assess whether group differences were specific to vmPFC, we examined connectivity in two additional regions per seed in which we expected no group differences in functional connectivity. For the right amygdala seed, we investigated connectivity with the anterior superior temporal gyrus (aSTG) and contralateral amygdala, regions with documented right amygdala connectivity (Roy et al., 2009). Connectivity with the aSTG was assessed by placing a sphere of 6-mm radius at coordinates reported by Roy et al. (aSTG: 34, -10, -26). Connectivity with the left amygdala was assessed using the hand-drawn amygdala ROI from the previous connectivity analysis. Group differences were considered significant at a corrected $p<0.05$ (uncorrected $p<0.005$, cluster size=14 voxels, 378 mm^3).

Results

Structural connectivity: DTI results

Fractional anisotropy (FA) is a scalar measure that is sensitive to the microstructural integrity and fiber coherence of white matter tracts (Pierpaoli and Basser, 1996). Here, we used FA to probe differences in white matter structural connectivity between psychopathic and non-psychopathic prisoners. Before examining FA values in the UF, we first computed a measure of whole-brain FA for each subject as the average FA value across all major white matter tracts. Overall, psychopaths had significantly lower whole-brain FA than non-psychopaths ($t=-3.5$, $p=0.002$). Therefore, in subsequent analyses of specific tracts, we computed a scaled FA value, equal to the FA value in the specific tract

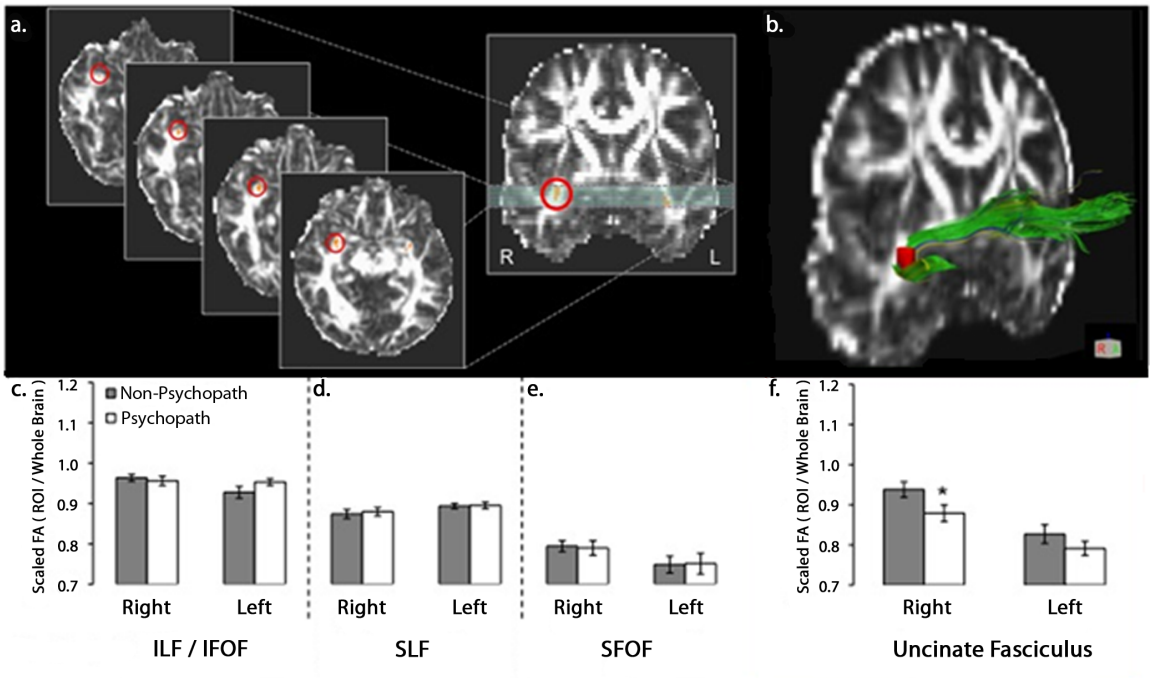

Figure 12. **DTI results: reduced white matter integrity is specific to the right UF in psychopaths. (a)** The UF ROI (circled in red) in serial axial slices and a single coronal slice. **(b)** The UF ROI (red) superimposed on an entire UF tract, as computed with tractography (see Methods for additional details). **(c-e)** Bar plots of mean scaled FA values in three comparison tracts, in each hemisphere: **(c)** inferior longitudinal fasciculus/inferior fronto-occipital fasciculus (ILF/IFOF), **(d)** superior longitudinal fasciculus (SLF), and **(e)** superior fronto-occipital fasciculus (SFOF). **(f)** Bar plots of mean scaled FA values in the UF. Psychopaths exhibited significantly lower scaled FA values only in right UF. Error bars indicate S.E.M.

of interest divided by the subject's whole-brain FA value. Using the scaled FA values, we addressed our first hypothesis—that psychopaths would have reduced structural integrity (lower FA values) in the UF. Indeed, relative to non-psychopaths, psychopaths had significantly lower scaled FA values in the right UF (t=-2.1, p=0.048) (**Figure 12a,b,f**). To assess the anatomical specificity of this finding, we computed scaled FA values for three additional major fiber tracts involving the frontal lobe: the superior fronto-occipital fasciculus, the superior longitudinal fasciculus, and the inferior longitudinal fasciculus/inferior fronto-occipital fasciculus. In none of these comparison tracts were FA values significantly different between psychopaths and non-psychopaths

(all p-values >0.14) (**Figure 12c,d,e**). These DTI data associate psychopathy with a reduction of white matter integrity in the right UF.

Functional connectivity: Rest-fMRI results

In light of our DTI findings in the right UF, we first examined resting functional connectivity between the right amygdala and vmPFC (**Figure 13a**). For each group (psychopaths and non-psychopaths), we computed the spatial map of voxels in vmPFC exhibiting a significant correlation with the BOLD signal derived from the right amygdala seed region (**Figure 13b**). To test the hypothesis that psychopaths would have reduced vmPFC-amygdala functional connectivity at rest, we then computed the spatial map of vmPFC voxels with significant differences in correlated activity with right amygdala (**Figure 13b**). In support of our hypothesis, we found a cluster of voxels in the right anterior vmPFC exhibiting significantly lower correlation with right amygdala in psychopaths than in non-psychopaths.

To address the anatomical specificity of this finding, we also assessed resting connectivity between the amygdala seed region and two other areas of the brain that have previously been shown to be functionally connected with the right amygdala: the contralateral (left) amygdala and a region of right anterior superior temporal gyrus (aSTG) (Roy et al., 2009). Although there were significant BOLD correlations between right and left amygdala as well as between right amygdala and right aSTG in both psychopaths and non-psychopaths, there were no significant between-group differences in amygdala connectivity with either area (both p-values>0.17). In other words, psychopaths exhibited normal functional connectivity between right amygdala and left

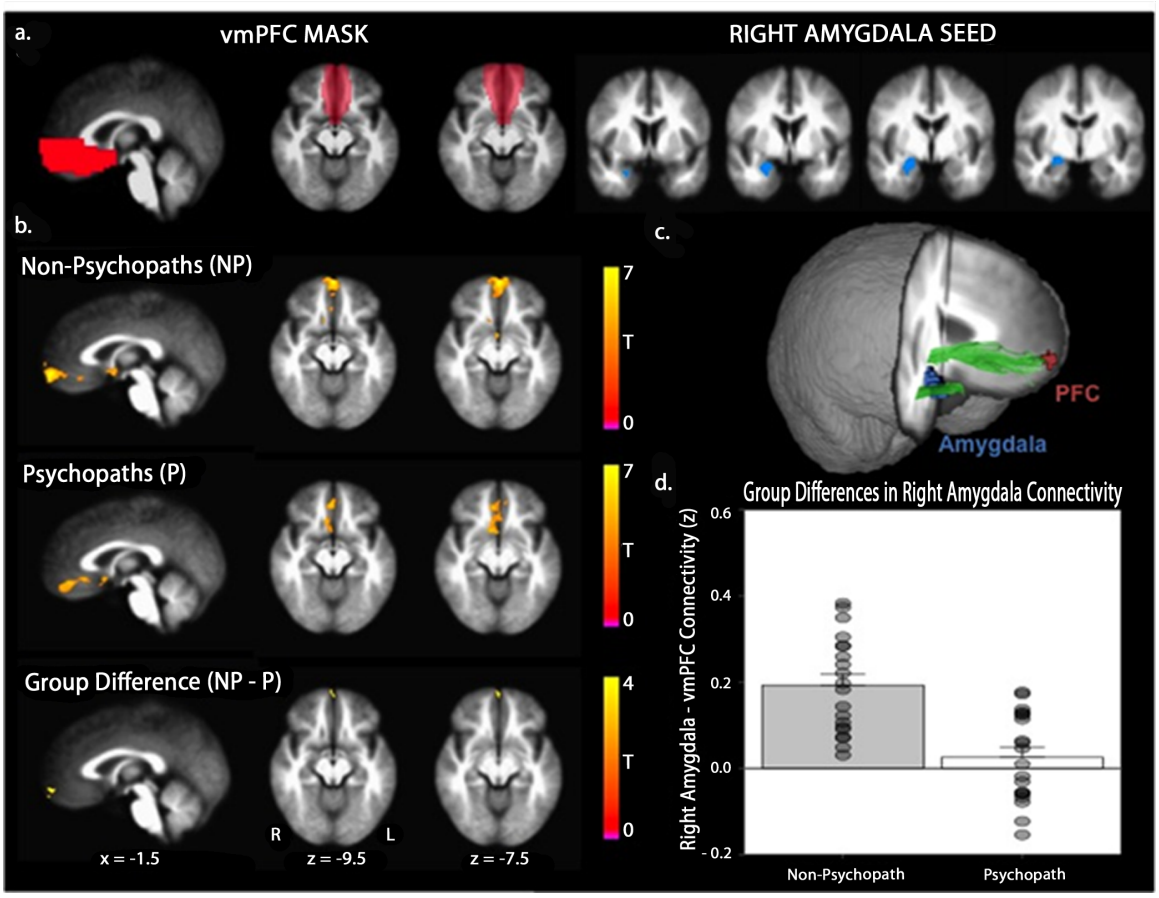

Figure 13. Functional connectivity between the right amygdala and anterior vmPFC is reduced in psychopaths. (a) Group differences in connectivity were assessed in the vmPFC mask (red) for correlation coefficients computed using the mean time series extracted from the hand drawn right amygdala seed (blue). **(b)** Mean right amygdala-vmPFC connectivity maps for non-psychopaths and psychopaths are shown separately on the group mean anatomical image, thresholded at a cluster corrected $p<0.05$. Scale bars depict the uncorrected T-statistic. Both groups exhibit significant resting connectivity between right amygdala and regions of vmPFC. The group difference map indicates an area in anterior vmPFC where non-psychopaths have significantly greater connectivity than psychopaths (x=-3, y=-66, z=-10, cluster size=14 voxels). **(c)** A three-dimensional rendering of the group mean anatomical image shows the location of the amygdala seed (blue) and significant vmPFC cluster (red) in relation to the UF (green). **(d)** The bar plot depicts the significant group difference in connectivity estimates (Fisher-z transformed correlation coefficients) within the vmPFC cluster. Error bars indicate S.E.M.. Filled circles represent values from individual subjects.

amygdala, as well as between right amygdala and right aSTG. These fMRI results associate psychopathy with a reduction in vmPFC-amygdala functional connectivity.

Discussion

In this study of psychopathic and non-psychopathic prison inmates, we found evidence of significantly reduced vmPFC-amygdala connectivity among psychopaths: lower FA in right UF and lower BOLD signal correlations with the amgydala at rest.

Regarding the finding of reduced structural connectivity in the right UF, ours is not the first study to use DTI to assess white matter structural integrity in psychopathy. The only previous study to do so also found that individuals with higher psychopathy scores had significantly lower FA values in right UF than those with lower psychopathy scores (Craig et al., 2009). Although the data presented here support the conclusion of the previous study (reduced structural connectivity between vmPFC and amygdala in psychopathy), our study has several notable methodological differences.

One advantage is a more rigorous subject classification scheme. The previous study included n=9 adult males with relatively high levels of psychopathy, defined as PCL-R score ≥25 (mean=28.4). We employed a more stringent PCL-R cutoff of ≥30 to define our psychopathic group, in accordance with the PCL-R recommendations (Hare, 2003) and in recognition of the fact that individuals with intermediate PCL-R scores (21-29) are in some experimental paradigms more similar to non-psychopaths (PCL-R ≤20) than actual psychopaths (PCL-R ≥30) (e.g., in tests of emotion-modulated startle (Patrick et al., 1993) and moral judgment (Koenigs et al., 2012). In addition, our psychopathic and non-psychopathic groups were well matched on demographic variables, intelligence, and substance abuse histories (**Table 7**).

A second distinguishing feature of the DTI component of our study is the single ROI-based approach to calculate UF FA values. The ROI we used was within the dense

insular segment, or "isthmus", of the UF. This ROI excludes terminal regions of the UF that intermingle with adjacent tracts (Ebeling and von Cramon, 1992). Combining this ROI approach with the correction for whole-brain FA differences allowed us to isolate regions of particular interest, while accounting for non-specific global differences throughout the brain.

Despite the methodological differences between studies, the fact that both DTI studies reveal the same specific finding supports a robust association between psychopathy and reduced FA in right UF.

Regarding the finding of reduced resting amygdala-vmPFC connectivity, although several previous fMRI studies have associated psychopathy with abnormal activation of the amygdala and vmPFC (see Koenigs et al., 2011 for review), our study is the first to demonstrate aberrant functional connectivity between vmPFC and amygdala in psychopathy using rest-fMRI. Moreover, the collection of neuroimaging data from n=20 psychopaths with PCL-R scores ≥30 is the largest such sample ever reported in an MRI study.

The finding of reduced vmPFC-amygdala correlation at rest coincides with our structural DTI data; both findings indicate diminished connectivity between vmPFC and amygdala in psychopathy. These convergent results support the central hypothesis of this study, and join a substantial corpus of research highlighting the importance of vmPFC-amygdala interactions in the regulation of emotion and social behavior (Barbas, 2000; Davidson, 2002; Milad et al., 2006; Delgado et al., 2008). Additionally, these neuroimaging findings are consistent with the longstanding psychological perspective that impaired decision-making in psychopathy is due to deficient integration of affective

information (Cleckley, 1976; Hiatt and Newman, 2006; Blair and Mitchell, 2009). The amygdala is understood to signal the affective salience of environmental stimuli (Davis and Whalen, 2001; Adolphs, 2010), and the anterior vmPFC is purported to discriminate the relative value of options and outcomes during decision-making (O'Doherty, 2004; Grabenhorst and Rolls, 2011). Accordingly, our finding of reduced functional connectivity between these regions suggests a plausible neurobiological mechanism underlying abnormal decision-making in psychopathy. More generally, the convergent DTI and rest-fMRI results suggest that the socio-affective deficits characterizing psychopathy may reflect impaired communication between vmPFC and amygdala.

This conclusion is supported by a previous study of adolescents with callous and unemotional traits, which revealed reduced functional connectivity between the amygdala and vmPFC during facial affect processing (Marsh et al., 2008). The convergence of findings across distinct demographic samples and experimental contexts suggests that reduced amygdala-vmPFC connectivity may be a consistent neurobiological feature of populations in which callous unemotionality and impaired empathy are major characteristics.

A goal for future research will be to use task-related fMRI to examine whether reduced vmPFC-amygdala connectivity is an invariant feature of the psychopathic brain, or if this abnormality is diminished or exaggerated during certain cognitive or affective tasks (e.g., reversal learning or emotion regulation). Additionally, it will be important to investigate with more anatomically precise imaging techniques whether the connectivity differences we observe in psychopaths are driven by particular subnuclei of the amygdala.

A limitation of the extreme groups design utilized in this study is that we are unable to determine whether our findings are driven by a particular factor of psychopathy (interpersonal-affective or impulsive-antisocial) or by particular behavioral characteristics (e.g., aggression). Future work in populations with more continuous distributions of psychopathy scores will be necessary to assess whether a particular dimensional factor drives the effects we report here.

Collectively, the structural and functional neuroimaging data presented here converge to specify diminished vmPFC-amygdala connectivity as a robust neural correlate of psychopathy. Human lesion studies have long implicated vmPFC dysfunction in the pathogenesis of "psychopathic" behavioral and affective traits (Eslinger and Damasio, 1985; Damasio et al., 1990; Koenigs et al., 2010). The imaging findings presented here provide direct evidence of dysfunctional vmPFC-amygdala connectivity in criminal psychopaths, and putatively identify a specific neurobiological abnormality underlying psychopathy. Furthermore, the identification of impaired structural connectivity between amygdala and vmPFC (structures typically linked to anxious and depressive psychopathology) in psychopathy, an externalizing disorder characterized by symptoms at the opposite end of the spectrum of emotional dysfunction, provides convincing support for the relevance of bidirectional prefrontal-amygdala interactions across a range of affective psychopathology.

Chapter 10. Summary and General Discussion

Taken together, the results summarized above indicate that modulation of emotion at neural, physiological, and behavioral levels, likely depends on complex, reciprocal interactions between vmPFC and a network of cortical and subcortical brain regions implicated in emotion processing. This perspective elaborates on a widely accepted neurobiological framework of emotion regulation, which proposes that activity in the vmPFC is critical for top-down regulation of amygdala activity, and further, that vmPFC-mediated control of amygdala activity is necessary for adaptive emotion regulatory processes (Quirk and Gehlert, 2003; Milad et al., 2006; Rauch et al., 2006). Whereas this model would predict that vmPFC damage should elicit heightened neural, physiological, and behavioral components of emotion and promote maladaptive patterns of emotional expression consistent with mood and anxiety disorders, humans with vmPFC lesions typically exhibit blunted behavioral and physiological emotional responses and a have reduced likelihood of developing anxious and depressive psychopathology (Damasio et al., 1990; Koenigs et al., 2008a; Koenigs et al., 2008b). To resolve this inconsistency, we conducted a series of experiments in a sample of four rare human patients with focal, bilateral vmPFC lesions to investigate the effects of vmPFC damage on the neural, physiological, and behavioral components of emotion. The experiments described in the preceding chapters each address facets of the larger question of how vmPFC modulates the expression of negative emotion.

In Chapter 6, we directly tested the top-down regulation model of vmPFC function by examining amygdala responses to aversive visual stimuli in human vmPFC lesion

patients using fMRI. In line with predictions from the model, we observed significant increases in right amygdala activation to aversive pictures in the vmPFC lesion group, relative to age- and sex-matched healthy comparison adults (**Figure 5, Table 3**). However, we did not observe similar increases in peripheral physiological indices of emotional arousal (i.e., cardiac deceleration) to the aversive picture stimuli (**Supplementary Figure 3**). The inconsistency between the neural and cardiovascular data indicate that, while the top-down regulation model appears to be valid in its assertion that efferent connections from vmPFC to amygdala are largely inhibitory and serve to decrease amygdala reactivity in healthy adults, the vmPFC must play some critical role in coordinating peripheral physiological responses beyond its role in modulating amygdala activity, whether directly through connections to brainstem and diencephalic nuclei involved in coordinating such responses, or perhaps through indirect connections with other brain regions implicated in affective processing.

In Chapter 7, we investigated the effect of vmPFC lesions on the neural correlates of anticipation, to test the possibility that anticipatory vmPFC activity could account for the divergence of neural and physiological responses in the previous study. Heightened negative emotion during anticipation (e.g., worry) is a cardinal symptom of anxiety disorders, and is therefore a relevant psychological process by which vmPFC could influence affective processing. By examining group differences in the phasic anticipatory response to cues predictive of ambiguous or certain outcomes (using the same task from Chapter 6), we found that the vmPFC lesion group exhibited markedly different patterns of insula activation during ambiguous, relative to certain, cues (**Figure 7**). Whereas healthy comparison subjects exhibited robust bilateral insula activity to ambiguous cues

and deactivation to certain cues, patients with vmPFC damage exhibited the opposite pattern of activity, showing increased insula activation to cues predicting certain aversive outcomes and decreased activation to ambiguous cues. Importantly, and unlike the previous study investigating amygdala responses to the pictures themselves, the level of uncertainty related anticipatory activity in bilateral insula clusters was significantly related to a peripheral physiological measure of adaptive flexibility and emotion regulation (HRV), both across all subjects and within the healthy comparison group (**Figure 9**). The concordance of neural and peripheral physiological findings in this second study supports the assertion that vmPFC likely plays a critical role in anticipatory processing that is directly relevant to the expression of peripheral autonomic components of an emotional response. In Chapter 8, we built upon these findings further by showing that the vmPFC lesion group had *reduced* resting cerebral blood flow in the bed nucleus of stria terminalis (BNST), a brain region with documented involvement in the expression of sustained anxiety (**Table 6**). As in the previous study of anticipatory processing, this finding of reduced perfusion in BNST is more consistent with the typically observed pattern of behavior in vmPFC lesion patients (i.e., reduced physiological and behavioral indices of anxiety).

Finally, in Chapter 9, we found evidence of reduced structural and functional connectivity between the amygdala and vmPFC in a population of prison inmates with psychopathy (**Figure 12, Figure 13**). This finding is consistent with previous systems-level neurobiological models of psychopathy, which propose that behavioral deficits characteristic of this population (e.g., blunted affect, reduced empathy, impaired decision-making) may reflect impaired bottom-up flow of salient, behaviorally relevant

information from the amygdala to vmPFC (Blair, 2007, 2008). Importantly, we observed the same general pattern of reduced amygdala-vmPFC connectivity in this population as has previously been reported in anxious and depressed populations (Kim and Whalen, 2009; Kim et al., 2010; Kim et al., 2011; Tromp et al., 2012), a finding typically interpreted as neural evidence of impaired *top-down* influence of vmPFC on amygdala. Thus, the results of this final study indicate that the flow of information between vmPFC and amygdala is likely bidirectional, and that bottom-up cortical influences from subcortical nuclei like the amygdala may be critically important for human emotion and social behavior.

In sum, we found direct evidence for a causal role of vmPFC activity in the modulation of brain activity across a network of interconnected cortical and subcortical brain regions implicated in emotion processing and expression. Some of the differences observed in the vmPFC lesion group (i.e., amygdala hyperactivity) were consistent with the proposed role of vmPFC in emotion regulation, whereas others (i.e., altered anticipatory processing and blunted peripheral physiological indices of emotion) more coherently reconciled the putative involvement of vmPFC in affective processing with previous human lesion data. Although the present results offer novel insights to changes in specific brain regions that interact with vmPFC, our findings are remarkably consistent with insights from earlier descriptions of patients with vmPFC damage. Particularly striking is this statement, from the 1985 description by Eslinger and Damasio of their vmPFC lesion patient, EVR:

> "The bidirectional action [between orbital and medial regions of the frontal lobe and principal limbic structures] described above is probably a central mechanism of frontal lobe operation,

> permitting two kinds of regulatory activity: (1) 'modulation' of innate hypothalamic drives that are informed of environmental rules and contingencies; and (2) activation of higher cortices by basic drives and tendencies." (Eslinger and Damasio, 1985)

Gleaned from the results of a single case study, this observation has proven to be quite prescient. Indeed, much of the data summarized in the previous four chapters are consistent with this idea that the vmPFC exerts its function through a combination of bottom-up and top-down interactions within a network of brain regions involved in higher order executive functions, like goals, planning, and action preparation, and evolutionarily older subcortical structures implicated in controlling somatic states related to maintaining homeostasis across varied environmental contexts. Critically, the vmPFC is ideally situated to coordinate and modulate activity across this network based on a host of psychological factors, like environmental or social context, expectancy, prior experience (memory), emotional state, attention and awareness, and current goals or control strategies.

The complex relationships among vmPFC damage, neural activity, and the behavioral and peripheral physiological expression of emotion demand a more nuanced approach to neural circuitry models of affective function. To date, the majority of research linking neural activity to negative affect has focused primarily on interactions between vmPFC and amygdala, yet the results described above highlight at least two other brain regions that may be critical for mediating the effects of vmPFC activity on emotional expression, and further, suggest that potential interactions with other interconnected brain regions may be critically important for affective processing.

A large corpus of data outlining the specific functional and connectional anatomy of particular vmPFC subregions can provide some insight to the mechanisms by which vmPFC could exert such far-reaching effects on brain regions and behaviors relevant to affective function. Below, I summarize evidence for the involvement of particular connections and subregions of vmPFC in coordinating different aspects of emotional processing, first in relation to the amygdala, then expanding scope to include a more diverse array of interconnected brain regions. I conclude by integrating the present results into a more parsimonious model of vmPFC function in affective psychopathology.

Neural circuitry underlying the expression of negative affect

Despite the preponderance of theoretical and empirical work directly linking amygdala activity to the expression of negative affect, anatomical tracing studies in rodents and non-human primates support comparable roles of vmPFC and amygdala in generating emotion-related physiological responses (Barbas et al., 2003). Indeed, many of the behavioral effects of vmPFC lesions are remarkably similar to those observed following amygdala lesions (Kling, 1972). Within the amygdala, there is convincing evidence that efferent projections from the central nucleus (CeA) are the primary drivers of affective somatomotor responses (LeDoux et al., 1988; Tye et al., 2011). Interestingly, amygdala subnuclei (especially CeA) and areas within vmPFC (especially the subgenual region including Brodmann areas 24, 25, and 32) send dense, overlapping projections to brainstem and diencephalic nuclei directly involved in coordinating peripheral autonomic expression; namely, lateral hypothalamus, bed nucleus of stria terminalis, parabrachial nucleus, dorsal motor nucleus of the vagus nerve, and periaqueductal gray (Price and

Amaral, 1981; Neafsey, 1990; Ongur and Price, 2000; Barbas et al., 2003; Ghashghaei et al., 2007). Stimulation of both amygdala and vmPFC has been shown elicit stereotyped changes in peripheral physiology and behavior (Kaada et al., 1949; Kapp et al., 1982; LeDoux et al., 1988; Neafsey, 1990), which can be interrupted with targeted lesions to more proximal brainstem and hypothalamic effectors (LeDoux et al., 1988). Thus, there exist viable anatomical and physiological mechanisms by which damage to vmPFC could directly attenuate behavioral and physiological expression of negative emotion, even in the face of amygdala hyperactivity.

The best studied of the efferent connections from vmPFC to amygdala terminate on GABAergic intercalated (ITC) cells (interneurons) and inhibitory projection neurons in the basolateral nucleus of the amygdala (BLA), both of which ultimately inhibit outflow from the CeA (Quirk et al., 2003; Berretta et al., 2005; Tye et al., 2011). Thus, the expected consequences of damaging or destroying these connections as the result of a vmPFC lesion would be enhanced CeA activity and enhanced somatomotor responses. This prediction has been borne out in rodent models (Quirk et al., 2000) and is in line with our finding of amygdala hyperactivity in the vmPFC lesion group (**Figure 5**), but is inconsistent with our observation that amygdala hyperactivity was accompanied by reduced (not increased) heart rate changes to the aversive stimuli. Our finding of reduced HRV in the vmPFC lesion group during the task and at rest, in concert with our observation that individual differences in anticipatory insula activity to uncertainty were positively correlated with HRV (**Figure 9**), suggests that direct projections from vmPFC to brainstem cardiovascular effectors, or perhaps indirect projections through the insula, may be more critical for directly modulating the physiological components of an

emotional response than projections to the amygdala (Neafsey, 1990; Allen et al., 1991; Shi and Cassell, 1998; Barbas et al., 2003). Our finding of reduced perfusion in the vmPFC lesion group in BNST (**Table 6**), which receives inputs from both amygdala and vmPFC and projects to the same somatomotor effectors in brainstem and hypothalamus (McDonald et al., 1999; Dong et al., 2001a; Dong et al., 2001b; Heimer et al., 1997; Tye et al., 2011; Kim et al., 2013), provides further evidence for distal effects of vmPFC lesions on regions downstream of the amygdala.

In addition to efferent projections to interneurons that ultimately inhibit the CeA, the vmPFC shares extensive reciprocal connections with the BLA, which are thought to be critical for modulating the behavioral and physiological expression of negative affect. Data from rodent models suggest that *ascending* inputs from BLA to targets within the vmPFC likely play a key role in this process (Little and Carter, 2013). For example, inactivation of ascending projections from BLA has been shown to reduce activity in medial prefrontal pyramidal neurons in the rodent, with corresponding reductions in freezing behavior (Sotres-Bayon et al., 2012; Little and Carter, 2013). Lesions of rodent BLA and vmPFC are each capable of blocking the expression of conditioned fear, further supporting a putative role for reciprocal connections between BLA and vmPFC in the expression of fear (Anglada-Figueroa and Quirk, 2005; Sierra-Mercado et al., 2006). These data are broadly consistent with previous work showing that activation of prefrontal cortex by amygdala induces risk assessment (Gozzi et al., 2010), sustained attention (Holland and Gallagher, 1999), and modulates fear and vigilance (Davis and Whalen, 2001).

Ascending connections from BLA to vmPFC could potentially account for our findings of reduced amygdala-vmPFC connectivity in the sample of psychopathic prison inmates studied in Chapter 9. Given the putative role of these projections in in the expression of negative affect, impaired communication between BLA and vmPFC in psychopathic prisoners could contribute to the observed similarities to patients with vmPFC lesions (e.g., blunted affect, reduced empathy, impaired decision-making). Interestingly, in Chapter 6, we observed similar effects of vmPFC damage on fMRI responses to aversive pictures regardless of whether we used a whole amygdala ROI or a CeA ROI (**Table 3**, **Supplementary Table 4)**. Thus, we are unable to determine conclusively whether vmPFC damage had divergent effects on particular amygdala subnuclei, like CeA and BLA. Further research using imaging techniques with improved spatial resolution will be necessary to more clearly delineate the specific contributions of vmPFC and amygdala subregions to human affective function.

Contributions of vmPFC subregions to affective processing

Another important anatomical distinction relevant to affective processing is between subregions of vmPFC. Previous work in human and animal models suggests a functional distinction between the subgenual PFC—a ventral and caudal subregion thought to be homologous to rodent infralimbic cortex (IL)—and pregenual/dorsomedial PFC, a more rostral and dorsal subregion with homology to the rodent prelimbic cortex (PL) (Ongur and Price, 2000; Quirk and Beer, 2006; Myers-Schulz and Koenigs, 2012). Whereas the IL sends dense projections to the ITC cells that ultimately inhibit CeA outflow, PL primarily projects to the BLA, which has been linked to fear expression (Quirk and Beer,

2006). In support of this distinction, individual neurons in PL and IL exhibit opposite response characteristics to conditioned fear stimuli (Gilmartin and McEchron, 2005). Importantly, there is evidence suggesting that the PL-BLA connections are excitatory (Likhtik et al., 2005), which could explain the positive associations observed in human neuroimaging studies between activity in pregenual/dorsomedial prefrontal cortex (homologous to PL) and fear acquisition (Phelps et al., 2004), more negative interpretations of face stimuli (Kim et al., 2003), emotional arousal (Taylor et al., 2003), and increased autonomic activity (Critchley, 2005; Wager et al., 2009).

In our sample of human neurosurgical patients with vmPFC lesions, damage was most pronounced in the subgenual region of vmPFC, thought to be homologous to rodent IL (**Figure 2**). However, the mechanism of injury in the vmPFC lesion group—surgical resection of an orbital meningioma—resulted in significant damage to white matter fibers passing through this region, likely interrupting connections from the PL-homologous region to subcortical structures like the amygdala. Thus, it is theoretically possible that cytotoxic lesions sparing the underlying white matter anatomy would yield a different pattern of results than those observed in Chapter 6, with enhanced amygdala activity accompanied by increased (rather than decreased) fear expression. Future work in larger samples with more heterogeneous lesions will be necessary to more clearly demarcate the functional contributions of specific vmPFC subregions and connections to the observed changes in affective processing.

Types of emotional regulation thought to depend on vmPFC

Before integrating the present results into a more comprehensive model of vmPFC function in affective psychopathology, it is useful to consider the component psychological processes thought to underlie effective emotion regulation. Accumulating evidence from human brain imaging points to a unique role for vmPFC in "reflexive" or "implicit" emotion regulation, a process critically dependent on the acquisition and use of expectancies about the valence and predictability of impending stimuli (Etkin et al., 2006; Etkin and Wager, 2007; Egner et al., 2008; Gyurak et al., 2011). Specifically, human functional imaging studies have observed vmPFC activity during emotional conflict monitoring (Etkin et al., 2006), extinction of conditioned fear (Phelps et al., 2004), and placebo anxiolysis (Petrovic et al., 2005), all of which involve passive or unconscious integration of ongoing goals, expectancies, and relevant contextual cues to guide ongoing behavior and emotional expression. This proposed implicit regulatory capacity is in line with previous research indicating that individual neurons in the orbitofrontal cortex of non-human primates integrate previously learned cue-outcome associations with information about internal states and goals. Individual neurons in vmPFC have been shown to encode the relative cost or value of competing outcomes (Kennerley et al., 2009; Kennerley and Wallis, 2009), and eventually, become active during the anticipation of these outcomes (Schoenbaum and Roesch, 2005). Interestingly, stimulation of particular subsets of neurons in this region can bias animals toward behavioral avoidance of an anticipated outcome (Amemori and Graybiel, 2012). This effect has been shown to accumulate over time and can be blocked by anxiolytic drug treatment, suggesting that this region may be critical for translating outcome expectancies into action tendencies

(Amemori and Graybiel, 2012). Thus, the encoding of expectancies by vmPFC could instantiate an internal representation of the likely consequences of a particular action, to guide behavior and facilitate subsequent learning. Furthermore, this process may be a relevant target for intervention in anxiety disorders.

The implicit regulatory function ascribed to vmPFC stands in contrast to more conscious regulation strategies involving overt evaluation and reappraisal, which are typically linked to activity in lateral prefrontal cortex (Ochsner et al., 2002; Ochsner et al., 2004; Wager et al., 2008). Phylogenetic comparison of prefrontal anatomy across mammalian species suggests that these lateral prefrontal regions are more recently evolved in humans, and thus may be better suited to enact higher-order cognitive appraisal of affective stimuli (Fuster, 2008a). However, even explicitly cognitive regulatory strategies likely depend on intact medial prefrontal cortex; the vast majority of projections from lateral prefrontal cortex to subcortical emotional effectors course through the medial prefrontal cortex and likely impinge on populations of vmPFC neurons that convey regulatory impulses to subcortical structures. In support of this interpretation, an fMRI study of emotion regulation via cognitive reappraisal found that ventrolateral PFC (vlPFC) was more active during reappraisal, that activity in this region correlated with reappraisal success, and that the effects of regulation on activity in subcortical structures was mediated by positive associations with the subgenual region of vmPFC (Wager et al., 2008). A recent functional connectivity analysis in humans provides further support for this medial/lateral distinction, finding divergent connectivity between lateral prefrontal cortex and regions involved in cognitive functions of language

and memory and between medial prefrontal cortex and limbic and autonomic regions (Zald et al., 2014).

Despite abundant data supporting functional specialization of particular prefrontal subregions in specific functional processes, it is important to acknowledge that it is effectively impossible to fully disentangle the functional properties of these regions. While it is evident from the results described herein that ventral and medial sectors of the prefrontal cortex exert substantial control over processes relevant to emotion and social behavior, modulating activity in limbic, hypothalamic, and brainstem structures directly implicated in the peripheral expression of affect, it would be inappropriate to categorically dissociate these functions from those thought to depend on the highly interconnected lateral prefrontal cortex. In his seminal textbook on prefrontal function, Fuster extends these ideas further:

> "It is equally erroneous to dissociate cognitive functions, especially executive functions, from the powerful role of those internal inputs and drives. Indeed, those inputs and drives are to some degree determinant of any decision and course of action, however exclusively cognitive those may appear. Strictly speaking, there is no cognition without affect and emotion." (Fuster, 2008b)

Thus, while we interpret our results as evidence for functional specialization of medial prefrontal cortex circuitry in the context-dependent modulation of emotional expression, it is unwise to ignore the contributions of densely interconnected structures involved in higher-order cognitive processes.

Relevance of observed findings to models of affective psychopathology

The results of this dissertation suggest that the top-down regulation model of vmPFC function in affective psychopathology, drawn from experimental insights in fear conditioning and extinction, is too narrow in scope to adequately explain the full range of behaviors affected by human vmPFC lesions. Rather, the novel findings reported herein, together with a large corpus of functional and anatomical data (summarized above), suggest a critical role for vmPFC in the acquisition and use of expectancies (i.e., internal representations of the likely consequences of a particular act) to guide the on-line experience of emotion and modulation of behavior. This functional specialization is likely based on a confluence of psychological processes that are integrated and deployed by medial prefrontal networks.

With regard to the implications of these findings for neurobiological models of mood and anxiety disorders, there is an important distinction between fear—the experiential phenomenon that has largely guided insight into disorders of negative affect—and anxiety, a construct more closely aligned with the phenomenological experience of anticipatory negative affect in patients with emotional psychopathology (i.e., "worry"). The most recent edition of the DSM (DSM-5) makes this distinction explicit: "fear is the emotional response to real or perceived imminent threat, whereas anxiety is anticipation of future threat" (American Psychiatric Association, 2013). In animal models, "fear-like" orienting responses to acute threat are associated with activity in the amygdala, whereas sustained negative affect characteristic of anxiety has been linked to BNST activity (Walker et al., 2003). Our results indicate that the neural phenomena (i.e., amygdala hyperactivity) underlying fear, the emotional response to imminent threat, is intact, and

even enhanced in human patients with vmPFC lesions. The inconsistency between the observed pattern of amygdala hyperactivity and the paucity of objective evidence of fear in our behavioral and physiological data could relate directly to the critical importance of bidirectional interactions between amygdala and prefrontal cortex in the experiential components of fear. For example, as described above, reciprocal connections between the vmPFC and BLA have been shown to be critical for the expression of fear behaviors in rodent models. Anxiety-related phenomena, which are mechanistically tied to the anticipatory processing of impending stimuli, are more in line with our neural, physiological and behavioral results. Specifically, our finding of disrupted insular cortex activity during the anticipation of ambiguous outcomes following vmPFC lesions, as well as the link between such responses and attenuated peripheral indices of emotion (HRV), are more consistent with the behavioral profile of vmPFC lesion patients; namely, that they exhibit blunted physiological indices of negative affect and are less likely to exhibit anxious and depressive symptomatology. Similarly, our finding of reduced BNST metabolism in the vmPFC lesion group, which has been more closely linked to state anxiety than phasic fear, further supports the critical role of vmPFC in the modulation of the phenomenological experience of anxiety. These assertions are largely consistent with a recently published model of anxiety linking the neural substrates of anticipation, especially under conditions of uncertainty, to psychological domains impaired in anxious psychopathology (Grupe and Nitschke, 2013).

These predictions should be evaluated in future studies comparing vmPFC lesion patients directly to patients with anxious and depressive psychopathology. Based on the present results, we might expect vmPFC lesion patients to exhibit similar patterns of

phasic amygdala activation to aversive or threatening stimuli as individuals with an anxiety disorder, but exhibit the opposite pattern (attenuation) of neural activity during the anticipation of potentially aversive or uncertain outcomes and in baseline BNST activity. By directly comparing predicted and observed outcomes in experiments probing responses to aversive stimuli, uncertain anticipation, and resting brain metabolism, future work could more conclusively determine the causal contributions of individual brain regions and psychological processing domains to affective psychopathology.

Taken together, the findings summarized in this dissertation clearly implicate vmPFC in the modulation of neural, physiological, and behavioral expressions of negative affect. Importantly, our findings highlight a need to refine and elaborate prevailing neurocircuitry models of affective psychopathology. Deliberate, hypothesis driven assessment of neural circuits responsible for particular domains of psychological or behavioral dysfunction that are shared across traditional diagnostic categories will be a key step toward improving the quality of neurobiological indices of psychiatric disease. This work has the potential to provide invaluable insight to clinicians, and may eventually inform the selection and implementation of pharmacological and behavioral treatments to individuals, and even brain regions, where they will be most effective.

.

Appendix 1. Supplementary Tables

Supplementary Table 1. IAPS numbers, content categories, and normative ratings of picture stimuli

Photo #	Pleasure	Arousal	Content	Valence
6230	2.37	7.35	AimedGun	Aversive
6313	1.98	6.94	Attack	Aversive
6560	2.16	6.53	Attack	Aversive
3170	1.46	7.21	BabyTumor	Aversive
2352.2	2.09	6.25	BloodyKiss	Aversive
3053	1.31	6.91	BurnVictim	Aversive
3102	1.4	6.58	BurnVictim	Aversive
3100	1.6	6.49	BurnVictim	Aversive
3110	1.79	6.7	BurnVictim	Aversive
9571	1.96	5.64	Cat	Aversive
9140	2.19	5.38	Cow	Aversive
3120	1.56	6.84	DeadBody	Aversive
9181	2.26	5.39	DeadCows	Aversive
9433	1.84	5.89	DeadMan	Aversive
9300	2.26	6	Dirty	Aversive
9570	1.68	6.14	Dog	Aversive
6020	2.93	5.81	ElectricChair	Aversive
9921	2.04	6.52	Fire	Aversive
9265	2.6	4.34	HungMan	Aversive
3130	1.58	6.97	Mutilation	Aversive
3060	1.79	7.12	Mutilation	Aversive
3071	1.88	6.86	Mutilation	Aversive
3030	1.91	6.76	Mutilation	Aversive
9253	2	5.53	Mutilation	Aversive
3150	2.26	6.55	Mutilation	Aversive
3400	2.35	6.91	SeveredHand	Aversive
9420	2.31	5.69	Soldier	Aversive
9400	2.5	5.99	Soldier	Aversive
9040	1.67	5.82	StarvingChild	Aversive
6570	2.19	6.24	Suicide	Aversive
3261	1.82	5.75	Tumor	Aversive
9320	2.65	4.93	Vomit	Aversive
6900	4.76	5.64	Aircraft	Neutral
7010	4.94	1.76	Basket	Neutral
5390	5.13	2.95	Boat	Neutral
7006	4.88	2.33	Bowl	Neutral
7491	4.82	2.39	Building	Neutral

7705	4.77	2.65	Cabinet	Neutral
2840	4.91	2.43	Chess	Neutral
7211	4.81	4.2	Clock	Neutral
7020	4.97	2.17	Fan	Neutral
7080	5.1	2.67	Fork	Neutral
7050	4.93	2.75	HairDryer	Neutral
7175	4.87	1.72	Lamp	Neutral
7170	4.9	3.15	LightBulb	Neutral
2190	4.83	2.41	Man	Neutral
7009	4.93	3.01	Mug	Neutral
7035	4.98	2.66	Mug	Neutral
5534	4.84	3.14	Mushrooms	Neutral
2200	4.79	3.18	NeutFace	Neutral
7550	5.17	3.52	Office	Neutral
6150	5.17	3.62	Outlet	Neutral
7233	5.01	2.51	Plate	Neutral
7000	5	2.42	RollingPin	Neutral
2383	4.72	3.41	Secretary	Neutral
2880	5.13	2.68	Shadow	Neutral
7004	4.89	2.09	Spoon	Neutral
5535	4.81	4.11	Stilllife	Neutral
2870	5.17	2.87	Teenager	Neutral
7002	4.97	3.16	Towel	Neutral
7130	4.77	3.35	Truck	Neutral
7150	4.72	2.61	Umbrella	Neutral
5410	5.78	3.42	Violinist	Neutral
2514	5.19	3.5	Woman	Neutral

Supplementary Table 2. Experimental ratings and reaction times of picture stimuli by valence

	Ratings[a]			Reaction time (ms)[a]		
Picture Valence	**NC**	**vmPFC**	***P***	**NC**	**vmPFC**	***P***
Aversive	3.63 (0.25)	3.67 (0.30)	0.75	841.30 (228.42)	880.00 (257.54)	0.67
Neutral	1.85 (0.16)	1.71 (0.21)	0.24	814.20 (253.99)	831.77 (244.75)	0.91

Means are presented with standard deviations in parentheses. [a]Excluding trials with no responses (NC: 6 subjects missed 1 rating, 1 subject missed 2 ratings; vmPFC: 2 subjects missed 1 rating, 1 subject missed 2 ratings).

Supplementary Table 3. Within-group comparisons of effects of cue type (certain/uncertain) on amygdala responses (PSC) to aversive and neutral pictures

		HC			vmPFC		
Amygdala ROI	**Picture Valence**	**Uncertain (?)**	**Certain (X/O)**	***P***	**Uncertain (?)**	**Certain (X/O)**	***P***
Right Functional	Aversive	0.07 (0.09)	0.09 (0.11)	0.557	0.21 (0.01)	0.16 (0.06)	0.25
	Neutral	0.00 (0.12)	0.00 (0.09)	0.836	0.06 (0.14)	0.08 (0.05)	1
Right Anatomical	Aversive	0.09 (0.11)	0.10 (0.11)	0.768	0.23 (0.12)	0.15 (0.06)	0.375
	Neutral	0.01 (0.12)	0.03 (0.11)	0.612	0.07 (0.18)	0.04 (0.06)	0.625
Left Functional	Aversive	0.09 (0.09)	0.10 (0.08)	0.403	0.17 (0.15)	0.09 (0.09)	0.375
	Neutral	0.00 (0.10)	0.01 (0.11)	0.643	0.05 (0.23)	-0.01 (0.11)	0.625
Left Anatomical	Aversive	0.10 (0.10)	0.11 (0.10)	0.756	0.21 (0.11)	0.11 (0.14)	0.375
	Neutral	0.01 (0.10)	0.03 (0.12)	0.507	0.06 (0.22)	0.00 (0.07)	0.875

Test statistic based on the specific paired difference test (HC: t-statistic from paired t-test with 18 degrees of freedom; vmPFC: W statistic from paired Wilcoxon rank sum test). MNI coordinates for each ROI are listed in Supplementary Table 4.

Supplementary Table 4. Group differences in percent signal change to aversive and neutral pictures in functional and anatomical ROIs (NC age 50+ group)

	Region of Interest				Aversive pictures				Neutral pictures			
Brain Region	**Size**	**Center of Mass**			**NC 50+ mean (SD)**	**vmPFC mean (SD)**	**W**	***P***	**NC 50+ mean (SD)**	**vmPFC mean (SD)**	**W**	***P***
		X	**Y**	**Z**								
R Amyg (Func)	39	22.6	-6.3	-9.6	0.07 (0.07)	0.18 (0.03)	2	**0.008**	-0.03 (0.05)	0.07 (0.07)	5	**0.036**
R Amyg (Anat)	18	25.3	-3.8	-15.5	0.08 (0.07)	0.19 (0.07)	5	**0.036**	0.00 (0.05)	0.05 (0.12)	14	0.454
R Amyg (CeA)	6	23.2	-7.5	-15	0.08 (0.05)	0.18 (0.06)	6	**0.054**	-0.03 (0.06)	0.06 (0.09)	8	0.106
L Amyg (Func)	72	-24.7	-2.7	-12	0.10 (0.07)	0.13 (0.11)	15	0.539	-0.01 (0.08)	0.02 (0.17)	15	0.539
L Amyg (Anat)	29	-23	-4.2	-16.7	0.12 (0.08)	0.16 (0.11)	14	0.454	0.01 (0.09)	0.03 (0.14)	15	0.539
L Amyg (CeA)	6	-22.2	-7.5	-15	0.11 (0.09)	0.19 (0.11)	13	0.37	-0.02 (0.07)	0.01 (0.19)	14	0.454
R ITG	684	46	-67.9	4	0.29 (0.13)	0.42 (0.11)	9	0.142	0.18 (0.10)	0.31 (0.07)	6	0.054
L MTG	597	-42.7	-71	6.6	0.26 (0.13)	0.35 (0.07)	8	0.106	0.17 (0.10)	0.25 (0.02)	4	**0.024**
Thal	337	0.9	-19.8	-2.2	0.13 (0.08)	0.18 (0.02)	10	0.188	0.04 (0.07)	0.11 (0.07)	11	0.24
R Lingual	283	6.7	-87.2	1.3	0.42 (0.16)	0.50 (0.14)	14	0.454	0.31 (0.13)	0.44 (0.08)	9	0.142
L ACC	72	-1.5	14.5	32.1	0.11 (0.06)	0.10 (0.06)	22	0.839	0.02 (0.07)	0.07 (0.06)	9	0.142
L MFG	68	-8.5	50.5	25.7	0.04 (0.11)	0.01 (0.12)	22	0.839	-0.06 (0.07)	-0.04 (0.06)	15	0.539
R Precun	64	0.1	-49.9	31.2	0.00 (0.06)	-0.02 (0.04)	26	0.454	-0.04 (0.06)	0.01 (0.03)	11	0.24
L PCC	62	-1.3	-18	32.6	0.04 (0.05)	-0.03 (0.12)	27	0.374	-0.02 (0.05)	0.02 (0.08)	13	0.374

p-values for significant group differences are in bold. Cluster size in number of voxels (3x3x3 mm^3).
Center of mass coordinates for each ROI presented in MNI space. Func, functionally-defined ROI; Anat, anatomically-defined ROI; CeA: central nucleus anatomically defined ROI.

Supplementary Table 5. Group comparisons of cerebral blood flow across all ROIs

	NC	vmPFC	W	*P*
Whole Brain	36.30 (8.73)	40.09 (13.65)	31	0.611
R Amyg (Func ROI)	1.11 (0.18)	1.02 (0.12)	49	0.409
R Amyg (Anat ROI)	1.10 (0.15)	1.01 (0.19)	46	0.557
R Amyg (CeA ROI)	1.18 (0.17)	1.06 (0.18)	55	0.188
L Amyg (Func ROI)	1.11 (0.15)	1.16 (0.10)	26	0.366
L Amyg (Anat ROI)	1.11 (0.15)	1.23 (0.11)	20	0.162
L Amyg (CeA ROI)	1.15 (0.19)	1.28 (0.13)	19	0.138
R ITG	0.90 (0.12)	0.83 (0.10)	52	0.286
L MTG	0.91 (0.12)	0.96 (0.11)	25	0.324
Thal	1.15 (0.10)	1.09 (0.04)	50	0.366
R Lingual	1.07 (0.21)	0.94 (0.12)	52	0.286
L ACC	1.48 (0.14)	1.37 (0.12)	54	0.218
L MFG	1.38 (0.13)	1.40 (0.16)	34	0.785
R Precun	1.40 (0.14)	1.30 (0.09)	58	0.116
L PCC	1.41 (0.14)	1.28 (0.06)	60	0.081

MNI coordinates for each ROI are listed in Supplementary Table 4.

Supplementary Table 6. Group comparisons of cerebral blood flow across all ROIs (NC age 50+ group)

	NC 50+	vmPFC	W	*P*
Whole Brain	34.39 (8.88)	40.09 (13.65)	15	0.539
R Amyg (Func ROI)	1.15 (0.16)	1.02 (0.12)	30	0.188
R Amyg (Anat ROI)	1.14 (0.15)	1.01 (0.19)	28	0.304
R Amyg (CeA ROI)	1.18 (0.17)	1.06 (0.18)	55	0.188
L Amyg (Func ROI)	1.16 (0.13)	1.16 (0.10)	18	0.839
L Amyg (Anat ROI)	1.16 (0.12)	1.23 (0.11)	13	0.374
L Amyg (CeA ROI)	1.15 (0.19)	1.28 (0.13)	19	0.138
R ITG	0.92 (0.09)	0.83 (0.10)	30	0.188
L MTG	0.92 (0.11)	0.96 (0.11)	11	0.240
Thal	1.17 (0.13)	1.09 (0.04)	28	0.304
R Lingual	1.06 (0.17)	0.94 (0.12)	30	0.188
L ACC	1.48 (0.12)	1.37 (0.12)	28	0.304
L MFG	1.35 (0.13)	1.40 (0.16)	15	0.539
R Precun	1.36 (0.13)	1.30 (0.09)	27	0.374
L PCC	1.40 (0.12)	1.28 (0.06)	32	0.106

MNI coordinates for each ROI are listed in Supplementary Table 4.

Supplementary Table 7. Lateralization of lesion volume in vmPFC lesion group

Subject	Left Volume[a]	Right Volume[a]	Full Volume[a]	Percent Right
vmPFC-1	25814	33189	59003	56.25%
vmPFC-2	14824	28614	43438	65.87%
vmPFC-3	41351	48100	89451	53.77%
vmPFC-4	14085	43447	57532	75.52%

Lesion volumes estimated by dividing lesion masks at the midline (x=0) and calculating the number of voxels in each hemisphere, in MNI space. [a]Volumes presented in mm^3.

Appendix 2. Supplementary Figures

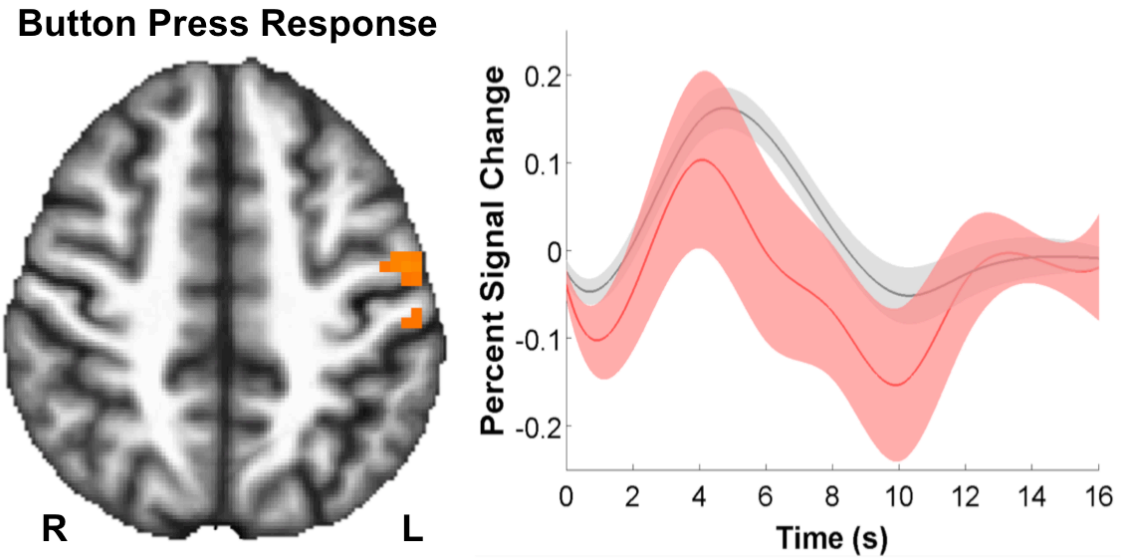

Supplementary Figure 1. Button Press Response. Estimated hemodynamic response functions in response to button press during the rating period are similar between groups. Left, cluster of activated voxels from a button press > baseline comparison in the NC group. Right, estimated response timecourse for vmPFC (red) and NC (black) subjects (width of shaded area corresponds to ±1 s.e.m.)

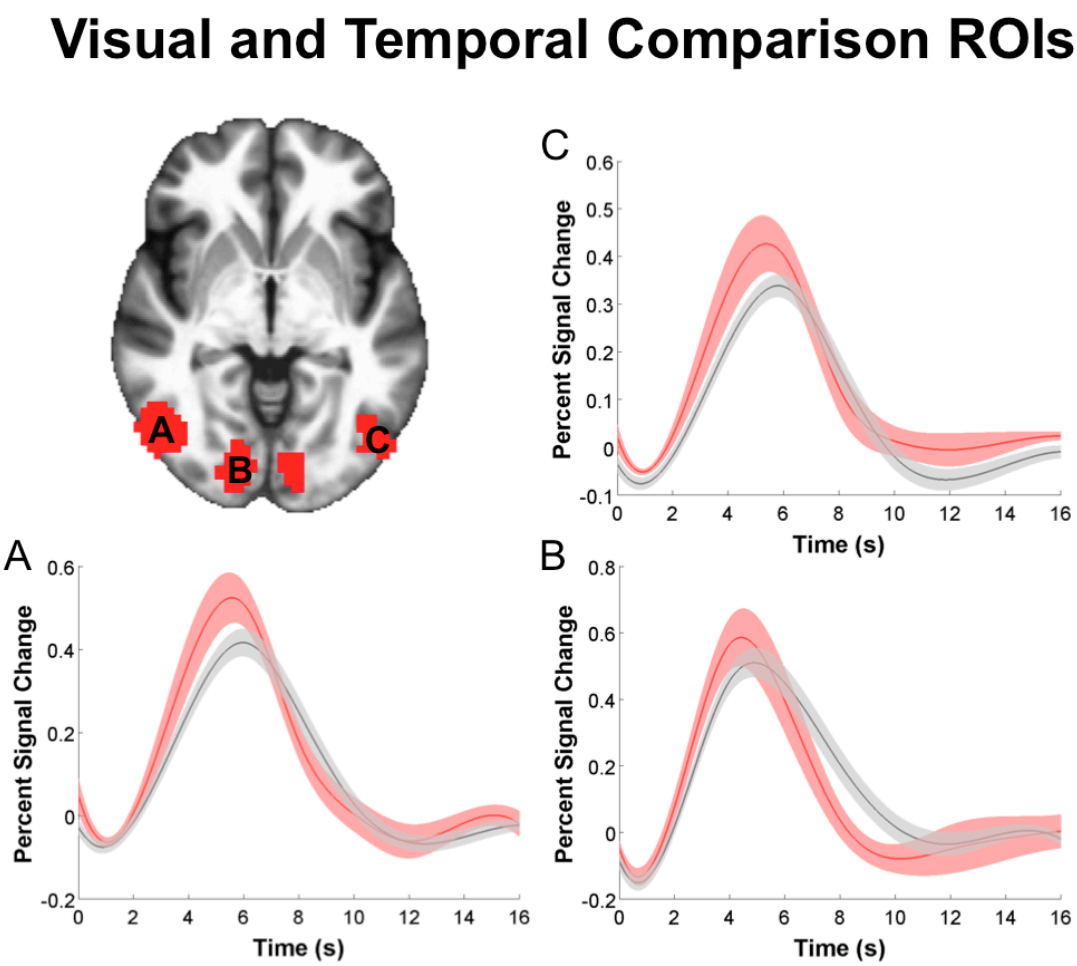

Supplementary Figure 2. Estimated hemodynamic response functions in response to aversive pictures in visual and temporal clusters are similar between groups. Top left, task-derived visual and temporal regions of interest (ROIs; red) used to extract timecourse data. (A-C) estimated response timecourse for vmPFC (red) and NC (black) subjects in response to aversive pictures (width of shaded area corresponds to ±1 s.e.m.). Letters indicate the cluster location: A = right inferior temporal gyrus, B = bilateral lingual gyrus (visual cortex), C = left middle temporal gyrus.

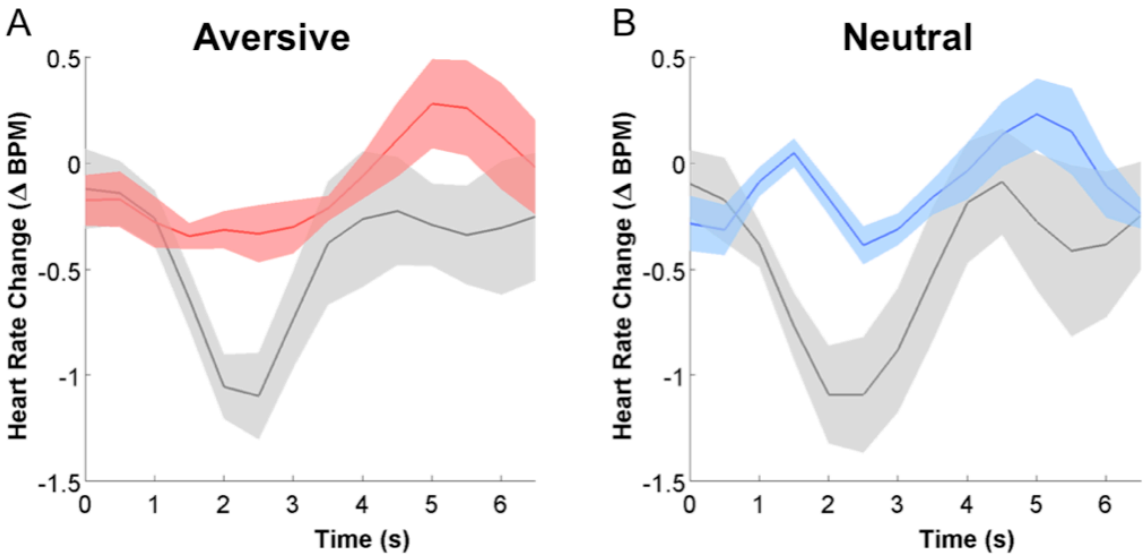

Supplementary Figure 3. vmPFC lesions attenuate heart rate deceleration to aversive pictures. Estimated heart rate timecourse for vmPFC (red) and NC (black) subjects in response to (A) aversive pictures and (B) neutral pictures, relative to pre-picture baseline. Width of shaded area corresponds to ±1 s.e.m. BPM = beats per minute. The same general pattern of group differences (although non-significant) was observed in the subsample of age- and gender-matched NC participants to both aversive (NC subsample: -1.23±0.74; vmPFC: -0.52±0.31; W=5, *P*=0.11) and neutral pictures (NC subsample: -1.38±1.01; vmPFC: -0.60±0.30; W=7, *P*=0.23).

Appendix 3. Summary of Results

1) Human vmPFC lesions are associated with enhanced right amygdala activation to aversive visual stimuli, supporting a causal role of vmPFC on amygdala activity (**Chapter 6**).
2) The vmPFC lesion group exhibited blunted cardiac physiological responses to aversive visual stimuli, despite exhibiting increased amygdala activity, suggesting that amygdala hyperactivity is *not* associated with increased physiological arousal (as would be predicted based on previous theoretical work linking amygdala to the peripheral expression of negative affect) (**Chapter 6**).
3) Healthy adults exhibited robust bilateral insula activation to ambiguous, relative to certain, anticipatory cues (**Chapter 7**).
4) The vmPFC lesion group exhibited altered insula activation during the uncertain anticipation of potentially aversive stimuli, consistent with a putative role for vmPFC in context-dependent regulation of neural activity (**Chapter 7**).
5) Patients with vmPFC lesions exhibited lower HRV both at rest and during the cued anticipation task, suggesting that lesions alter context-dependent modulation of cardiac physiology (**Chapter 7**).
6) Across all subjects (vmPFC lesion patients and healthy comparison adults), the magnitude of uncertainty-related activation in bilateral insula was related to individual differences in HRV, suggesting that vmPFC-insula interactions may

be critical for the putative role of vmPFC in context-dependent emotion regulation (**Chapter 7**).

7) Human vmPFC lesions were associated with reduced resting perfusion of the BNST, a region linked to the expression of state-anxiety (**Chapter 8**).

8) Psychopathic prison inmates exhibited reduced structural and functional connectivity between vmPFC and amygdala, suggesting that deficient *bidirectional* interactions between these brain regions may account for a wide range of affective psychopathology (**Chapter 9**).

References

Adolphs R (2010) What does the amygdala contribute to social cognition? Ann N Y Acad Sci 1191:42-61.

Adolphs R, Gosselin F, Buchanan TW, Tranel D, Schyns P, Damasio AR (2005) A mechanism for impaired fear recognition after amygdala damage. Nature 433:68-72.

Aldao A, Nolen-Hoeksema S, Schweizer S (2010) Emotion-regulation strategies across psychopathology: A meta-analytic review. Clin Psychol Rev 30:217-237.

Alexander DC, Barker GJ (2005) Optimal imaging parameters for fiber-orientation estimation in diffusion MRI. Neuroimage 27:357-367.

Allen GV, Saper CB, Hurley KM, Cechetto DF (1991) Organization of visceral and limbic connections in the insular cortex of the rat. J Comp Neurol 311:1-16.

Allen JJ, Chambers AS, Towers DN (2007) The many metrics of cardiac chronotropy: a pragmatic primer and a brief comparison of metrics. Biological psychology 74:243-262.

Almeida JR, Versace A, Mechelli A, Hassel S, Quevedo K, Kupfer DJ, Phillips ML (2009) Abnormal amygdala-prefrontal effective connectivity to happy faces differentiates bipolar from major depression. Biol Psychiatry 66:451-459.

Alvarez RP, Chen G, Bodurka J, Kaplan R, Grillon C (2011) Phasic and sustained fear in humans elicits distinct patterns of brain activity. Neuroimage 55:389-400.

Amaral DG, Price JL (1984) Amygdalo-cortical projections in the monkey (Macaca fascicularis). J Comp Neurol 230:465-496.

Amemori K, Graybiel AM (2012) Localized microstimulation of primate pregenual cingulate cortex induces negative decision-making. Nat Neurosci 15:776-785.

American Psychiatric Association A (2013) Diagnostic and statistical manual of mental disorders, fifth edition, 5th Edition. Arlington, VA: American Psychiatric Publishing.

Andersson JLR, Jenkinson M, Smith S (2007) Non-linear registration, aka Spatial normalisation. FMRIB technical report TR07JA2 In.

Anglada-Figueroa D, Quirk GJ (2005) Lesions of the basal amygdala block expression of conditioned fear but not extinction. J Neurosci 25:9680-9685.

APA (1994) Diagnostic and Statistical Manual of Mental Disorders 4th ed. Washington D.C.: American Psychiatric Press.

Appelhans BM, Luecken LJ (2006) Heart rate variability as an index of regulated emotional responding. Review of general psychology 10:229.

Aupperle RL, Allard CB, Grimes EM, Simmons AN, Flagan T, Behrooznia M, Cissell SH, Twamley EW, Thorp SR, Norman SB, Paulus MP, Stein MB (2012) Dorsolateral prefrontal cortex activation during emotional anticipation and neuropsychological performance in posttraumatic stress disorder. Archives of General Psychiatry 69:360-371.

Avants B, Gee JC (2004) Geodesic estimation for large deformation anatomical shape averaging and interpolation. Neuroimage 23 Suppl 1:S139-150.

Avery SN, Clauss JA, Winder DG, Woodward N, Heckers S, Blackford JU (2014) BNST neurocircuitry in humans. Neuroimage 91:311-323.

Baas D, Aleman A, Kahn RS (2004) Lateralization of amygdala activation: a systematic review of functional neuroimaging studies. Brain Res Brain Res Rev 45:96-103.

Barbas H (2000) Connections underlying the synthesis of cognition, memory, and emotion in primate prefrontal cortices. Brain Res Bull 52:319-330.

Barbas H, Saha S, Rempel-Clower N, Ghashghaei T (2003) Serial pathways from primate prefrontal cortex to autonomic areas may influence emotional expression. BMC Neurosci 4:25.

Barrash J, Tranel D, Anderson SW (2000) Acquired personality disturbances associated with bilateral damage to the ventromedial prefrontal region. Dev Neuropsychol 18:355-381.

Bechara A, Damasio AR, Damasio H, Anderson SW (1994) Insensitivity to future consequences following damage to human prefrontal cortex. Cognition 50:7-15.

Bechara A, Damasio H, Tranel D, Damasio AR (1997) Deciding advantageously before knowing the advantageous strategy. Science 275:1293-1295.

Bechara A, Damasio H, Damasio AR, Lee GP (1999) Different contributions of the human amygdala and ventromedial prefrontal cortex to decision-making. J Neurosci 19:5473-5481.

Beck AT, Steer RA, Brown GK (1996) Manual for the Beck Depression Inventory-II. San Antonio, TX: Psychological Corporation.

Bereza BG, Machado M, Einarson TR (2009) Systematic review and quality assessment of economic evaluations and quality-of-life studies related to generalized anxiety disorder. Clin Ther 31:1279-1308.

Berretta S, Pantazopoulos H, Caldera M, Pantazopoulos P, Pare D (2005) Infralimbic cortex activation increases c-Fos expression in intercalated neurons of the amygdala. Neuroscience 132:943-953.

Blair KS, Geraci M, Hollon N, Otero M, DeVido J, Majestic C, Jacobs M, Blair RJ, Pine DS (2010) Social norm processing in adult social phobia: atypically increased ventromedial frontal cortex responsiveness to unintentional (embarrassing) transgressions. Am J Psychiatry 167:1526-1532.

Blair RJ (2007) The amygdala and ventromedial prefrontal cortex in morality and psychopathy. Trends Cogn Sci 11:387-392.

Blair RJ (2008) The amygdala and ventromedial prefrontal cortex: functional contributions and dysfunction in psychopathy. Philos Trans R Soc Lond B Biol Sci 363:2557-2565.

Blair RJ, Cipolotti L (2000) Impaired social response reversal. A case of 'acquired sociopathy'. Brain 123 (Pt 6):1122-1141.

Blair RJ, Mitchell DG (2009) Psychopathy, attention and emotion. Psychol Med 39:543-555.

Blumer D, Benson DF (1975) Personality changes with frontal and temporal lesions. In: Psychiatric Aspects of Neurological Disease (Benson DF, Blumer D, eds). New York: Stratton.

Bradley MM, Codispoti M, Cuthbert BN, Lang PJ (2001) Emotion and motivation I: defensive and appetitive reactions in picture processing. Emotion 1:276-298.

Brett M, Leff AP, Rorden C, Ashburner J (2001) Spatial normalization of brain images with focal lesions using cost function masking. Neuroimage 14:486-500.

Bruce SE, Yonkers KA, Otto MW, Eisen JL, Weisberg RB, Pagano M, Shea MT, Keller MB (2005) Influence of psychiatric comorbidity on recovery and recurrence in generalized anxiety disorder, social phobia, and panic disorder: a 12-year prospective study. The American journal of psychiatry 162:1179-1187.

Camille N, Coricelli G, Sallet J, Pradat-Diehl P, Duhamel JR, Sirigu A (2004) The involvement of the orbitofrontal cortex in the experience of regret. Science 304:1167-1170.

Campos JJ, Mumme DL, Kermoian R, Campos RG (1994) A functionalist perspective on the nature of emotion. Monogr Soc Res Child Dev 59:284-303.

Carp J (2012) The secret lives of experiments: methods reporting in the fMRI literature. Neuroimage 63:289-300.

Cereda C, Ghika J, Maeder P, Bogousslavsky J (2002) Strokes restricted to the insular cortex. Neurology 59:1950-1955.

Chen G, Saad ZS, Britton JC, Pine DS, Cox RW (2013) Linear mixed-effects modeling approach to FMRI group analysis. Neuroimage 73:176-190.

Clark L, Bechara A, Damasio H, Aitken MR, Sahakian BJ, Robbins TW (2008) Differential effects of insular and ventromedial prefrontal cortex lesions on risky decision-making. Brain 131:1311-1322.

Cleckley H (1976) The Mask of Sanity 5th edition. St. Louis: Mosby.

Codispoti M, Bradley MM, Lang PJ (2001) Affective reactions to briefly presented pictures. Psychophysiology 38:474-478.

Cook PA, Bai Y, Nedjati-Gilani S, Seunarine KK, Hall MG, Parker GJ (2006) Camino: Open-Source Diffusion-MRI Reconstruction and Processing. In: 14th Scientific Meeting of the International Society for Magnetic Resonance in Medicine. Seattle, WA.

Costafreda SG, Brammer MJ, David AS, Fu CH (2008) Predictors of amygdala activation during the processing of emotional stimuli: a meta-analysis of 385 PET and fMRI studies. Brain Res Rev 58:57-70.

Cotter D, Mackay D, Landau S, Kerwin R, Everall I (2001) Reduced glial cell density and neuronal size in the anterior cingulate cortex in major depressive disorder. Archives of General Psychiatry 58:545-553.

Cox RW (1996) AFNI: software for analysis and visualization of functional magnetic resonance neuroimages. Comput Biomed Res 29:162-173.

Craig AD (2002) How do you feel? Interoception: the sense of the physiological condition of the body. Nat Rev Neurosci 3:655-666.

Craig MC, Catani M, Deeley Q, Latham R, Daly E, Kanaan R, Picchioni M, McGuire PK, Fahy T, Murphy DG (2009) Altered connections on the road to psychopathy. Mol Psychiatry 14:946-953, 907.

Critchley HD (2005) Neural mechanisms of autonomic, affective, and cognitive integration. J Comp Neurol 493:154-166.

Critchley HD, Mathias CJ, Dolan RJ (2001) Neural activity in the human brain relating to uncertainty and arousal during anticipation. Neuron 29:537-545.

Cuijpers P, Karyotaki E, Weitz E, Andersson G, Hollon SD, van Straten A (2014) The effects of psychotherapies for major depression in adults on remission, recovery and improvement: A meta-analysis. J Affect Disord 159C:118-126.

Cuthbert BN, Insel TR (2013) Toward the future of psychiatric diagnosis: the seven pillars of RDoC. BMC medicine 11:126.

Dai W, Garcia D, de Bazelaire C, Alsop DC (2008) Continuous flow-driven inversion for arterial spin labeling using pulsed radio frequency and gradient fields. Magnetic resonance in medicine : official journal of the Society of Magnetic Resonance in Medicine / Society of Magnetic Resonance in Medicine 60:1488-1497.

Damasio AR (1994) Descartes' error: emotion, reason and the human brain. New York: G.P. Putnam.

Damasio AR, Tranel D, Damasio H (1990) Individuals with sociopathic behavior caused by frontal damage fail to respond autonomically to social stimuli. Behav Brain Res 41:81-94.

Damasio H, Grabowski T, Frank R, Galaburda AM, Damasio AR (1994) The return of Phineas Gage: clues about the brain from the skull of a famous patient. Science 264:1102-1105.

Darwin C (1872) The expression of the emotions in man and animals. London: John Murray.

Davidson RJ (2002) Anxiety and affective style: role of prefrontal cortex and amygdala. Biol Psychiatry 51:68-80.

Davidson RJ, Jackson DC, Kalin NH (2000) Emotion, plasticity, context, and regulation: perspectives from affective neuroscience. Psychol Bull 126:890-909.

Davis M, Shi C (1999) The extended amygdala: are the central nucleus of the amygdala and the bed nucleus of the stria terminalis differentially involved in fear versus anxiety? Ann N Y Acad Sci 877:281-291.

Davis M, Whalen PJ (2001) The amygdala: vigilance and emotion. Mol Psychiatry 6:13-34.

Dawson M, Schell D (2007) The Electrodermal System. In: Handbook of psychophysiology, 3rd Edition (Cacioppo JT, Berntson GG, Tassinary LG, eds). Cambridge [England] ; New York: Cambridge University Press.

Delgado MR, Nearing KI, Ledoux JE, Phelps EA (2008) Neural circuitry underlying the regulation of conditioned fear and its relation to extinction. Neuron 59:829-838.

Di Martino A, Scheres A, Margulies DS, Kelly AM, Uddin LQ, Shehzad Z, Biswal B, Walters JR, Castellanos FX, Milham MP (2008) Functional connectivity of human striatum: a resting state FMRI study. Cerebral cortex 18:2735-2747.

Dolan RJ, Vuilleumier P (2003) Amygdala automaticity in emotional processing. Annals of the New York Academy of Sciences 985:348-355.

Dong HW, Petrovich GD, Swanson LW (2001a) Topography of projections from amygdala to bed nuclei of the stria terminalis. Brain Res Brain Res Rev 38:192-246.

Dong HW, Petrovich GD, Watts AG, Swanson LW (2001b) Basic organization of projections from the oval and fusiform nuclei of the bed nuclei of the stria terminalis in adult rat brain. J Comp Neurol 436:430-455.

Drevets WC (2003) Neuroimaging abnormalities in the amygdala in mood disorders. Ann N Y Acad Sci 985:420-444.

Drevets WC, Bogers W, Raichle ME (2002) Functional anatomical correlates of antidepressant drug treatment assessed using PET measures of regional glucose metabolism. Eur Neuropsychopharmacol 12:527-544.

Drevets WC, Price JL, Furey ML (2008) Brain structural and functional abnormalities in mood disorders: implications for neurocircuitry models of depression. Brain structure & function 213:93-118.

Drevets WC, Videen TO, Price JL, Preskorn SH, Carmichael ST, Raichle ME (1992) A functional anatomical study of unipolar depression. J Neurosci 12:3628-3641.

Drevets WC, Price JL, Simpson JR, Jr., Todd RD, Reich T, Vannier M, Raichle ME (1997) Subgenual prefrontal cortex abnormalities in mood disorders. Nature 386:824-827.

Dunsmoor JE, Bandettini PA, Knight DC (2007) Impact of continuous versus intermittent CS-UCS pairing on human brain activation during Pavlovian fear conditioning. Behav Neurosci 121:635-642.

Ebeling U, von Cramon D (1992) Topography of the uncinate fascicle and adjacent temporal fiber tracts. Acta Neurochir (Wien) 115:143-148.

Egner T, Etkin A, Gale S, Hirsch J (2008) Dissociable neural systems resolve conflict from emotional versus nonemotional distracters. Cerebral cortex 18:1475-1484.

Eslinger PJ, Damasio AR (1985) Severe disturbance of higher cognition after bilateral frontal lobe ablation: patient EVR. Neurology 35:1731-1741.

Etkin A, Wager TD (2007) Functional neuroimaging of anxiety: a meta-analysis of emotional processing in PTSD, social anxiety disorder, and specific phobia. Am J Psychiatry 164:1476-1488.

Etkin A, Schatzberg AF (2011) Common abnormalities and disorder-specific compensation during implicit regulation of emotional processing in generalized anxiety and major depressive disorders. Am J Psychiatry 168:968-978.

Etkin A, Egner T, Peraza DM, Kandel ER, Hirsch J (2006) Resolving emotional conflict: a role for the rostral anterior cingulate cortex in modulating activity in the amygdala. Neuron 51:871-882.

Ewbank MP, Barnard PJ, Croucher CJ, Ramponi C, Calder AJ (2009) The amygdala response to images with impact. Social cognitive and affective neuroscience 4:127-133.

Feinstein JS, Adolphs R, Damasio A, Tranel D (2011) The human amygdala and the induction and experience of fear. Curr Biol 21:34-38.

Feinstein JS, Buzza C, Hurlemann R, Follmer RL, Dahdaleh NS, Coryell WH, Welsh MJ, Tranel D, Wemmie JA (2013) Fear and panic in humans with bilateral amygdala damage. Nat Neurosci 16:270-272.

Fellows LK (2011) Orbitofrontal contributions to value-based decision making: evidence from humans with frontal lobe damage. Annals of the New York Academy of Sciences 1239:51-58.

Fellows LK, Farah MJ (2003) Ventromedial frontal cortex mediates affective shifting in humans: evidence from a reversal learning paradigm. Brain 126:1830-1837.

First MB, ed (2002) Structured Clinical Interview for DSM-IV-TR Axis I Disorders, Research Version, Non-patient Edition. (SCID-I/NP). New York: Biometrics Research, New York State Psychiatric Institute.

Forman SD, Cohen JD, Fitzgerald M, Eddy WF, Mintun MA, Noll DC (1995) Improved Assessment of Significant Activation in Functional Magnetic Resonance Imaging (fMRI): Use of a Cluster-Size Threshold. Magnetic Resonance in Medicine 33:636-647.

Fox AS, Shelton SE, Oakes TR, Converse AK, Davidson RJ, Kalin NH (2010) Orbitofrontal cortex lesions alter anxiety-related activity in the primate bed nucleus of stria terminalis. J Neurosci 30:7023-7027.

Fox PT, Raichle ME (1986) Focal physiological uncoupling of cerebral blood flow and oxidative metabolism during somatosensory stimulation in human subjects. Proc Natl Acad Sci U S A 83:1140-1144.

Fuster JM (2008a) Chapter 2 - Anatomy of the Prefrontal Cortex. In: The Prefrontal Cortex (Fourth Edition) (Fuster JM, ed), pp 171-219. San Diego: Academic Press.

Fuster JM (2008b) Chapter 5 - Human Neuropsychology. In: The Prefrontal Cortex (Fourth Edition) (Fuster JM, ed), pp 171-219. San Diego: Academic Press.

Garfinkle EJ, Behar E (2012) Advances in psychotherapy for generalized anxiety disorder. Current psychiatry reports 14:203-210.

Ghashghaei HT, Hilgetag CC, Barbas H (2007) Sequence of information processing for emotions based on the anatomic dialogue between prefrontal cortex and amygdala. Neuroimage 34:905-923.

Gibbons RD, Hur K, Brown CH, Davis JM, Mann JJ (2012) Benefits from antidepressants: synthesis of 6-week patient-level outcomes from double-blind placebo-controlled randomized trials of fluoxetine and venlafaxine. Archives of General Psychiatry 69:572-579.

Gilmartin MR, McEchron MD (2005) Single neurons in the medial prefrontal cortex of the rat exhibit tonic and phasic coding during trace fear conditioning. Behav Neurosci 119:1496-1510.

Gorman JM, Sloan RP (2000) Heart rate variability in depressive and anxiety disorders. American heart journal 140:S77-S83.

Gozzi A, Jain A, Giovannelli A, Bertollini C, Crestan V, Schwarz AJ, Tsetsenis T, Ragozzino D, Gross CT, Bifone A (2010) A neural switch for active and passive fear. Neuron 67:656-666.

Grabenhorst F, Rolls ET (2011) Value, pleasure and choice in the ventral prefrontal cortex. Trends Cogn Sci 15:56-67.

Grafman J, Schwab K, Warden D, Pridgen A, Brown HR, Salazar AM (1996) Frontal lobe injuries, violence, and aggression: a report of the Vietnam Head Injury Study. Neurology 46:1231-1238.

Greenberg T, Carlson JM, Cha J, Hajcak G, Mujica-Parodi LR (2013) Ventromedial prefrontal cortex reactivity is altered in generalized anxiety disorder during fear generalization. Depress Anxiety 30:242-250.

Greicius MD, Flores BH, Menon V, Glover GH, Solvason HB, Kenna H, Reiss AL, Schatzberg AF (2007) Resting-state functional connectivity in major depression: abnormally increased contributions from subgenual cingulate cortex and thalamus. Biol Psychiatry 62:429-437.

Gross JJ (2002) Emotion regulation: affective, cognitive, and social consequences. Psychophysiology 39:281-291.

Grupe DW, Nitschke JB (2013) Uncertainty and anticipation in anxiety: an integrated neurobiological and psychological perspective. Nat Rev Neurosci 14:488-501.
Grupe DW, Oathes DJ, Nitschke JB (2013) Dissecting the anticipation of aversion reveals dissociable neural networks. Cerebral cortex 23:1874-1883.
Gyurak A, Gross JJ, Etkin A (2011) Explicit and implicit emotion regulation: a dual-process framework. Cogn Emot 25:400-412.
Hare RD (1965) Psychopathy, Fear Arousal and Anticipated Pain. Psychol Rep 16:499-502.
Hare RD (2003) The Hare psychopathy checklist-revised (2nd ed.). Toronto: Multi-Health Systems.
Hare RD, Frazelle J, Cox DN (1978) Psychopathy and physiological responses to threat of an aversive stimulus. Psychophysiology 15:165-172.
Hare TA, Camerer CF, Rangel A (2009) Self-control in decision-making involves modulation of the vmPFC valuation system. Science 324:646-648.
Harlow JM (1848) Passage of an iron rod through the head. The Boston Medical and Surgical Journal 39:389-393.
Harlow JM (1868) Recovery from the passage of an iron bar through the head. Publications of the Massachusetts Medical Society 2:327-347.
Harrison BJ, Pujol J, Soriano-Mas C, Hernandez-Ribas R, Lopez-Sola M, Ortiz H, Alonso P, Deus J, Menchon JM, Real E, Segalas C, Contreras-Rodriguez O, Blanco-Hinojo L, Cardoner N (2012) Neural correlates of moral sensitivity in obsessive-compulsive disorder. Arch Gen Psychiatry 69:741-749.
Heberlein AS, Padon AA, Gillihan SJ, Farah MJ, Fellows LK (2008) Ventromedial frontal lobe plays a critical role in facial emotion recognition. J Cogn Neurosci 20:721-733.
Heimer L, Harlan RE, Alheid GF, Garcia MM, de Olmos J (1997) Substantia innominata: a notion which impedes clinical-anatomical correlations in neuropsychiatric disorders. Neuroscience 76:957-1006.
Heller AS, Johnstone T, Light SN, Peterson MJ, Kolden GG, Kalin NH, Davidson RJ (2013) Relationships between changes in sustained fronto-striatal connectivity and positive affect in major depression resulting from antidepressant treatment. The American journal of psychiatry 170:197-206.
Hermann A, Schafer A, Walter B, Stark R, Vaitl D, Schienle A (2007) Diminished medial prefrontal cortex activity in blood-injection-injury phobia. Biol Psychol 75:124-130.
Hermann A, Schafer A, Walter B, Stark R, Vaitl D, Schienle A (2009) Emotion regulation in spider phobia: role of the medial prefrontal cortex. Soc Cogn Affect Neurosci 4:257-267.
Hiatt KD, Newman JP (2006) Understanding psychopathy: The cognitive side. In: Handbook of Psychopathy (Patrick CJ, ed), pp 334-352. New York: Guilford Press.
Holland PC, Gallagher M (1999) Amygdala circuitry in attentional and representational processes. Trends in cognitive sciences 3:65-73.
Hua K, Zhang J, Wakana S, Jiang H, Li X, Reich DS, Calabresi PA, Pekar JJ, van Zijl PC, Mori S (2008) Tract probability maps in stereotaxic spaces: analyses of white matter anatomy and tract-specific quantification. Neuroimage 39:336-347.

Insel T, Cuthbert B, Garvey M, Heinssen R, Pine DS, Quinn K, Sanislow C, Wang P (2010) Research domain criteria (RDoC): toward a new classification framework for research on mental disorders. Am J Psychiatry 167:748-751.

James W (1884) What is an emotion? Mind:188-205.

Jennings JH, Sparta DR, Stamatakis AM, Ung RL, Pleil KE, Kash TL, Stuber GD (2013) Distinct extended amygdala circuits for divergent motivational states. Nature 496:224-228.

Jezzard P, Clare S (1999) Sources of distortion in functional MRI data. Hum Brain Mapp 8:80-85.

Johnstone T, van Reekum CM, Urry HL, Kalin NH, Davidson RJ (2007) Failure to regulate: counterproductive recruitment of top-down prefrontal-subcortical circuitry in major depression. J Neurosci 27:8877-8884.

Johnstone T, Ores Walsh KS, Greischar LL, Alexander AL, Fox AS, Davidson RJ, Oakes TR (2006) Motion correction and the use of motion covariates in multiple-subject fMRI analysis. Hum Brain Mapp 27:779-788.

Jones DK, Basser PJ (2004) "Squashing peanuts and smashing pumpkins": how noise distorts diffusion-weighted MR data. Magn Reson Med 52:979-993.

Jose AD, Collison D (1970) The normal range and determinants of the intrinsic heart rate in man. Cardiovasc Res 4:160-167.

Kaada BR, Pribram KH, Epstein JA (1949) Respiratory and vascular responses in monkeys from temporal pole, insula, orbital surface and cingulate gyrus; a preliminary report. J Neurophysiol 12:347-356.

Kalin NH, Shelton SE, Fox AS, Oakes TR, Davidson RJ (2005) Brain regions associated with the expression and contextual regulation of anxiety in primates. Biological Psychiatry 58:796-804.

Kapp BS, Gallagher M, Underwood MD, McNall CL, Whitehorn D (1982) Cardiovascular responses elicited by electrical stimulation of the amygdala central nucleus in the rabbit. Brain Res 234:251-262.

Kapur S, Phillips AG, Insel TR (2012) Why has it taken so long for biological psychiatry to develop clinical tests and what to do about it? Mol Psychiatry 17:1174-1179.

Keedwell P, Drapier D, Surguladze S, Giampietro V, Brammer M, Phillips M (2009) Neural markers of symptomatic improvement during antidepressant therapy in severe depression: subgenual cingulate and visual cortical responses to sad, but not happy, facial stimuli are correlated with changes in symptom score. J Psychopharmacol 23:775-788.

Kennerley SW, Wallis JD (2009) Evaluating choices by single neurons in the frontal lobe: outcome value encoded across multiple decision variables. Eur J Neurosci 29:2061-2073.

Kennerley SW, Dahmubed AF, Lara AH, Wallis JD (2009) Neurons in the frontal lobe encode the value of multiple decision variables. Journal of Cognitive Neuroscience 21:1162-1178.

Kessler RC, Chiu WT, Demler O, Merikangas KR, Walters EE (2005a) Prevalence, severity, and comorbidity of 12-month DSM-IV disorders in the National Comorbidity Survey Replication. Archives of General Psychiatry 62:617-627.

Kessler RC, Berglund P, Demler O, Jin R, Merikangas KR, Walters EE (2005b) Lifetime prevalence and age-of-onset distributions of DSM-IV disorders in the National Comorbidity Survey Replication. Archives of general psychiatry 62:593-602.

Kim H, Somerville LH, Johnstone T, Alexander AL, Whalen PJ (2003) Inverse amygdala and medial prefrontal cortex responses to surprised faces. Neuroreport 14:2317-2322.

Kim MJ, Whalen PJ (2009) The structural integrity of an amygdala-prefrontal pathway predicts trait anxiety. J Neurosci 29:11614-11618.

Kim MJ, Gee DG, Loucks RA, Davis FC, Whalen PJ (2010) Anxiety dissociates dorsal and ventral medial prefrontal cortex functional connectivity with the amygdala at rest. Cereb Cortex 21:1667-1673.

Kim MJ, Loucks RA, Palmer AL, Brown AC, Solomon KM, Marchante AN, Whalen PJ (2011) The structural and functional connectivity of the amygdala: From normal emotion to pathological anxiety. Behav Brain Res 223:403-410.

Kim SY, Adhikari A, Lee SY, Marshel JH, Kim CK, Mallory CS, Lo M, Pak S, Mattis J, Lim BK, Malenka RC, Warden MR, Neve R, Tye KM, Deisseroth K (2013) Diverging neural pathways assemble a behavioural state from separable features in anxiety. Nature 496:219-223.

Kling A (1972) Effects of amygdalectomy on social-affective behavior in non-human primates. In: The neurobiology of the amygdala (Eleftheriou BE, ed), pp 511-536. New York: Plenum Press.

Koenigs M, Grafman J (2009a) The functional neuroanatomy of depression: distinct roles for ventromedial and dorsolateral prefrontal cortex. Behav Brain Res 201:239-243.

Koenigs M, Grafman J (2009b) Posttraumatic stress disorder: the role of medial prefrontal cortex and amygdala. Neuroscientist 15:540-548.

Koenigs M, Kruepke M, Newman JP (2010) Economic decision-making in psychopathy: a comparison with ventromedial prefrontal lesion patients. Neuropsychologia 48:2198-2204.

Koenigs M, Baskin-Sommers A, Zeier J, Newman JP (2011) Investigating the neural correlates of psychopathy: a critical review. Mol Psychiatry 16:792-799.

Koenigs M, Kruepke M, Zeier J, Newman JP (2012) Utilitarian moral judgment in psychopathy. Social cognitive and affective neuroscience 7:708-714.

Koenigs M, Huey ED, Calamia M, Raymont V, Tranel D, Grafman J (2008a) Distinct regions of prefrontal cortex mediate resistance and vulnerability to depression. J Neurosci 28:12341-12348.

Koenigs M, Huey ED, Raymont V, Cheon B, Solomon J, Wassermann EM, Grafman J (2008b) Focal brain damage protects against post-traumatic stress disorder in combat veterans. Nat Neurosci 11:232-237.

Kross E, Davidson M, Weber J, Ochsner K (2009) Coping with emotions past: the neural bases of regulating affect associated with negative autobiographical memories. Biol Psychiatry 65:361-366.

Kuhn S, Gallinat J (2012) Gray Matter Correlates of Posttraumatic Stress Disorder: A Quantitative Meta-Analysis. Biol Psychiatry.

Kwan CL, Crawley AP, Mikulis DJ, Davis KD (2000) An fMRI study of the anterior cingulate cortex and surrounding medial wall activations evoked by noxious cutaneous heat and cold stimuli. Pain 85:359-374.

Lane RD, McRae K, Reiman EM, Chen K, Ahern GL, Thayer JF (2009) Neural correlates of heart rate variability during emotion. Neuroimage 44:213-222.

Lang PJ, Bradley MM, Cuthbert BN (2008) International affective picture system (IAPS): Affective ratings of pictures and instruction manual. Technical Report A-8. Gainesville, FL: University of Florida.

Lanteaume L, Khalfa S, Regis J, Marquis P, Chauvel P, Bartolomei F (2007) Emotion induction after direct intracerebral stimulations of human amygdala. Cerebral cortex 17:1307-1313.

Lazar M, Weinstein DM, Tsuruda JS, Hasan KM, Arfanakis K, Meyerand ME, Badie B, Rowley HA, Haughton V, Field A, Alexander AL (2003) White matter tractography using diffusion tensor deflection. Hum Brain Mapp 18:306-321.

LeDoux JE, Iwata J, Cicchetti P, Reis DJ (1988) Different projections of the central amygdaloid nucleus mediate autonomic and behavioral correlates of conditioned fear. J Neurosci 8:2517-2529.

Likhtik E, Pelletier JG, Paz R, Pare D (2005) Prefrontal control of the amygdala. J Neurosci 25:7429-7437.

Little JP, Carter AG (2013) Synaptic mechanisms underlying strong reciprocal connectivity between the medial prefrontal cortex and basolateral amygdala. J Neurosci 33:15333-15342.

Lorberbaum JP, Kose S, Johnson MR, Arana GW, Sullivan LK, Hamner MB, Ballenger JC, Lydiard RB, Brodrick PS, Bohning DE, George MS (2004) Neural correlates of speech anticipatory anxiety in generalized social phobia. Neuroreport 15:2701-2705.

Maclean PD (1954) The limbic system and its hippocampal formation; studies in animals and their possible application to man. Journal of neurosurgery 11:29-44.

Mai JK, Assheuer J, Paxinos G (2003) Atlas of the Human Brain, 2nd ed. San Diego: Elsevier Academic Press.

Maldjian JA, Laurienti PJ, Kraft RA, Burdette JH (2003) An automated method for neuroanatomic and cytoarchitectonic atlas-based interrogation of fMRI data sets. Neuroimage 19:1233-1239.

Manji HK, Moore GJ, Rajkowska G, Chen G (2000) Neuroplasticity and cellular resilience in mood disorders. Molecular psychiatry 5:578-593.

Marsh AA, Finger EC, Mitchell DG, Reid ME, Sims C, Kosson DS, Towbin KE, Leibenluft E, Pine DS, Blair RJ (2008) Reduced amygdala response to fearful expressions in children and adolescents with callous-unemotional traits and disruptive behavior disorders. Am J Psychiatry 165:712-720.

Matthews SC, Strigo IA, Simmons AN, Yang TT, Paulus MP (2008) Decreased functional coupling of the amygdala and supragenual cingulate is related to increased depression in unmedicated individuals with current major depressive disorder. J Affect Disord 111:13-20.

Mayberg HS, Brannan SK, Tekell JL, Silva JA, Mahurin RK, McGinnis S, Jerabek PA (2000) Regional metabolic effects of fluoxetine in major depression: serial changes and relationship to clinical response. Biol Psychiatry 48:830-843.

Mayberg HS, Lozano AM, Voon V, McNeely HE, Seminowicz D, Hamani C, Schwalb JM, Kennedy SH (2005) Deep brain stimulation for treatment-resistant depression. Neuron 45:651-660.

Mayberg HS, Liotti M, Brannan SK, McGinnis S, Mahurin RK, Jerabek PA, Silva JA, Tekell JL, Martin CC, Lancaster JL, Fox PT (1999) Reciprocal limbic-cortical function and negative mood: converging PET findings in depression and normal sadness. Am J Psychiatry 156:675-682.

McDonald AJ, Mascagni F, Guo L (1996) Projections of the medial and lateral prefrontal cortices to the amygdala: a Phaseolus vulgaris leucoagglutinin study in the rat. Neuroscience 71:55-75.

McDonald AJ, Shammah-Lagnado SJ, Shi C, Davis M (1999) Cortical afferents to the extended amygdala. Annals of the New York Academy of Sciences 877:309-338.

McEvoy PM, Mahoney AE (2012) To be sure, to be sure: intolerance of uncertainty mediates symptoms of various anxiety disorders and depression. Behavior therapy 43:533-545.

McEwen BS, Sapolsky RM (1995) Stress and cognitive function. Current opinion in neurobiology 5:205-216.

McGrath CL, Kelley ME, Holtzheimer PE, Dunlop BW, Craighead WE, Franco AR, Craddock RC, Mayberg HS (2013) Toward a neuroimaging treatment selection biomarker for major depressive disorder. JAMA Psychiatry 70:821-829.

Melzig CA, Weike AI, Hamm AO, Thayer JF (2009) Individual differences in fear-potentiated startle as a function of resting heart rate variability: implications for panic disorder. Int J Psychophysiol 71:109-117.

Milad MR, Quirk GJ (2002) Neurons in medial prefrontal cortex signal memory for fear extinction. Nature 420:70-74.

Milad MR, Rauch SL, Pitman RK, Quirk GJ (2006) Fear extinction in rats: implications for human brain imaging and anxiety disorders. Biol Psychol 73:61-71.

Miller EK, Cohen JD (2001) An integrative theory of prefrontal cortex function. Annu Rev Neurosci 24:167-202.

Mori S, Wakana S, Nagae-Poetscher L, van Zijl PCM (2005) MRI Atlas of Human White Matter. Amsterdam: Elsevier.

Myers-Schulz B, Koenigs M (2012) Functional anatomy of ventromedial prefrontal cortex: implications for mood and anxiety disorders. Mol Psychiatry 17:132-141.

Nacewicz BM, Dalton KM, Johnstone T, Long MT, McAuliff EM, Oakes TR, Alexander AL, Davidson RJ (2006) Amygdala volume and nonverbal social impairment in adolescent and adult males with autism. Arch Gen Psychiatry 63:1417-1428.

Neafsey EJ (1990) Prefrontal cortical control of the autonomic nervous system: anatomical and physiological observations. Prog Brain Res 85:147-165; discussion 165-146.

Nitschke JB, Sarinopoulos I, Mackiewicz KL, Schaefer HS, Davidson RJ (2006) Functional neuroanatomy of aversion and its anticipation. Neuroimage 29:106-116.

Nitschke JB, Sarinopoulos I, Oathes DJ, Johnstone T, Whalen PJ, Davidson RJ, Kalin NH (2009) Anticipatory activation in the amygdala and anterior cingulate in generalized anxiety disorder and prediction of treatment response. The American journal of psychiatry 166:302-310.

O'Doherty JP (2004) Reward representations and reward-related learning in the human brain: insights from neuroimaging. Curr Opin Neurobiol 14:769-776.
Ochsner KN, Gross JJ (2005) The cognitive control of emotion. Trends in cognitive sciences 9:242-249.
Ochsner KN, Gross JJ (2008) Cognitive emotion regulation insights from social cognitive and affective neuroscience. Current Directions in Psychological Science 17:153-158.
Ochsner KN, Bunge SA, Gross JJ, Gabrieli JD (2002) Rethinking feelings: an FMRI study of the cognitive regulation of emotion. Journal of Cognitive Neuroscience 14:1215-1229.
Ochsner KN, Ray RD, Cooper JC, Robertson ER, Chopra S, Gabrieli JD, Gross JJ (2004) For better or for worse: neural systems supporting the cognitive down- and up-regulation of negative emotion. Neuroimage 23:483-499.
Okonkwo OC, Xu G, Oh JM, Dowling NM, Carlsson CM, Gallagher CL, Birdsill AC, Palotti M, Wharton W, Hermann BP, Larue A, Bendlin BB, Rowley HA, Asthana S, Sager MA, Johnson SC (2012) Cerebral Blood Flow is Diminished in Asymptomatic Middle-Aged Adults with Maternal History of Alzheimer's Disease. Cerebral cortex.
Oler JA, Birn RM, Patriat R, Fox AS, Shelton SE, Burghy CA, Stodola DE, Essex MJ, Davidson RJ, Kalin NH (2012) Evidence for coordinated functional activity within the extended amygdala of non-human and human primates. Neuroimage 61:1059-1066.
Ongur D, Price JL (2000) The organization of networks within the orbital and medial prefrontal cortex of rats, monkeys and humans. Cereb Cortex 10:206-219.
Ongur D, Drevets WC, Price JL (1998) Glial reduction in the subgenual prefrontal cortex in mood disorders. Proc Natl Acad Sci U S A 95:13290-13295.
Oppenheimer SM, Gelb A, Girvin JP, Hachinski VC (1992) Cardiovascular effects of human insular cortex stimulation. Neurology 42:1727-1732.
Papez JW (1937) A proposed mechanism of emotion. Archives of Neurology and Psychiatry 38:725-743.
Patrick CJ, Bradley MM, Lang PJ (1993) Emotion in the criminal psychopath: startle reflex modulation. J Abnorm Psychol 102:82-92.
Petrovic P, Dietrich T, Fransson P, Andersson J, Carlsson K, Ingvar M (2005) Placebo in emotional processing--induced expectations of anxiety relief activate a generalized modulatory network. Neuron 46:957-969.
Phan KL, Wager T, Taylor SF, Liberzon I (2002) Functional neuroanatomy of emotion: a meta-analysis of emotion activation studies in PET and fMRI. Neuroimage 16:331-348.
Phelps EA, LeDoux JE (2005) Contributions of the amygdala to emotion processing: from animal models to human behavior. Neuron 48:175-187.
Phelps EA, Delgado MR, Nearing KI, LeDoux JE (2004) Extinction learning in humans: role of the amygdala and vmPFC. Neuron 43:897-905.
Pierpaoli C, Basser PJ (1996) Toward a quantitative assessment of diffusion anisotropy. Magn Reson Med 36:893-906.
Pizzagalli DA (2011) Frontocingulate dysfunction in depression: toward biomarkers of treatment response. Neuropsychopharmacology 36:183-206.

Ploghaus A, Tracey I, Gati JS, Clare S, Menon RS, Matthews PM, Rawlins JN (1999) Dissociating pain from its anticipation in the human brain. Science 284:1979-1981.

Poldrack RA (2007) Region of interest analysis for fMRI. Social cognitive and affective neuroscience 2:67-70.

Postuma RB, Dagher A (2006) Basal ganglia functional connectivity based on a meta-analysis of 126 positron emission tomography and functional magnetic resonance imaging publications. Cerebral cortex 16:1508-1521.

Power JD, Barnes KA, Snyder AZ, Schlaggar BL, Petersen SE (2012) Spurious but systematic correlations in functional connectivity MRI networks arise from subject motion. Neuroimage 59:2142-2154.

Price JL, Amaral DG (1981) An autoradiographic study of the projections of the central nucleus of the monkey amygdala. J Neurosci 1:1242-1259.

Qin P, Northoff G (2011) How is our self related to midline regions and the default-mode network? Neuroimage 57:1221-1233.

Quirk GJ, Gehlert DR (2003) Inhibition of the amygdala: key to pathological states? Ann N Y Acad Sci 985:263-272.

Quirk GJ, Beer JS (2006) Prefrontal involvement in the regulation of emotion: convergence of rat and human studies. Current opinion in neurobiology 16:723-727.

Quirk GJ, Garcia R, Gonzalez-Lima F (2006) Prefrontal mechanisms in extinction of conditioned fear. Biol Psychiatry 60:337-343.

Quirk GJ, Russo GK, Barron JL, Lebron K (2000) The role of ventromedial prefrontal cortex in the recovery of extinguished fear. J Neurosci 20:6225-6231.

Quirk GJ, Likhtik E, Pelletier JG, Pare D (2003) Stimulation of medial prefrontal cortex decreases the responsiveness of central amygdala output neurons. J Neurosci 23:8800-8807.

Rauch SL, Shin LM, Phelps EA (2006) Neurocircuitry models of posttraumatic stress disorder and extinction: human neuroimaging research--past, present, and future. Biol Psychiatry 60:376-382.

Rorden C, Karnath HO, Bonilha L (2007) Improving lesion-symptom mapping. Journal of Cognitive Neuroscience 19:1081-1088.

Rosenkranz JA, Moore H, Grace AA (2003) The prefrontal cortex regulates lateral amygdala neuronal plasticity and responses to previously conditioned stimuli. J Neurosci 23:11054-11064.

Roy AK, Shehzad Z, Margulies DS, Kelly AM, Uddin LQ, Gotimer K, Biswal BB, Castellanos FX, Milham MP (2009) Functional connectivity of the human amygdala using resting state fMRI. Neuroimage 45:614-626.

Royer S, Martina M, Pare D (2000) Bistable behavior of inhibitory neurons controlling impulse traffic through the amygdala: role of a slowly deinactivating K+ current. J Neurosci 20:9034-9039.

Sabatinelli D, Lang PJ, Bradley MM, Costa VD, Keil A (2009) The timing of emotional discrimination in human amygdala and ventral visual cortex. J Neurosci 29:14864-14868.

Sapolsky RM (1996) Why stress is bad for your brain. Science 273:749-750.

Sarinopoulos I, Grupe DW, Mackiewicz KL, Herrington JD, Lor M, Steege EE, Nitschke JB (2010) Uncertainty during anticipation modulates neural responses to aversion in human insula and amygdala. Cerebral cortex 20:929-940.

Sawamoto N, Honda M, Okada T, Hanakawa T, Kanda M, Fukuyama H, Konishi J, Shibasaki H (2000) Expectation of pain enhances responses to nonpainful somatosensory stimulation in the anterior cingulate cortex and parietal operculum/posterior insula: an event-related functional magnetic resonance imaging study. J Neurosci 20:7438-7445.

Schoenbaum G, Roesch M (2005) Orbitofrontal cortex, associative learning, and expectancies. Neuron 47:633-636.

Schoenbaum G, Roesch MR, Stalnaker TA, Takahashi YK (2009) A new perspective on the role of the orbitofrontal cortex in adaptive behaviour. Nat Rev Neurosci 10:885-892.

Sheline YI, Barch DM, Donnelly JM, Ollinger JM, Snyder AZ, Mintun MA (2001) Increased amygdala response to masked emotional faces in depressed subjects resolves with antidepressant treatment: an fMRI study. Biol Psychiatry 50:651-658.

Shi CJ, Cassell MD (1998) Cortical, thalamic, and amygdaloid connections of the anterior and posterior insular cortices. J Comp Neurol 399:440-468.

Shin LM, Rauch SL, Pitman RK (2006) Amygdala, medial prefrontal cortex, and hippocampal function in PTSD. Annals of the New York Academy of Sciences 1071:67-79.

Sierra-Mercado D, Jr., Corcoran KA, Lebron-Milad K, Quirk GJ (2006) Inactivation of the ventromedial prefrontal cortex reduces expression of conditioned fear and impairs subsequent recall of extinction. Eur J Neurosci 24:1751-1758.

Simmons A, Strigo I, Matthews SC, Paulus MP, Stein MB (2006) Anticipation of aversive visual stimuli is associated with increased insula activation in anxiety-prone subjects. Biol Psychiatry 60:402-409.

Singer T, Critchley HD, Preuschoff K (2009) A common role of insula in feelings, empathy and uncertainty. Trends in cognitive sciences 13:334-340.

Smith SM (2002) Fast robust automated brain extraction. Hum Brain Mapp 17:143-155.

Solomon RC (2010) The Philosophy of Emotions. In: Handbook of emotions (Lewis MJ, Barrett LF, Haviland-Jones JM, eds). New York: Guilford Press.

Somerville LH, Whalen PJ, Kelley WM (2010) Human bed nucleus of the stria terminalis indexes hypervigilant threat monitoring. Biol Psychiatry 68:416-424.

Somerville LH, Wagner DD, Wig GS, Moran JM, Whalen PJ, Kelley WM (2013) Interactions between transient and sustained neural signals support the generation and regulation of anxious emotion. Cereb Cortex 23:49-60.

Sotres-Bayon F, Sierra-Mercado D, Pardilla-Delgado E, Quirk GJ (2012) Gating of fear in prelimbic cortex by hippocampal and amygdala inputs. Neuron 76:804-812.

Spielberger CD, Gorsuch RL, Lushene R, Vagg PR, Jacobs GA (1983) Manual for the State-Trait Anxiety Inventory. Palo Alto, CA: Consulting Psychologists Press.

Stearns PN (2010) History of Emotions: Issues of Change and Impact. In: Handbook of emotions (Lewis MJ, Barrett LF, Haviland-Jones JM, eds). New York: Guilford Press.

Stern ER, Welsh RC, Gonzalez R, Fitzgerald KD, Abelson JL, Taylor SF (2012) Subjective uncertainty and limbic hyperactivation in obsessive-compulsive disorder. Hum Brain Mapp.

Summerfield C, Egner T, Greene M, Koechlin E, Mangels J, Hirsch J (2006) Predictive codes for forthcoming perception in the frontal cortex. Science 314:1311-1314.

Talairach J, Tournoux P (1988) Co-planar Stereotaxic Atlas of the Human Brain. New York: Theime Medical.

Taylor SF, Phan KL, Decker LR, Liberzon I (2003) Subjective rating of emotionally salient stimuli modulates neural activity. Neuroimage 18:650-659.

Tharp DR (1980) Practice administration department established at dental school. Alumni Bull Sch Dent Indiana Univ:15-18.

Thayer JF, Ahs F, Fredrikson M, Sollers JJ, 3rd, Wager TD (2012) A meta-analysis of heart rate variability and neuroimaging studies: implications for heart rate variability as a marker of stress and health. Neurosci Biobehav Rev 36:747-756.

Thompson RA (1994) Emotion regulation: a theme in search of definition. Monogr Soc Res Child Dev 59:25-52.

Tranel D, Bechara A, Damasio H, Damasio AR (1998) Neural correlates of emotional imagery. Int J Psychophys 30:107.

Tranel D, Gullickson G, Koch M, Adolphs R (2006) Altered experience of emotion following bilateral amygdala damage. Cogn Neuropsychiatry 11:219-232.

Tromp DP, Grupe DW, Oathes DJ, McFarlin DR, Hernandez PJ, Kral TR, Lee JE, Adams M, Alexander AL, Nitschke JB (2012) Reduced structural connectivity of a major frontolimbic pathway in generalized anxiety disorder. Arch Gen Psychiatry 69:925-934.

Tsuchida A, Doll BB, Fellows LK (2010) Beyond reversal: a critical role for human orbitofrontal cortex in flexible learning from probabilistic feedback. J Neurosci 30:16868-16875.

Tye KM, Prakash R, Kim SY, Fenno LE, Grosenick L, Zarabi H, Thompson KR, Gradinaru V, Ramakrishnan C, Deisseroth K (2011) Amygdala circuitry mediating reversible and bidirectional control of anxiety. Nature 471:358-362.

Uchida RR, Del-Ben CM, Busatto GF, Duran FL, Guimaraes FS, Crippa JA, Araujo D, Santos AC, Graeff FG (2008) Regional gray matter abnormalities in panic disorder: a voxel-based morphometry study. Psychiatry Res 163:21-29.

Urry HL, van Reekum CM, Johnstone T, Kalin NH, Thurow ME, Schaefer HS, Jackson CA, Frye CJ, Greischar LL, Alexander AL, Davidson RJ (2006) Amygdala and ventromedial prefrontal cortex are inversely coupled during regulation of negative affect and predict the diurnal pattern of cortisol secretion among older adults. J Neurosci 26:4415-4425.

Versace A, Thompson WK, Zhou D, Almeida JR, Hassel S, Klein CR, Kupfer DJ, Phillips ML (2010) Abnormal left and right amygdala-orbitofrontal cortical functional connectivity to emotional faces: state versus trait vulnerability markers of depression in bipolar disorder. Biol Psychiatry 67:422-431.

Wager TD, Phan KL, Liberzon I, Taylor SF (2003) Valence, gender, and lateralization of functional brain anatomy in emotion: a meta-analysis of findings from neuroimaging. Neuroimage 19:513-531.

Wager TD, Davidson ML, Hughes BL, Lindquist MA, Ochsner KN (2008) Prefrontal-subcortical pathways mediating successful emotion regulation. Neuron 59:1037-1050.

Wager TD, Waugh CE, Lindquist M, Noll DC, Fredrickson BL, Taylor SF (2009) Brain mediators of cardiovascular responses to social threat: part I: Reciprocal dorsal and ventral sub-regions of the medial prefrontal cortex and heart-rate reactivity. Neuroimage 47:821-835.

Wakana S, Caprihan A, Panzenboeck MM, Fallon JH, Perry M, Gollub RL, Hua K, Zhang J, Jiang H, Dubey P, Blitz A, van Zijl P, Mori S (2007) Reproducibility of quantitative tractography methods applied to cerebral white matter. Neuroimage 36:630-644.

Walker DL, Toufexis DJ, Davis M (2003) Role of the bed nucleus of the stria terminalis versus the amygdala in fear, stress, and anxiety. European journal of pharmacology 463:199-216.

Wang R, Benner T, Sorensen AG, Wedeen VJ (2007) Diffusion Toolkit: A software package for diffusion imaging data processing and tractography. Proc Intl Soc Mag Reson Med 15:3720.

Watson D, Clark LA, Tellegen A (1988) Development and validation of brief measures of positive and negative affect: the PANAS scales. Journal of personality and social psychology 54:1063-1070.

Weber CS, Thayer JF, Rudat M, Wirtz PH, Zimmermann-Viehoff F, Thomas A, Perschel FH, Arck PC, Deter HC (2010) Low vagal tone is associated with impaired post stress recovery of cardiovascular, endocrine, and immune markers. Eur J Appl Physiol 109:201-211.

Whalen PJ, Johnstone T, Somerville LH, Nitschke JB, Polis S, Alexander AL, Davidson RJ, Kalin NH (2008) A functional magnetic resonance imaging predictor of treatment response to venlafaxine in generalized anxiety disorder. Biological psychiatry 63:858-863.

Wilkinson GS, Robertson GJ (2006) WRAT4: Wide Range Achievement Test. Lutz, FL: Psychological Assessment Resources.

Wolf RC, Philippi CL, Motzkin JC, Baskaya MK, Koenigs M (2014) Ventromedial prefrontal cortex mediates visual attention during facial emotion recognition. Brain.

Xu G, Rowley HA, Wu G, Alsop DC, Shankaranarayanan A, Dowling M, Christian BT, Oakes TR, Johnson SC (2010) Reliability and precision of pseudo-continuous arterial spin labeling perfusion MRI on 3.0 T and comparison with 15O-water PET in elderly subjects at risk for Alzheimer's disease. NMR Biomed 23:286-293.

Yeterian EH, Pandya DN, Tomaiuolo F, Petrides M (2012) The cortical connectivity of the prefrontal cortex in the monkey brain. Cortex 48:58-81.

Zachary RA (1986) Shipley Institute of Living Scale: Revised Manual. Los Angeles: Western Psychological Services.

Zald DH, Mattson DL, Pardo JV (2002) Brain activity in ventromedial prefrontal cortex correlates with individual differences in negative affect. Proc Natl Acad Sci U S A 99:2450-2454.

Zald DH, McHugo M, Ray KL, Glahn DC, Eickhoff SB, Laird AR (2014) Meta-analytic connectivity modeling reveals differential functional connectivity of the medial and lateral orbitofrontal cortex. Cerebral cortex 24:232-248.

Zhang Y, Brady M, Smith S (2001) Segmentation of brain MR images through a hidden Markov random field model and the expectation-maximization algorithm. IEEE Trans Med Imaging 20:45-57.